



Rialtas na hÉireann
Government of Ireland



Geological Survey
Suirbhéireacht Gheolaíochta
Ireland | Éireann

GW Flood Project: Monitoring, Modelling and Mapping Karst Groundwater Flooding in Ireland



Geological Survey Ireland



Trinity College Dublin
Coláiste na Tríonóide, Baile Átha Cliath
The University of Dublin



**INSTITUTE of
TECHNOLOGY
CARLOW**

Institiúid Teicneolaíochta Cheatharlach

Document Information

Project title: *GW Flood Project: Monitoring, Modelling and Mapping Karst Groundwater Flooding in Ireland*

Current Document version 1.2

Date 19/08/2020

Prepared By	Date	Comment
Ted McCormack	25/06/2020	
Owen Naughton	01/04/2020	
Rebecca Bradford	01/04/2020	
Joan Companyà	01/04/2020	
Patrick Morrissey	01/04/2020	
Laurence Gill	01/04/2020	

Reviewed By	Date	Comment
Monica Lee	10/04/2020	
Philip Schuler	23/04/2020	
Damien Doherty	23/04/2020	
Koen Verbruggen	25/05/2020	

Approved By	Date	Comment
Monica Lee	01/07/2020	
Koen Verbruggen	01/07/2020	

Version History

Ver. No.	Ver. Date	Comment	Revised By
1.0	24/4/2020		Ted McCormack
1.1	03/7/2020		Ted McCormack
1.2	19/08/2020	Minor syntax corrections	Ted McCormack



Geological Survey Ireland

Founded in 1845, Geological Survey Ireland is Ireland's public earth science knowledge centre and is a division of the Department of Communications, Climate Action and Environment. We are committed to providing free, open and accurate data and maps on Ireland's subsurface to landowners, the public, industry, and all other stakeholders, within Ireland and internationally. In addition, we act as a project partner in interpreting data and developing models and viewers to allow people to understand underground. We deal with a diverse array of topics including bedrock, groundwater, seabed mapping, natural disasters, and public health risks. www.gsi.ie

Acknowledgments

This work was carried out as part of the scientific project “GW Flood: Groundwater Flood Monitoring, Modelling and Mapping”, funded by Geological Survey Ireland, a division of the Department of Communications, Climate Action and Environment (DCCA). The project was initiated based on the Programme for a Partnership Government (2016) which stated that resources would be provided for “*studies into individual problematic (prone to flooding) Turlough systems, if requested by a local authority or another relevant State agency*”. The authors would like to gratefully acknowledge the assistance provided by Geological Survey Ireland staff and past project team member James McActeer. The authors acknowledge the contribution of the project steering committee, namely Richard Dooley (OPW), Mark Adamson (OPW), Conor Quinlan (EPA), Enda Mooney (NPWS), Eugene Dwyer (Roscommon Co.Co.), Maire NiChionna (Galway Co.Co.), Enda Gallagher (Galway Co.Co) and Paul Johnston (TCD).

The authors would like to thank Met Éireann for the provision of rainfall and evapotranspiration data, the European Space Agency Copernicus Programme for provision of satellite imagery, the Office of Public Works for the provision of LIDAR, hydrometric and aerial photography data and Ryan Hanley Consulting Engineers for the assistance in the South Galway and Neale catchments. The authors would also like to thank Roscommon, Galway, Mayo and Clare County Councils for assistance with fieldwork operations.



Disclaimer

Although every effort has been made to ensure the accuracy of the material contained in this report, complete accuracy cannot be guaranteed. Neither Geological Survey Ireland, nor the authors accept any responsibility whatsoever for loss or damage occasioned, or claimed to have been occasioned, in part or in full as a consequence of any person acting or refraining from acting, as a result of a matter contained in this report.

Reference

McCormack, T., Naughton, O., Bradford, R., Campanyà, J., Morrissey, P., Gill, L., Lee, M., (2020) *GW Flood Project: Monitoring, Modelling and Mapping Karst Groundwater Flooding in Ireland*, Geological Survey Ireland Report

Basemaps © Ordnance Survey Ireland Licence No. EN 0047217

Cover photo shows groundwater flooding near Gort, Co. Galway in February 2020. Photo courtesy of Galway County Council.



Executive Summary

Introduction

In response to the serious flooding of winter 2015/2016 specifically related to turloughs, the Programme for a Partnership Government (2016) stated that resources would be provided for “*studies into individual problematic (prone to flooding) Turlough systems, if requested by a local authority or another relevant State agency*”. Geological Survey Ireland (GSI), a division of the Department of Communications, Climate Action and Environment (DCCAE), and the leading national authority on groundwater science, delivered on this commitment by initiating a new three-year project (GWFlood) to investigate the drivers and extent of karst groundwater flooding in Ireland. The remit of this project was to advance understanding of karst groundwater flooding in Ireland, address the deficit of data available, and enable local and national authorities to make scientifically informed decisions regarding groundwater flood risk management in karst areas. To achieve this, the GSI in collaboration with Trinity College Dublin (TCD) initially and later with the Institute of Technology Carlow (ITC), developed a monitoring, mapping and modelling programme to address the knowledge gap regarding karst groundwater systems. This report describes the implementation of a turlough monitoring network and the methodology used to produce the historic and predictive groundwater flood maps.

Monitoring Karst Groundwater Flooding

The installation of monitoring infrastructure commenced in October 2016 and over 60 exploratory monitoring stations were installed at locations of recurrent groundwater flooding (turloughs) in counties Galway, Clare, Mayo, Roscommon, Longford and Westmeath. A subset of 18 sites which are representative of the spectrum of groundwater flooding conditions were upgraded as permanent telemetered stations providing real-time information on groundwater levels. Data from these monitoring stations were used to help to develop an understanding of the hydrodynamics and flooding potential of turlough systems across key catchments and provide model calibration data.



Modelling Karst Groundwater Flooding

The production of national groundwater flood maps faced two significant challenges: the absence of hydrometric data at flood sites and the lack of a methodology for predictive groundwater flood mapping. In this context, a methodology for generating hydrometric information from multi-temporal Synthetic Aperture Radar (SAR) imagery was established and hydrological models of flood sites were developed. Two model types were used: 1) generic (global) models capable of reproducing groundwater flooding time series from antecedent rainfall and soil moisture conditions, and 2) a distributed groundwater model of the Gort Lowlands catchment developed by Trinity College Dublin (TCD).

Mapping Karst Groundwater Flooding

SAR imagery was collected from the European Space Agency Copernicus Programme Sentinel-1 Mission and used to develop two types of groundwater flood maps. The first, the historic flood map, shows the extent of observed groundwater flood events and is largely based on SAR mapping of the 2015/2016 event combined with observed flood information. The second, the predictive flood maps, have also been developed for areas of recurrent groundwater flooding (turloughs), with flood extents predicted for a range of annual exceedance probabilities (AEP).

Historic Groundwater Flood Map

The historic groundwater flood map shows maximum observed flood extents for locations of recurrent groundwater flooding in limestone regions. The map is primarily based on the winter 2015/2016 flood event, which in most areas represented the largest groundwater flood event on record. It was developed using all available SAR imagery between the 1st of December 2015 and the 31st of March 2016 as well as any available historic records (from winter 2015/2016 or otherwise). The map consists of 3,598 polygons which cover a total flooded area of 283.3 km². The classification of a flood as “groundwater” was determined based on the intrinsic geological and hydrogeological characteristics of the flood environment as well as the duration and seasonality of the flood. Floods which were determined to have both groundwater and surface water components are included in the



flood map. When possible, a topographic correction algorithm was used to lessen interference from vegetation to SAR derived flood extents.

Predictive Groundwater Flood Map

The predictive groundwater flood map presents the probabilistic flood extents for locations of recurrent karst groundwater flooding. It consists of a series of stacked polygons at each site representing the flood extent for specific annual exceedance probabilities (AEP's). The map is focussed primarily (but not entirely) on flooding at seasonally inundated wetlands known as turloughs. These sites were chosen for inclusion in the predictive map based on existing turlough databases as well as manual interpretation of SAR imagery. The mapping process tied together the observed and SAR-derived hydrograph data, hydrological modelling, stochastic weather generation and extreme value analysis to generate predictive groundwater flood maps for 440 qualifying sites. Whist the map includes flood extents at the majority of known turloughs, it should be noted that it is not a comprehensive datasets of groundwater flooding. The map is limited to locations where the flood pattern was detectable and capable of being hydrologically modelled to a sufficient level of confidence.

Recommendations

Upon completion of the GWFlood project, a series of recommendations were outlined:

1. Capacity Building in Long-Term Groundwater Observation

The deficit of long-term multidisciplinary observational data of Irish groundwater systems could be addressed by applying the multidisciplinary scientific approach taken by the GWFlood project to key groundwater and wetland systems.

2. Non-karst Groundwater Flooding

Explore the impact of flooding from non karst systems such as permeable superficial deposits or urban groundwater.

3. Further Development of Remote Sensing Mapping Tools

Extend the remote sensing mapping tools developed during the GWFlood project to generate new products such as automated national flood maps and near real time satellite derived hydrographs.



4. Groundwater Flood Forecasting

Examine the potential application of near real-time monitoring and modelling developed during this project to groundwater flood forecasting.

5. Impacts of Climate Change on Groundwater Flooding

Interpret the latest climate change projection data for Ireland using GWFlood models to assess the potential impact of climate change on groundwater flooding.

In January 2020 GSI initiated a new three year climate change focussed project, GWClimate. This project was designed to build from the experience gained through the GWFlood project and will address many of the GWFlood project recommendations.



Table of Contents

1	Introduction.....	1
2	Groundwater Flooding.....	3
2.1	Groundwater Flooding in Ireland	4
2.2	Groundwater Flooding Mechanisms in Lowland Karst.....	6
2.3	Mapping Groundwater Flooding	9
3	GWflood Project.....	11
3.1	GWflood Project Outputs	12
3.2	Collaborations - Gort Lowlands Hydraulic Modelling Research Project	13
4	Turlough Water Level Monitoring Network	14
4.1	Exploratory Monitoring Network	14
4.2	Telemetric Monitoring Network	21
5	Mapping Methodology	24
5.1	Data Collection	24
5.2	Remote Sensing Hydrological Monitoring	25
5.3	Remote Sensing Hydrograph Generation	26
5.4	Hydrological Modelling.....	26
5.5	Historic Groundwater Flood map.....	27
5.6	Predictive Groundwater Flood map	27
6	Preparation of National DTM.....	29
6.1	List of data sources and datasets	29
6.2	Procedure for merging DTM datasets	32
6.3	DTM products.....	36
7	Flood Mapping Using Sentinel-1 SAR	39
7.1	Synthetic Aperture Radar.....	39



7.1	Water Delineation using SAR	41
8	Hydrograph Generation using SAR.....	53
8.1	Site Selection.....	53
8.2	Hydrograph Generation Methodology	55
8.3	Calibration.....	60
8.4	Results.....	61
9	Hydrological Modelling: Global.....	64
9.1	Modelling Overview.....	64
9.2	Global Modelling	65
9.3	Stochastic Weather Generation and Predictive Level Estimation.....	69
10	Hydrological Modelling: Distributive (Gort Lowlands)	70
10.1	Project Overview.....	70
10.2	Model Description.....	72
10.3	Main Project Outcomes.....	76
11	Historic Groundwater Flood Map	78
11.1	Filtering and Classification.....	78
11.2	Topographic Correction.....	85
11.3	Application of Supplementary Evidence	89
11.4	Dataset Merging	89
11.5	Manual Editing.....	90
11.6	Historic Flood Map Limitations and Assumptions	90
11.7	Shapefile Description	91
12	Predictive Groundwater Flood Map.....	93
12.1	Mapping Methodology.....	94
12.2	TCD Gort Lowlands Sites	97
12.3	Predictive Flood Map Limitations and Assumptions.....	98



12.4	Shapefile Description	99
13	Project Recommendations and Future Developments.....	101
13.1	Recommendations	101
13.2	Future Developments.....	103
14	References	104



Table of Acronyms

AEP	Annual Exceedance Probability
Amax	Annual Maxima
API	Antecedent Precipitation Index
CFRAM	Catchment Flood Risk Assessment and Management
CPI	Current Precipitation Index
DCCAE	Department of Communications, Climate Action and Environment
DTM	Digital Terrain Model
dGPS	Differential Global Positioning System
EMSRI	Emergency Management Service Rapid Mapping (Copernicus)
EPA	Environmental Protection Agency
ESA	European Space Agency
ET	Evapotranspiration
GIS	Geographic Information System
GSI	Geological Survey Ireland
GNSS	Global Navigation Satellite System
GPS	Global Positioning System
GRD	Ground Range Detected
GW	Groundwater
GWDTE	Groundwater Dependent Terrestrial Ecosystem
HAND	Height Above Nearest Drainage
ITC	Institute of Technology Carlow
IfSAR	Interferometric Synthetic Aperture Radar
IW	Interferometric Wide Swath
LiDAR	Light detection and ranging
NSE	Nash-Sutcliffe Efficiency
NPWS	National Parks and Wildlife Service
OPW	Office of Public Works
OSI	Ordnance Survey Ireland
PBIAS	Percentage bias
PFRA	Preliminary Flood Risk Assessment
RMSE	Root Mean Square Error
SMD	Soil Moisture Deficit
SAC	Special Area of Conservation
SPA	Special Protection Area
SAR	Synthetic Aperture Radar
SW	Surface water
TCD	Trinity College Dublin
TII	Transport Infrastructure Ireland
USGS	United States Geological Survey



1 Introduction

The winter of 2015/2016 saw the most extensive groundwater flooding ever witnessed in Ireland. Homes were flooded or cut off, roads submerged and agriculture disrupted by karst derived groundwater flooding, with some affected areas remaining inundated for many months. In the aftermath of the floods, the lack of data on groundwater flooding and fit-for-purpose flood hazard maps were identified as serious impediments to managing groundwater flood risk in vulnerable communities. In response, the Programme for Government (2016) stated that resources would be provided for “*studies into individual problematic (prone to flooding) Turlough systems*”. Geological Survey Ireland (GSI), as the leading national authority on groundwater science, initiated a new groundwater flood project (GWFlood) to deliver on the Programme for Government and address these deficits.

The remit of this project was to advance understanding of karst groundwater flooding in Ireland, address the deficit of data available, and enable local and national authorities to make scientifically informed decisions regarding groundwater flood risk management. To achieve this, GSI, in collaboration with Trinity College Dublin (TCD) and Institute of Technology Carlow (ITC), developed a monitoring, mapping and modelling programme to address the knowledge gap regarding karst groundwater systems. The study addressed the gap in groundwater hydrometric data by establishing a permanent telemetric network, as well as developing mapping and modelling tools to address issues surrounding groundwater flood mapping and flood frequency estimation.

In addition to the monitoring network, the key deliverables from this project were two flood maps. The first, the historic flood map, shows the extent of observed groundwater flood events and is largely based on mapping of the 2015/2016 event combined with historic observed flood information. The second, the predictive flood map, was developed for areas of recurrent groundwater flooding (chiefly turloughs) with flood extents predicted for a range of annual exceedance probabilities (AEP).



This report describes the implementation of a turlough monitoring network and the methodology used to produce the historic and predictive groundwater flood maps. Flood receptors were not identified nor were risks and consequences defined.



2 Groundwater Flooding

Groundwater flooding can be defined as flooding caused by the emergence of water originating from subsurface permeable strata induced by exceptional and/or prolonged recharge (Morris et al., 2007). It rarely poses a risk to life but instead commonly causes prolonged damage and disruption because of the relatively long flood duration (Morris et al., 2007, Cobby et al., 2009). Groundwater flooding has distinctive characteristics that present unique difficulties in quantifying the location and likelihood of flood occurrence (Hughes et al., 2011). Unlike fluvial or coastal flooding, where the flood location is concentrated along the river network or coastline, groundwater flooding is controlled by locally variable geological and hydraulic factors and can occur in a discontinuous manner across a wide geographical area (Naughton et al., 2017a).

The literature on groundwater flooding remains comparatively sparse in contrast to fluvial and pluvial flooding with relatively limited reporting of the phenomenon worldwide (Hughes et al., 2011, Abboud et al., Finch et al., 2004a, Gotkowitz et al., 2014). However, attention on groundwater flooding as a geohazard has increased in recent decades due to an increased frequency of extreme groundwater flood events across Europe (Ascott et al., 2017, Finch et al., 2004b, Pinault et al., 2005, Naughton et al., 2017b). The introduction of the EU Floods Directive (2007/60/EC), requiring States to consider flooding from groundwater sources, has reinforced the need to improve our understanding of the processes influencing this phenomenon.

In the UK, a series of groundwater flood events in the early 2000s motivated a number of investigations into the causes of groundwater flooding and how to manage it (Jacobs, 2004, Morris et al., 2007). Based on this experience, Hughes et al. (2011) outlines four reasons for a rise in water table causing groundwater flooding:

- 1. Groundwater level rise in response to prolonged extreme rainfall**

This form of flooding, also known as bedrock flooding, occurs in unconfined aquifers as a response to prolonged extreme rainfall. During these rainfall events,



low storage aquifers cannot accept more recharge and water rises above the ground surface, emerging as either point or diffuse flooding. The resultant floods may occur a few days or several weeks after a major recharge event and can last a number of weeks.

2. Groundwater flow in alluvial deposits by-passing river channel flood defences

This form of flooding, also known as permeable superficial deposits flooding, occurs in permeable superficial aquifers that are hydraulically connected to a river channel. Flooding occurs when water moves laterally out through the permeable sides of a river channel into lower lying alluvial deposits that overlie relatively impermeable bedrock (Mott MacDonald, 2010).

3. Cessation of groundwater abstraction

Reducing groundwater abstraction rates in areas of long-term abstraction (e.g. urban areas or mines) can lead to groundwater rebound and cause flooding in areas that were developed after abstraction commenced.

4. Underground structures creating barriers to groundwater flow

This form of flooding can occur in urban areas where basements are constructed at sufficient density to artificially obstruct the movement of groundwater. Such obstructions can cause localised increases in groundwater level and flood unsealed basements.

While each of these forms of groundwater flooding may occur in Ireland to a certain degree, by far the most extensive form of groundwater flooding is related to water table rise in Carboniferous limestone aquifers due to prolonged rainfall.

2.1 Groundwater Flooding in Ireland

Groundwater Flooding in Ireland is primarily associated with the limestone areas of the western lowlands, which extend from the River Fergus in Co. Clare in the south upwards to the areas east of Lough Mask and Corrib in Co. Galway and southern Co. Mayo. The prevalence of groundwater flooding in the western counties is fundamentally linked to bedrock geology. Groundwater flow systems in these areas are characterised by high spatial heterogeneity, low storage, high diffusivity, and extensive interactions between



groundwater and surface water, which leaves them susceptible to groundwater flooding (Naughton et al., 2017a). During intense or prolonged rainfall, the solutionally-enlarged flow paths are unable to drain recharge and available sub-surface storage rapidly reaches capacity. Consequently, surface flooding occurs in low-lying topographic depressions known as turloughs, which represent the principal form of extensive, recurrent groundwater flooding in Ireland (Mott MacDonald, 2010, Naughton et al., 2012). There are over 400 recorded examples of turloughs across the country, with the majority located in the limestone lowlands in counties Roscommon, Galway, Mayo and Clare (see Figure 1).

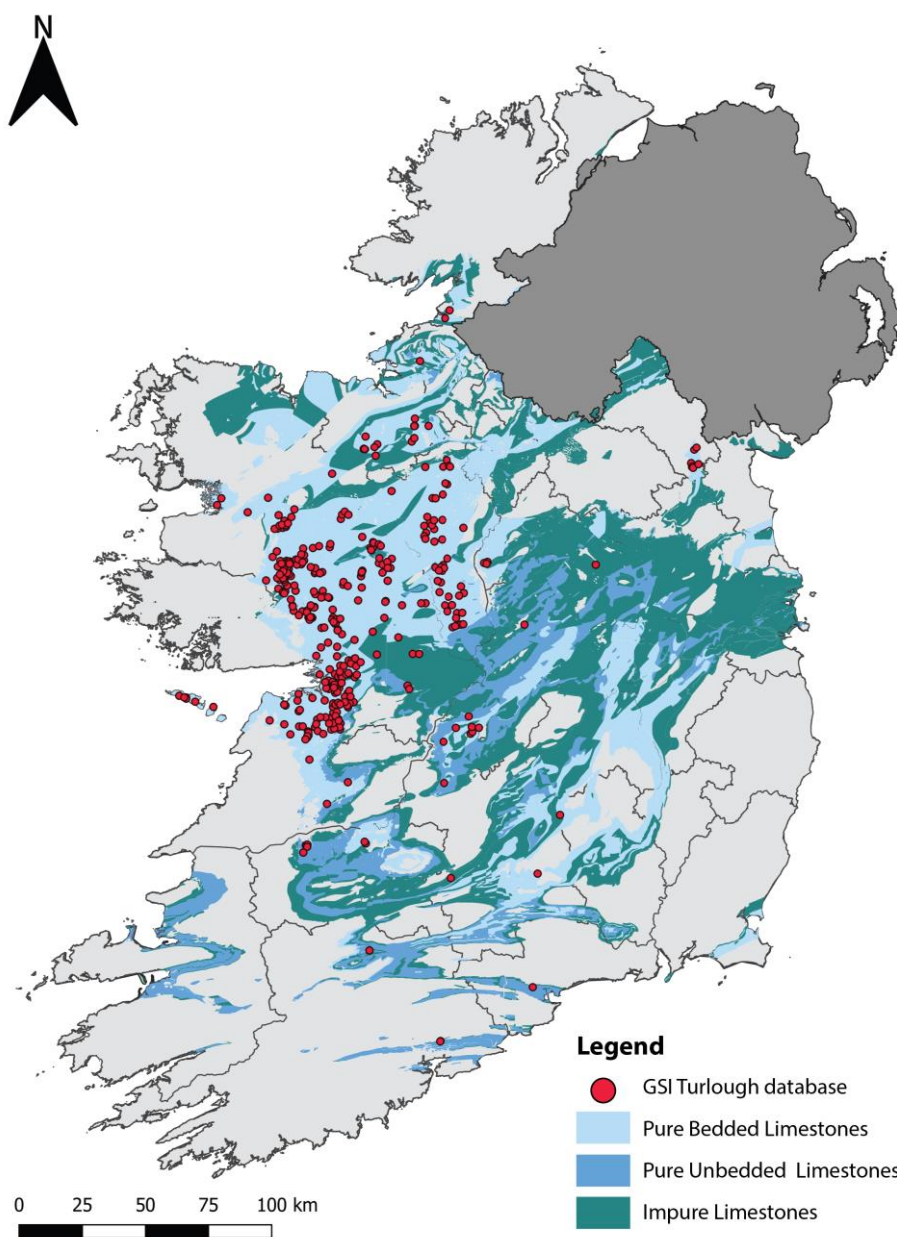


Figure 1: Locations of limestone and turloughs in Ireland (limestone layers derived from GSI Hydrostratigraphic Rock Unit Groups map).

Unlike fluvial flooding where the flood is typically caused by high intensity rainfall, groundwater flooding is primarily driven by cumulative rainfall over a prolonged period. It is this accumulation of water over a period of weeks or months that determines flood severity and duration. Furthermore, the long-term hydrometric data required for traditional flood frequency analysis does not exist for groundwater flooding, impeding the calculation of flood risk (combination of likelihood of an event and the damage caused by the event) as required in flood defence scheme assessments.

The last decade has seen the worst groundwater flooding in living memory. The dramatic floods during the winters of 2009/2010 and 2015/2016 caused widespread damage and disruption to communities across the country, particularly in the extensive karstic limestone lowlands on the western seaboard. The winter of 2015/2016 saw unprecedented levels of rainfall across the Republic of Ireland. Over 600 mm of rainfall fell across the island of Ireland between December and February, representing 190% of the long-term average and making it the wettest winter on record in a rainfall time series stretching back to 1850 (McCarthy et al., 2016, Noone et al., 2016). The sustained heavy rainfall caused exceptional and widespread flooding, with rivers across the country bursting their banks and registering some of the highest levels on record. The winter also saw the most extensive groundwater flooding ever witnessed on the karstic limestone plains in the west of Ireland (Naughton et al., 2017b). In these regions, homes were flooded or cut off, roads submerged, and agriculture disrupted, with some affected areas remaining inundated for months after flooding had subsided elsewhere.

2.2 Groundwater Flooding Mechanisms in Lowland Karst

Groundwater flooding in lowland karst environments can manifest in a variety of ways. Naughton et al. (2017b) identified the principal mechanisms as:

- Turlough flooding (Figure 2a)
- Backwater flooding (Figure 2a)
- Overtopping of sinks (Figure 2b)
- Discharge from springs and resurgences (Figure 2c and Figure 2d)



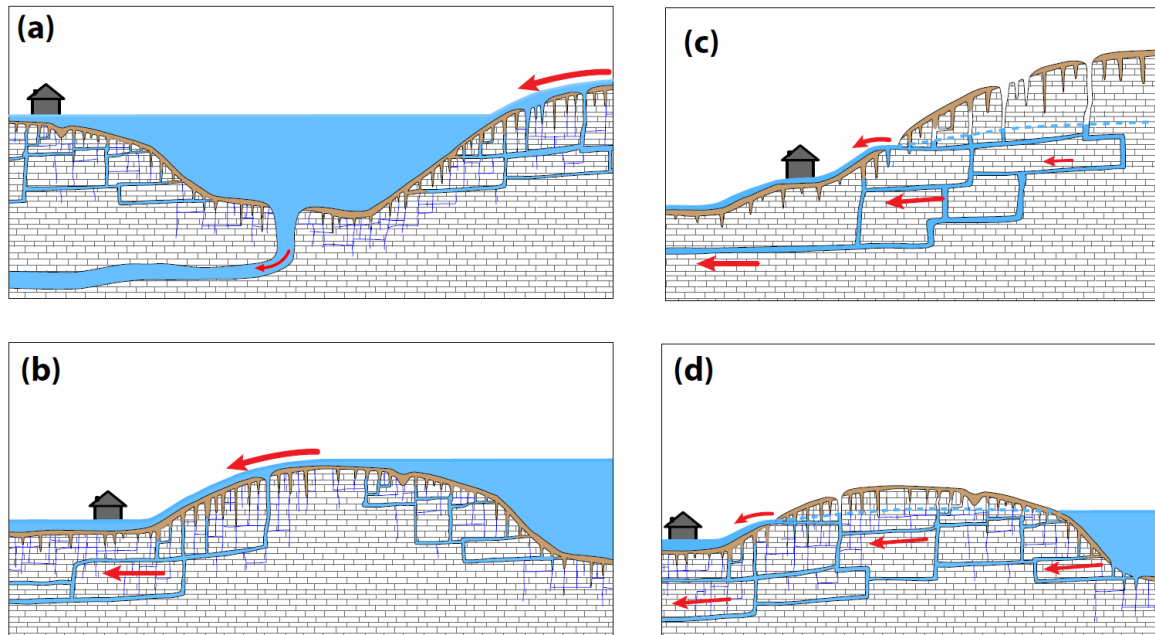


Figure 2: Groundwater flood mechanisms in lowland karst groundwater flow systems: (a) turlough/backwater flooding of sinks; (b) overtopping of basins and sinks; (c) discharge from spring and resurgences at the periphery of upland areas; and (d) lateral flow through shallow epikarst pathways (Naughton et al., 2017b).

2.2.1 Turlough Flooding

Turloughs are the principal form of recurrent, extensive groundwater flooding in Ireland. Most turloughs fill by rising groundwater levels through estavelles or springs in addition to direct precipitation and some surface runoff, and ultimately they empty through estavelles and swallow holes (Sheehy Skeffington et al., 2006). Filling normally occurs in late autumn due to periods of intense or prolonged rainfall, with emptying typically occurring from March onwards. The timing and extent of flooding can vary significantly between sites depending on the nature of and connections to the karstic groundwater system. Under normal hydrological conditions the inundation within turlough basins does not represent a flood hazard; in fact, it is an ecohydrological supporting condition for the flood-dependent turlough ecosystems. However, water levels can exceed normal bounds under extreme conditions and inundate surrounding buildings, agricultural land and infrastructure.

The hydrological budget of turloughs can be separated into two conceptual models: through-flow and surcharge tank systems. In a through-flow system, the turlough basin

effectively acts as a sink, receiving recharge from the surrounding vadose zone, shallow groundwater systems and/or point recharge (Figure 3a). In a surcharged tank system (Figure 3b), the main recharge and discharge processes do not occur simultaneously. Instead, the water budget is controlled by a bidirectional flow system located at or near the turlough base, with the turlough acting as overflow storage for the underlying conduit network.

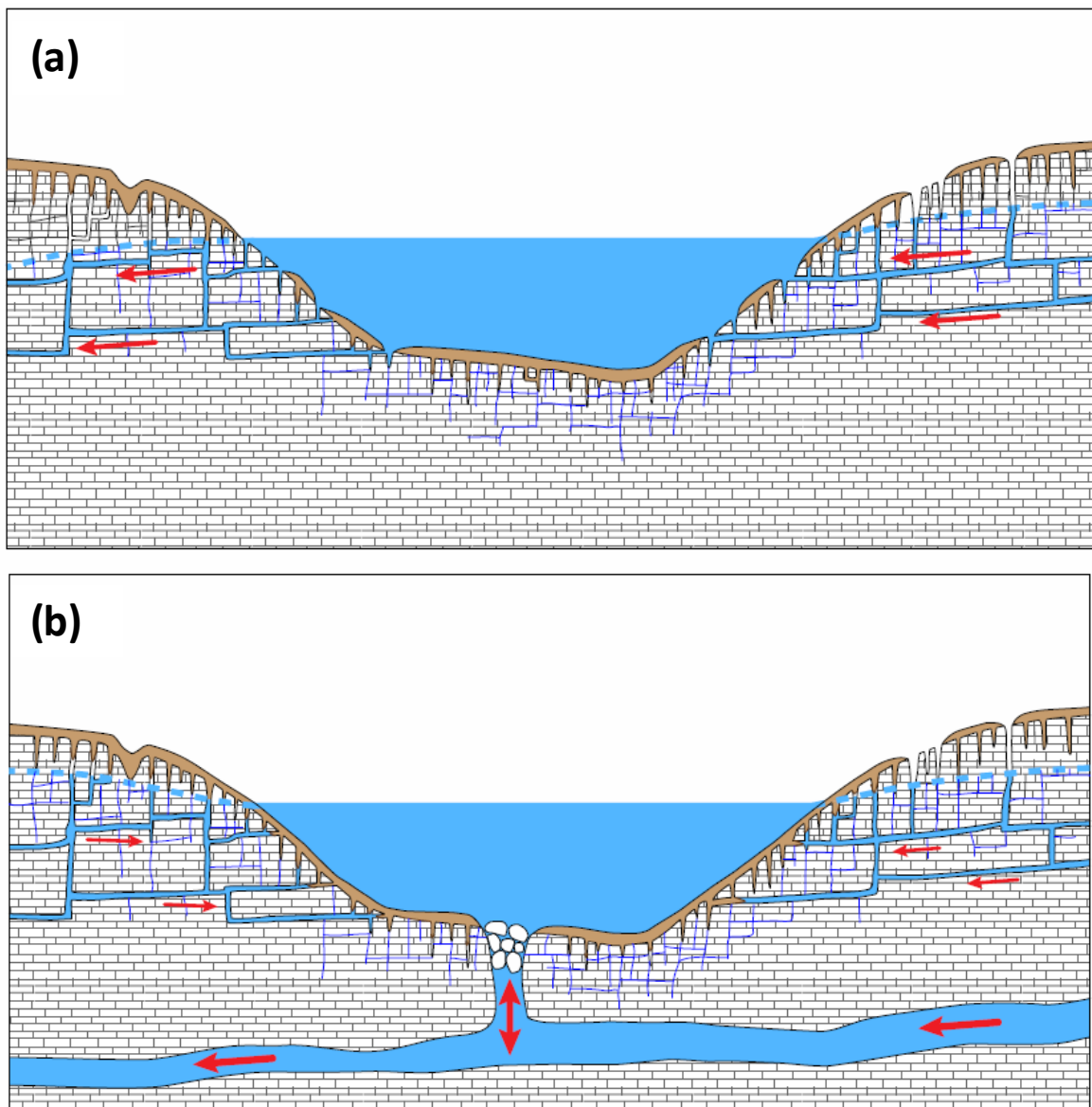


Figure 3: Conceptual diagrams representing possible turlough water budgets: (a) through-flow and (b) surcharge tank (Naughton et al., 2017b).

2.2.2 Backwater Flooding of Sinks

Backwater flooding occurs when excess point recharge (sinking streams or rivers) causes the inundation of dolines or sinks capable of accommodating recharge under normal conditions (Figure 2a). This mode is analogous to the recharge-related sinkhole flooding described by Zhou (2007), whereby flooding occurs when the capacity of the sinkhole is not sufficient to transfer storm water runoff into the subsurface.

2.2.3 Overtopping of Basins and Sinks

This flood mechanism is intrinsically linked to flooding within turlough and sink depressions because it occurs when floodwaters build up in surface depressions to such an extent that the level exceeds and overtops the surrounding topographic divide. When overtopping occurs, ephemeral overland flow routes develop, bypassing the groundwater flow systems normally governing water movement through the catchment (Figure 2b).

2.2.4 Discharge from Springs and Resurgences

Flooding in lowland karst aquifers can also be caused by high discharges of groundwater, via springs and resurgences, during which time the hydrodynamic force of the floodwater is the main cause of damage. This flood mechanism can be separated into two discharge scenarios: (1) groundwater springs and risings on the periphery of upland areas exceeding normal discharge levels and causing flooding around and downstream of the resurgence (Figure 2c), and (2) shallow flow paths within the epikarst zone are activated by high groundwater levels, triggering ephemeral springs and flooding of adjacent depressions (Figure 2d).

2.3 Mapping Groundwater Flooding

Flood maps are a key element of effective flood risk planning and management. Such maps support raising awareness among local authorities, government agencies and the general public of the risks posed by flooding and provide valuable information on the location and likelihood of flooding, thereby helping to reduce the impact of future flood events. The EU Floods Directive (Directive 2007/60/EC) requires all EU Member States including Ireland to reduce and manage the risks that all forms of flooding pose through the mapping of



probabilistic flood extents and the establishment of flood risk management plans. For flooding from groundwater sources, the Floods Directive stipulates that EU Member States may decide that the preparation of flood hazard maps shall be limited to floods with a low probability, or extreme event scenarios.

The abovementioned approach guided the groundwater flood mapping during the first implementation phase of the Floods Directive, where an evidence-based method was used to map areas vulnerable to groundwater flooding (Mott MacDonald, 2010). However, available data were severely limited, and the extreme floods of 2015/2016 highlighted the need to revise and update groundwater flood maps in order to accurately represent the magnitude and extent of groundwater flooding in the Irish landscape. Furthermore, an absence of methods for estimating groundwater flood frequency was identified as a key limitation in groundwater flood management, particularly in light of the increased frequency of groundwater flooding in recent decades and the future risks posed by climate change. It was in this context that the work of the GWFlood project was instigated.



3 GWFlood Project

In response to the serious flooding of winter 2015/2016 specifically related to turloughs, the Programme for a Partnership Government (2016), under the area of Climate Change and Flooding, contains the following objective: *“Turlough Systems: We will provide resources to the OPW to commission studies into individual problematic (prone to flooding) Turlough systems, if requested by a local authority or another relevant State agency”*. GSI, a division of the Department of Communications, Climate Action and Environment (DCCA), delivered on this commitment by planning and executing a three-year project investigating the drivers and extent of karst groundwater flooding in Ireland.

GSI, in collaboration with TCD and ITC developed the GWFlood project. Project objectives were to address the knowledge deficit on groundwater flooding and provide tools for effective groundwater flood risk management. This was to be achieved through:

- Establishing a groundwater flood monitoring network
- Developing remote groundwater flood monitoring methods
- Devising and applying a predictive (probabilistic) flood mapping approach
- Producing national groundwater flood maps
- Communication and dissemination of results

To achieve these objectives, the GWFlood project assembled expertise in the fields of groundwater flood monitoring, modelling and remote sensing. The project team consisted of three full time GSI staff and one research fellow, operating between October 2016 and December 2019. Additional technical guidance was provided by a technical advisory committee which met three times over the course of the project. The committee consisted of representatives from government stakeholder groups associated with groundwater flooding in Ireland including the OPW, EPA, NPWS and relevant local authorities.



3.1 GWFlood Project Outputs

The primary deliverables of the GWFlood project were the establishment of a hydrometric monitoring network and the production of groundwater flood maps.

3.1.1 Turlough Monitoring Network

Hydrometric information is a crucial component to understanding the dynamics of surface and groundwater flow systems. Hydrometric data such as stage and discharge are recorded across the country in rivers, lakes and coastlines, providing data vital to local authorities and planning agencies for effective flood risk management. However, consistent long-term hydrometric data do not exist for groundwater flooding applications. A primary output of the GWFlood project was the establishment of a monitoring network to provide these baseline data. These data were utilised for the calibration and validation of remote sensing data and hydrological modelling. Further details of the exploratory and permanent monitoring networks are provided in Section 4.

3.1.2 Groundwater Flood Maps

Historically the mapping of groundwater flooding in Ireland has been relatively sparse and incomplete in comparison to other forms of flooding such as fluvial or coastal flooding. This is primarily due to technical challenges in monitoring of groundwater floods, a relatively poor understanding of groundwater flood mechanisms, and the absence of analytical tools to assess groundwater flood frequency.

Remedying the lack of monitoring data poses significant technical challenges. In Ireland, groundwater flooding occurs in isolated basins across the landscape. The large number and wide distribution of these basins makes them impractical to monitor using traditional field instrumentation. In this context, the GWFlood Project endeavoured to develop a data collection and flood mapping methodology for ungauged sites using ESA Copernicus Programme Synthetic Aperture Radar imagery.

Two types of flood maps were developed. The first, the historic flood map, shows the extent of observed groundwater flood events and is largely based on mapping of the



2015/2016 event combined with observed flood information. The second, the predictive flood maps, have also been developed for areas of recurrent groundwater flooding (turloughs), with flood extents predicted for a range of annual exceedance probabilities (AEP). The procedure for developing the flood maps is described in Sections 5 to 12.

3.1.3 Communications, Dissemination and Engagement

The goals of providing an expert advisory service and disseminating project outputs were achieved via extensive engagement with public agencies, local authorities and community groups throughout the project, supplemented by a series of national and international presentations and publications (Naughton et al., 2018, Naughton et al., 2017b) . Notably, the project was showcased by the European Space Agency as an user story of how public administrations across Europe are using Copernicus data to address challenges affecting them (Naughton and McCormack, 2018). In addition, the project contributed to external groundwater flood relief schemes through contributing to tracer studies (Doherty et al., 2018, Doherty, 2019, Kelly, 2018) and participating in steering committees for flood schemes in Co. Galway and Co. Clare.

3.2 Collaborations - Gort Lowlands Hydraulic Modelling Research Project

In addition to instigating the nationally focussed GWFlood project, the winter 2015/2016 flood event also prompted a series of local flood relief schemes by local Authorities and the OPW. In County Galway, a scheme was initiated to investigate potential flood relief measures for the Gort Lowlands. At the outset of this scheme, the OPW and Galway County Council sought to utilise the significant research experience of the area gained by the Department of Civil, Structural and Environmental Engineering, TCD. To facilitate this, the GWFlood project provided 30 months funding for a postdoctoral researcher. The objective of this research project was to enhance a pre-existing hydrological model of the catchment (Gill et al., 2013a, McCormack et al., 2014) and work with Galway County Council to research the effects of various engineered flood mitigation measures on local and catchment hydrology. This research project is described in more detail in Section 10.



4 Turlough Water Level Monitoring Network

Installation of monitoring infrastructure commenced in October 2016. Over 60 exploratory monitoring stations were installed in counties Galway, Clare, Mayo, Roscommon, Longford and Westmeath. Data from these sites helped to develop an understanding of the hydrodynamics and flooding potential of turlough systems across key catchments and provide model calibration data. Exploratory data were also used to inform the site selection process for the permanent monitoring network. The installation of permanent monitoring stations began in summer 2017 and was completed in mid-2019. A subset of 18 sites representative of the spectrum of groundwater flooding conditions were established as permanent telemetered stations providing real-time information on water levels.

4.1 Exploratory Monitoring Network

4.1.1 Site Selection

The initial approach for the site selection process involved collating a comprehensive database of karst groundwater flood sites and systems from which exploratory and telemetric monitoring sites would be selected. Due to constraints imposed by the seasonality of groundwater flooding, rapid high-level site selection processes commenced in October 2016 to ensure sites were installed before the winter flooding. The exploratory monitoring sites were selected based on factors including: 1) karst feature databases, 2) historic data, 3) earth observation data, and 4) stakeholder engagement.

The National Karst Landform Database, a geospatial inventory of recorded karst landforms in the Republic of Ireland maintained by GSI, together with additional turloughs databases in Ireland (Coxon, 1986, Mayes, 2008, O'Neill and Martin, 2015), were queried. Sites subject to recurrent groundwater flooding were identified and extracted as possible sites for the exploratory network. Sites with historical monitoring data were also considered (e.g. Naughton et al. (2012)) to support long-term hydrological observations. Remote sensing-derived flood maps prepared by the Copernicus Emergency Mapping Service



(activations: EMSRI149, EMSRI154 and EMSRI156), were consulted to detect the location and prevalence of groundwater flooding across the worst affected regions, thus selecting the ones that had larger impact in society during the winter of 2015/2016. Based on this initial screening, local authorities and stakeholders in the worst affected regions during the 2015/2016 flooding event were contacted to corroborate findings and to identify any areas of significant groundwater flood hazard overlooked in the screening process. Subsequently, 60 exploratory sites (see Table 1 and Figure 4) were established, the majority of them grouped in three main clusters in the regions of counties Roscommon, Mayo, Galway-Clare (Figure 5).

Table 1: List of the exploratory monitoring network stations (Logger type - L: Level, T: Temperature, C: Electrical conductivity). Sites with absent date refer to Loggers remain onsite recording data. Asterisks in location attribute show stations that are now part of the telemetric network.

Location	County	Date Installed	Date Removed	Logger Type	Easting (ITM)	Northing (ITM)
Ballycar Lough*	Clare	12/03/2019	12/09/2019	LT	541026	668626
Knockaunroe	Clare	30/11/2016		LT	531567	693882
Lough Aleenaun*	Clare	30/11/2016	15/08/2019	LT	524812	695538
Lough Bunny	Clare	30/11/2016	11/07/2018	LT	537311	696443
Lough Gash	Clare	12/03/2019		LT	539050	667889
Lough Gealain	Clare	30/11/2016	11/09/2019	LT	531365	694745
Lough Loum	Clare	15/06/2017	20/09/2017	LTC	539664	700737
Tulla*	Clare	30/11/2016	28/05/2019	LT	536619	702217
Ardacong North	Galway	22/06/2017	29/07/2019	LT	542952	755673
Ardacong South	Galway	22/06/2017	29/07/2019	LT	543607	754326
Ballinduff	Galway	25/11/2016	07/08/2019	LT	546022	708041
Ballyboy	Galway	06/06/2017	07/08/2019	LT	548087	712961
Ballylee North	Galway	06/06/2017	08/08/2019	LTC	548024	706624
Ballylee South	Galway	06/06/2017		LTC	547480	706169
Belclare	Galway	22/06/2017	29/07/2019	LT	537999	749917
Belclare	Galway	22/06/2017	29/07/2019	LT	537999	749917
Blackrock*	Galway	30/11/2016	08/08/2019	LT	549682	708077
Caherglassaun*	Galway	24/11/2016	04/05/2018	LT	541184	706330
Cahermore	Galway	01/12/2016	28/08/2019	LT	541473	707889
Caranavoodaun*	Galway	14/09/2016	14/11/2018	LTC	545275	715315
Castletown Sink	Galway	07/06/2017	08/08/2019	LTC	545885	704921
Cockstown	Galway	06/06/2017	08/08/2019	LT	548452	710258
Coolcam	Galway	21/06/2017	15/08/2018	LT	557301	770656
Coole*	Galway	24/11/2016	08/08/2019	LT	543070	704291
Garryland East	Galway	24/11/2016	09/05/2018	LTC	541515	703740
Garryland West	Galway	24/11/2016		LTC	541294	703846
Glenamaddy	Galway	21/06/2017	17/10/2018	LT	563710	761365
Hawkhill	Galway	25/11/2016	08/08/2019	LTC	541131	702381
Kiltartan River	Galway	01/12/2016	25/07/2019	LT	545060	705762
Labane*	Galway	01/12/2016	14/11/2018	LT	546232	710181
Lough Coy	Galway	30/11/2016	08/08/2019	LT	548933	707496
Managh	Galway	25/11/2016	09/05/2018	LT	540270	701489
Newtown Coole	Galway	24/11/2016	08/08/2019	LT	542584	702688
Newtown RC	Galway	25/11/2016		LT	543097	702256



Rathbaun	Galway	29/06/2017	14/08/2018	LT	534312	761103
Roo West	Galway	30/11/2016	11/09/2019	LTC	538555	702265
Termon North	Galway	01/12/2016	11/09/2019	LT	541901	697755
Termon South*	Galway	25/11/2016	15/08/2019	LT	541078	697275
Fortwilliam*	Longford	14/09/2016	16/10/2018	LTC	601350	762960
Balla	Mayo	21/06/2017	14/08/2018	LT	526523	783887
Ballyshingadaun	Mayo	23/06/2017	11/09/2019	LT	519411	757130
Cahernagollum	Mayo	22/06/2017	29/07/2019	LT	516580	761879
Cross Spring	Mayo	29/06/2017	29/07/2019	LTC	519080	755108
Cuilaun South	Mayo	21/06/2017	28/08/2019	LT	540368	770475
Drumadoon	Mayo	21/06/2017	14/08/2018	LT	524401	785705
Garracloon*	Mayo	22/06/2017	15/04/2019	LT	518511	756383
Kildotia	Mayo	12/12/2017	29/07/2019	LT	520716	757832
Kiltagorra	Mayo	12/12/2017	29/07/2019	LTC	520503	757611
Neale*	Mayo	22/06/2017	14/08/2018	LT	518941	759799
Polldowagh	Mayo	22/06/2017	29/07/2019	LT	518968	756007
Shrule*	Mayo	28/06/2017	15/04/2019	LT	526339	753805
Skealaghan*	Mayo	22/06/2017	29/07/2019	LT	524795	762940
Turloughatsallain	Mayo	29/06/2017	29/07/2019	LT	515073	756326
Turloughmore	Mayo	22/06/2017	29/07/2019	LTC	520614	758895
Moylan Lough*	Monaghan	05/07/2019	30/09/2019	LT	685244	808863
Ardmullan	Roscommon	18/11/2016	20/08/2019	LT	595410	749670
Ballinturly	Roscommon	18/11/2016		LT	583710	760210
Brean Drum	Roscommon	28/06/2017	22/05/2018	LT	578352	801125
Ballygalda (Correal Cross)*	Roscommon	18/11/2016	16/10/2018	LT	585110	760840
Brierfield	Roscommon	04/08/2016		LT	581756	777114
Carrowkeel	Roscommon	18/11/2016	15/08/2018	LT	584400	761590
Carrowreagh	Roscommon	18/11/2016		LT	578510	775190
Castleplunket*	Roscommon	17/11/2016	14/05/2019	LT	577640	777865
Four Roads	Roscommon	18/11/2016	20/08/2019	LT	583930	751730
Funshinagh *	Roscommon	04/08/2016	20/08/2019	LTC	594267	749818
Lisduff	Roscommon	18/11/2016	15/08/2018	LT	584220	755730
Lough Croan	Roscommon	18/11/2016	15/08/2018	LT	587980	749520
Rathnalulleagh	Roscommon	17/11/2016	16/10/2018	LTC	577890	773680
Shad Lough	Roscommon	17/11/2016	22/05/2018	LT	582490	775700
Moate	Westmeath	06/06/2017	15/08/2018	LT	617435	738811



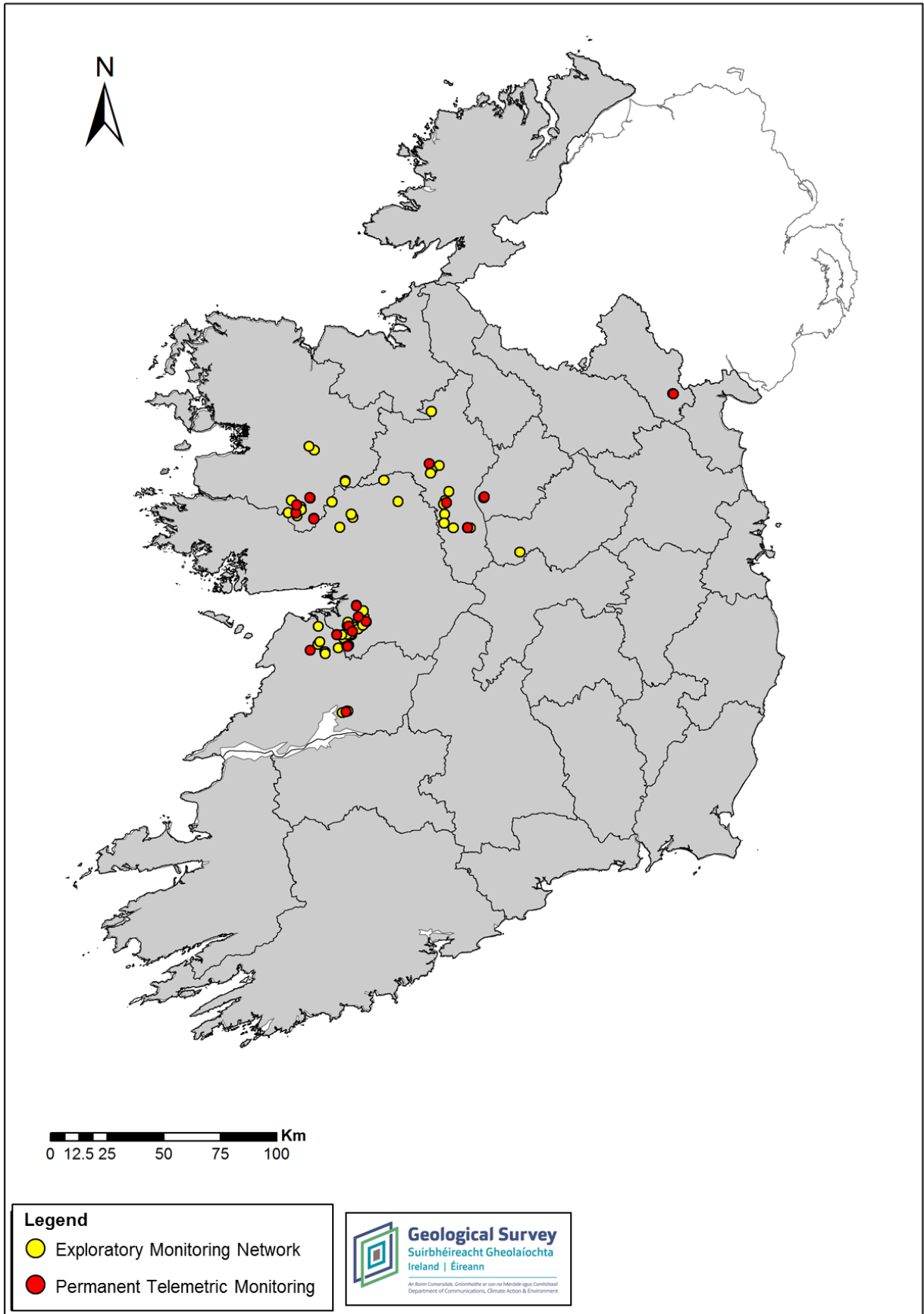


Figure 4: Exploratory (2016-2019) and permanent telemetric monitoring networks.

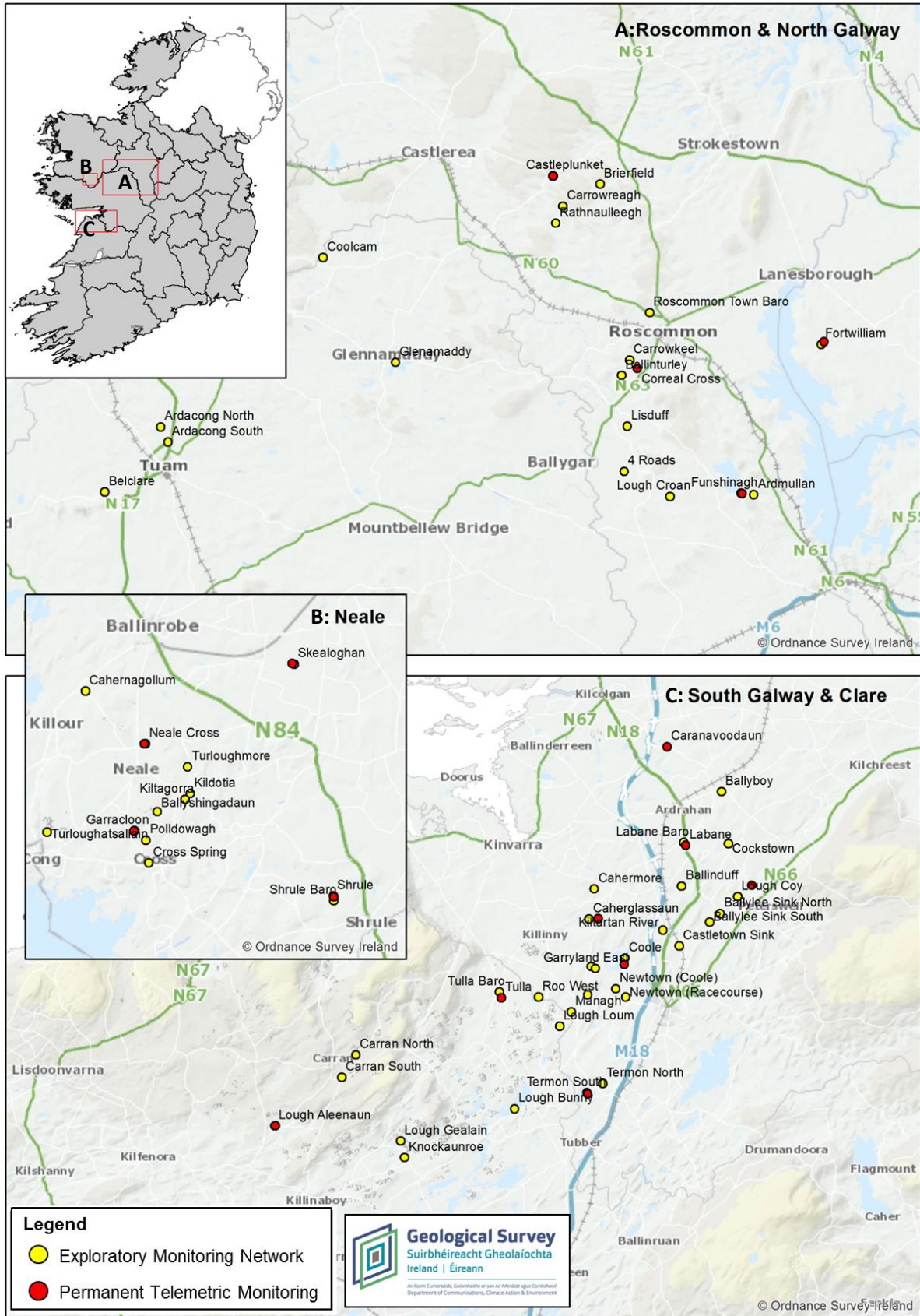


Figure 5: Exploratory and permanent telemetric monitoring network clusters.



4.1.2 Exploratory Station Installation

Installation of the exploratory monitoring equipment commenced in October 2016 and took place over an 18-month period. Custom-built instrument enclosures were used to house the loggers at each site for easy deployment and recovery during flooded conditions (Figure 6). Water levels, temperature, and conductivity (at a select few sites) were recorded on the hour at hourly intervals using Solinst Levelloggers[®], which were placed at or near the deepest point in each turlough basin. Solinst Barologger Edges[®] were installed within each cluster of sites to compensate for atmospheric pressure fluctuation. Each Barologger was positioned within a 30 km radius and/or 300 m elevation change to a cluster of monitoring sites, and recorded data on the hour every hour. The Barologgers were installed above the known groundwater flood maximum. Data from Levelloggers and Barologgers were downloaded manually approximately every six months, and access to the loggers was performed by foot or by boat, depending on flooding conditions.



Figure 6: Exploratory monitoring equipment. Custom built monitoring box and Solinst Levelloggers used for data recording.

Water level elevation was also collected through the duration of the monitoring period using a GPS Trimble[®] R10 LT GNSS Advanced Rover with Virtual Reference Station (VRS) capability in order to adjust logger water levels to ordnance datum. GPS measurements were taken typically every 2-3 months to correct for any logger movement and calibration purposes, and helped to reduce the impact of issues encountered during the monitoring

period, which included: 1) livestock in fields preventing access to the monitoring equipment, 2) upturned monitoring boxes, 3) loggers stolen or vandalised, 4) rope and float cut impeding recovering during flooded condition, and 5) logger failure.

4.1.3 Data Processing

Logger data were compensated with barometric data to get water level above the logger, and the GPS measurements were then used to adjust water levels to ordnance datum and to correct for any movement of the logger. In addition to groundwater levels, volume and area of the flooding for each turlough was calculated using Digital Terrain Models (DTMs). Sample hydrographs are shown below in Figure 7.

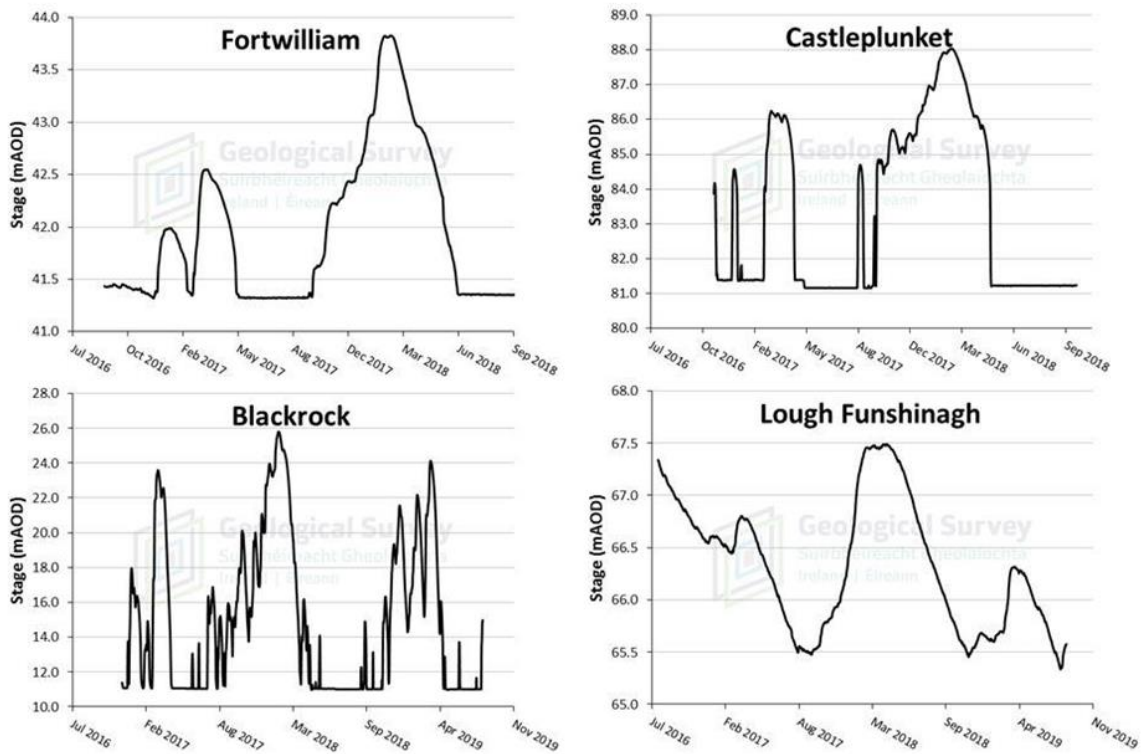


Figure 7: Sample hydrograph data from exploratory monitoring network stations at Blackrock turlough (Co. Galway), Fortwilliam turlough (Co. Longford), Castleplunket turlough and Lough Funshinagh (both Co. Roscommon).

4.2 Telemetric Monitoring Network

4.2.1 Site Selection

The installation of the telemetered monitoring network (Figure 4– red points) began in summer 2017 and completed in 2019, with a subset of 18 sites representative of the spectrum of groundwater flooding conditions providing real-time information on groundwater flood conditions (See Table 2 for telemetric monitoring station details). The telemetered sites were selected based on the following factors:

1. Hydrological regime – statistical analysis

Stage and volume data from the exploratory network were analysed to quantify the spectrum of groundwater flooding behaviour, where each potential site lay on that spectrum and how each site compared to others in the surrounding groundwater system.

2. Historic data

Long term data has largely been confined to the Gort Lowlands catchment in South Galway due to a long history of flooding in the region. As such, this area was prioritised in order to support long term hydrographs for karst features.

3. Flood risk/receptor density

Sites where the groundwater flooding poses significant economic and social disruption were prioritised.

4. Ecological value

Turloughs are classified as Groundwater Dependant Terrestrial Ecosystems (GWDTEs) under the Water Framework Directive (2000/60/EC) and as a Priority Habitat in Annex 1 of the EU Habitats Directive (92/43/EEC). Sites of ecological significance were prioritised in support of ecosystem assessment.

5. Geographical distribution

An objective of the telemetric network was to represent the hydrological regime across the country within karst systems. The geographical representation was assessed on a catchment basis.



Table 2: Permanent telemetric monitoring stations (Logger type - L: Level, T: Temperature, C: Electrical Conductivity).

Location	GSI -Code	County	Date Installed	Logger Type	Easting (ITM)	Northing (ITM)
Ballycar Lough	GSI_18	Clare	27/08/2019	LT	540719	668278
Lough Aleenaun	GSI_16	Clare	15/08/2019	LT	524822	695560
Tulla	GSI_07	Clare	10/09/2018	LT	536677	702256
Blackrock	GSI_02	Galway	09/05/2018	LTC	549463	708190
Caherglassaun	GSI_04	Galway	12/10/2017	LTC	541837	706258
Caranvoodaun	GSI_05	Galway	10/09/2018	LT	545265	715265
Coole	GSI_03	Galway	26/02/2019	LT	543322	703780
Labane	GSI_17	Galway	21/08/2019	LT	546174	710211
Termon South	GSI_08	Galway	10/09/2018	LT	541328	697112
Fortwilliam	GSI_09	Longford	16/10/2018	LT	601729	763339
Garracloon	GSI_12	Mayo	25/09/2018	LT	518495	756305
Neale	GSI_15	Mayo	14/05/2019	LT	518917	759821
Shrulle	GSI_13	Mayo	25/09/2018	LT	526404	753746
Skealoghan	GSI_14	Mayo	25/09/2018	LT	524713	763045
Moylan Lough	GSI_19	Monaghan	30/09/2019	LT	685284	808863
Ballygalda (Correal Cross)	GSI_10	Roscommon	16/10/2018	LT	585024	760859
Castleplunket	GSI_01	Roscommon	18/09/2017	LT	577470	777964
Lough Funshinagh	GSI_11	Roscommon	14/02/2019	LT	594389	749828

4.2.2 Telemetric Station Installation

A heavy duty precast concrete box (Figure 8a) was designed and built for the telemetric monitoring sites. The 58x44x44cm hollow box was designed with holes to allow water to freely circulate with a logger housed inside recording depth and temperature hourly using Van Essen TD-Diver pressure transducer data logger. The data are transmitted through an optical reader to an Eijkelkamp GDT-S Prime modem housed within a waterproof enclosure (Figure 8b) via a direct read cable buried underground. The modem transmits data recurrently via SMS to an online web portal. The precast concrete enclosure is installed at or close to the lowest point of the basin and is designed for the long-term protection of equipment from damage due to livestock and vandalism. The telemetry modem is installed above the peak flood level to ensure the equipment will not be submerged during an extreme flood event. Sites with a long distance of buried cable had junction boxes installed at intervals along the cable path to aid cable installation and future maintenance.

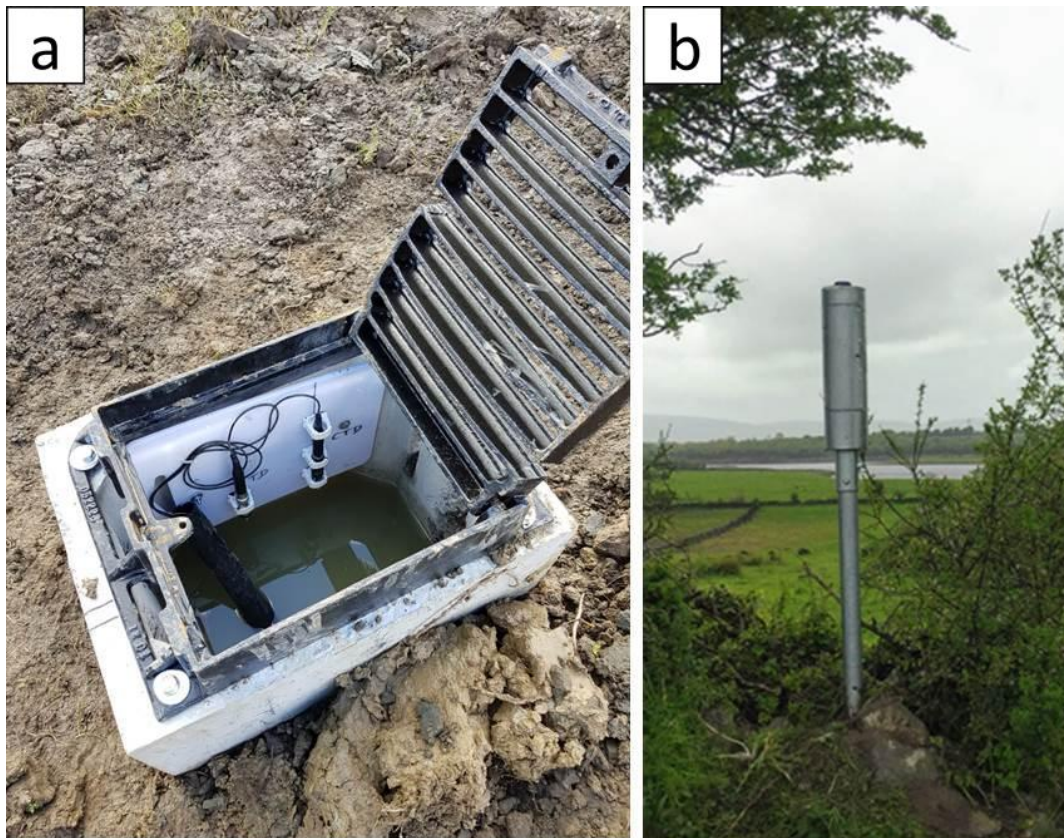


Figure 8: (a) Precast concrete monitoring box and (b) Telemetry housing unit.

The steps for installation included:

1. Screening reports were prepared for each site to ensure there were no potential effects of the proposed plan on and in combination with other plans to one or more Natura 2000 sites (Special Protection Areas, SPA or Special Areas of Conservation, SAC).
2. Desk study of the area. Initially looked at maps to decide the shortest and most direct route for the pipe layout, also looking at flood maps and DTM's to ensure the telemetry unit will be out flooding reach.
3. Site walkovers were carried out and landowner permission granted. When necessary, route for the pipe layout was modified after site walk over and after contacting with landowners.
4. Permitting for pole installation, by contacting local authorities, and arrangements for digging the trench for the pipes and installing the pole.
5. Installation was carried out during summer months when turloughs were empty or at their lowest.

5 Mapping Methodology

The production of the national historic and predictive groundwater flood maps faced two significant challenges: the absence of hydrometric data at flood sites and the lack of a methodology for predictive groundwater flood mapping. In this context, a methodology for generating hydrometric information from multi-temporal SAR imagery was established, followed by the development of hydrological models capable of reproducing groundwater flooding time series from antecedent rainfall and soil moisture conditions. These advances enabled, for the first time, the systematic mapping and modelling of groundwater flood extents across Ireland. The mapping workflow is described in the following sections and is summarised in Figure 9.

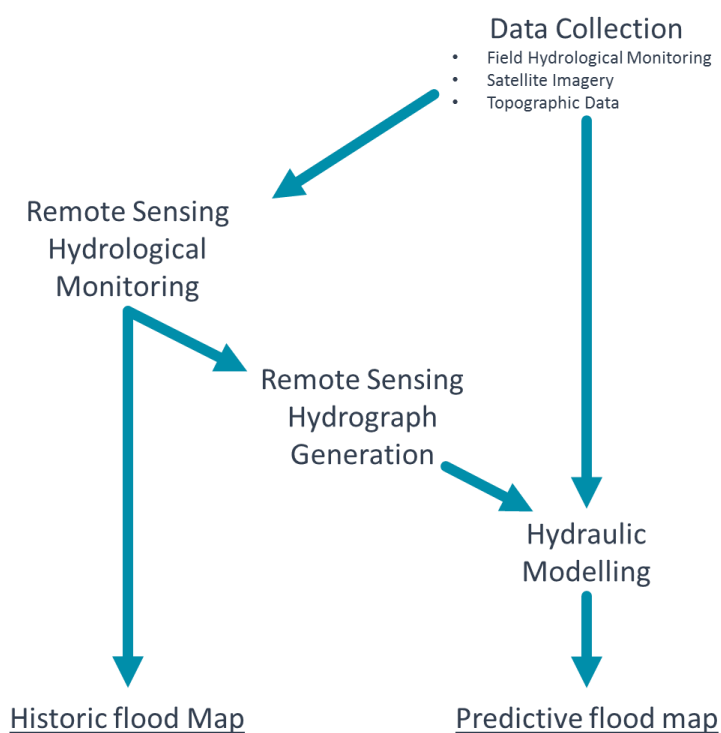


Figure 9: Groundwater Flood Map Workflow.

5.1 Data Collection

5.1.1 Field Hydrological Monitoring

Through the GWFlood monitoring network, hydrometric data were collected from over 60 locations. This data were used for the calibration and validation of remote sensing data and hydrological modelling.



5.1.2 Satellite Imagery

Sentinel-1 SAR data were collected from the ESA Copernicus Programme through the Copernicus Open Access Hub. All data collected over Ireland between February 2015 and August 2019 were downloaded and stored. Selected Sentinel-2 and Landsat images were also downloaded from Copernicus Open Access Hub and the USGS Earth Explorer services, respectively.

5.1.3 Topographic Data

A national DTM for the Republic of Ireland was compiled from best available datasets, incorporating topographic data from IfSAR NEXTMAP (OPW), LiDAR (OPW, GSI, TII), drone-based photogrammetry (GSI) and dGPS datasets (TCD, GSI). All datasets were resampled to a horizontal resolution of 5m to match that of the national IfSAR NEXTMap DTM. The processes used to merge all DTM data into a seamless national DTM is described in Section 6.

5.2 Remote Sensing Hydrological Monitoring

A prerequisite for both the historic and predictive flood maps is observation data. Historically there has been no systematic collection of hydrometric data of groundwater flooding, however, and so the required data does not exist. To address this information gap, the GWFlood project has developed a remote sensing procedure to optimise and automate the mapping of groundwater flood extents from SAR data. This procedure enabled the systematic collection of data at previously unachievable spatial and temporal scales.

SAR systems, such as the ESA Copernicus Programme Sentinel-1 satellites, emit radar pulses and record the return signal at the satellite. The strength of this signal, also called backscatter, is largely dependent on surface roughness and geometry. Flat surfaces such as water operate as specular reflectors resulting in minimal backscatter signal returning to the satellite (see Figure 10). Interpretation of SAR images involves a degree of ambiguity due to factors such as speckle effects and dielectric properties, but overall SAR systems offer a powerful tool for surface water delineation. Furthermore, by combining satellite



derived flood extents with high resolution topographic mapping, it is possible to extract water level information from each satellite image. This methodology enhances the accuracy of once-off flood extent maps as well as enabling the generation of historic flood hydrographs for previously unmonitored sites. For more information on this process, see Section 7.

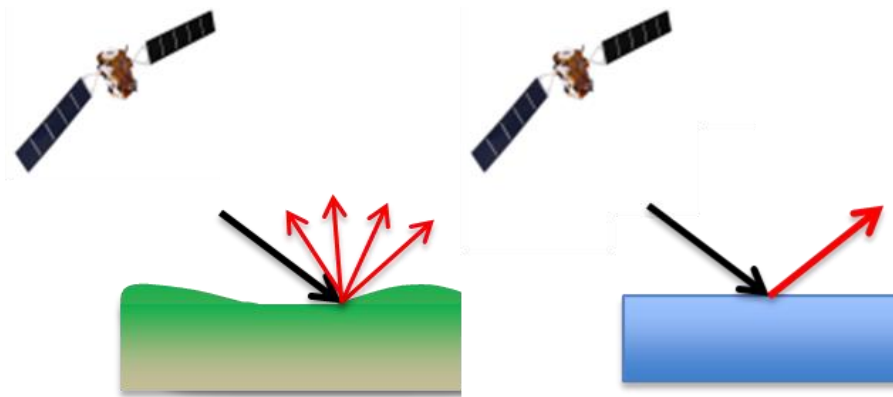


Figure 10: Illustration of SAR backscatter characteristics for land (left) and flat surfaces (right).

5.3 Remote Sensing Hydrograph Generation

The distributed nature of groundwater flooding in karst lowlands makes it impractical to monitor using traditional field instrumentation. To remedy this, the SAR mapping methodology was further developed in order to reconstruct hydrometric data at priority locations. This methodology enabled, for the first time, the systematic concurrent monitoring of almost 300 flood locations in Ireland. For more information on this process, see Section 8.

5.4 Hydrological Modelling

Predictive flood mapping requires long-term hydrological time series to estimate future occurrence probabilities. No such records exist for karst groundwater flow systems in Ireland; however, long-term records of rainfall are available. A global hydrological modelling methodology was developed to quantify the relationship between rainfall and turlough flooding to reconstruct the requisite long-term hydrological timeseries from observed and stochastic rainfall data.

Site-specific hydrological models capable of reproducing groundwater flooding time series from antecedent rainfall and soil moisture conditions were calibrated using a combination of logger measured and SAR generated hydrographic data. Long-term meteorological series were then used as model input to reconstruct long-term volume time series suitable for flood frequency analysis. A stochastic weather generator was calibrated for each site using observed meteorological data and used to construct long-term (>2000 years) synthetic rainfall series. This stochastic rainfall series, together with long-term average evapotranspiration (ET), were considered as input data to the site models to produce a long-term hydrological time series. Statistical distributions were fitted to annual maxima series and predictive groundwater flood extents derived, mapped and combined into a national predictive groundwater map. For further information, see Section 9.

5.5 Historic Groundwater Flood map

The historic groundwater flood map is a national-scale flood map presenting the maximum historic observed extent of karst groundwater flooding. The map is primarily based on the winter 2015/2016 flood event, which in most areas represented the largest groundwater flood event on record. The map was produced based on the SAR imagery of the 2015/2016 event as well as any available supplementary evidence.

The map consists of 3,598 polygons which cover a total flooded area of 283.3 km². The classification of floods as groundwater derived was automated based on a series of rules (e.g. 'must overlay limestone', 'must be seasonal' etc.). Floods classified as surface water were also mapped and used to generate a complementary product to the historical groundwater flood map. For further information, see Section 11.

5.6 Predictive Groundwater Flood map

The predictive groundwater flood map presents the probabilistic flood extents for locations of recurrent karst groundwater flooding. It consists of a series of stacked polygons at each site representing the flood extent for specific AEP's. The map is focussed primarily (but not entirely) on flooding at seasonally inundated wetlands known as



turloughs. Sites were chosen for inclusion in the predictive map based on existing turlough databases as well as manual interpretation of SAR imagery.

The mapping process tied together the observed and SAR-derived hydrograph data, hydrological modelling, stochastic weather generation and extreme value analysis to generate predictive groundwater flood maps for 440 qualifying sites. In addition, the results of the TCD research project (Section 10) were incorporated into the map at 15 sites in the Gort Lowlands. It should be noted that not all turloughs are included in the predictive map as some sites could not be successfully monitored with SAR and/or modelled.



6 Preparation of National DTM

Digital terrain models (DTM) have a key role when constraining flooded areas from SAR images, facilitating the characterization of hydrological parameters nationwide without the need of direct measurements in the field. DTMs allow for direct relation between hydrological parameters such as stage, area, and volume. Sub-products of the DTM, including topographic basin mask (based on results from Tarboton et al. (1991)), topographic hill mask, and height above nearest drainage (HAND) (Rennó et al., 2008, Nobre et al., 2011) were also considered to reduce false positive floods from SAR images by defining regions that may or cannot be flooded. For all of these reasons, a substantial effort focused on creating a nationwide DTM for the Republic of Ireland with the best available data, incorporating several datasets from different sources.

NEXTMap® for the Republic of Ireland commissioned by OPW to INTERMAP technologies, LiDAR, and GPS (topography and bathymetry) datasets, were combined to achieve the best possible DTM, with particular focus on regions previously affected by groundwater flooding. All datasets were resampled to the horizontal resolution of the NEXTMap map which already covers the whole Republic of Ireland, having a final DTM map with 5 x 5 m horizontal resolution. The vertical resolution changes depending on the considered datasets. Vertical resolution of the NEXTMap is 70 cm, while for regions with LiDAR and GPS points the vertical resolution improved up to 10 cm.

6.1 List of data sources and datasets

The DTM datasets were provided by several institutions including the OPW, Transport Infrastructure Ireland (TII), Ordnance Survey Ireland (OSI), and TCD (Table 3). In addition, LiDAR datasets were commissioned specifically by GSI for karst feature mapping and flown in conjunction with acquisition by Coilte. Figure 11 shows the NEXTmap and LiDAR datasets considered in this study, where colours represent the source of the data.



Table 3: Number of datasets considered in this study and institution that provided them. Numbers within parentheses shows the horizontal resolution of the original LiDAR and IfSAR datasets.

	OPW	GSI	TII	OSI	TCD
Nextmap (IfSAR) - all Ireland	1 (5 x 5 m)				
LiDAR - regional	165 (2 x 2 m)	21 (1 x 1 m)	1 (1 x 1 m)	3 (2 x 2 m)	
GPS topography - local					21,066 points
GPS bathymetry - local	167,195 points				

6.1.1 NEXTMap (IfSAR)

NEXTMap® is an Interferometric SAR (ifSAR) derived DTM of the Republic of Ireland provided by INTERMAP technologies. The map is a highly reliable countrywide DTM with all cultural features digitally removed, along with an orthorectified radar image that accentuates topographic features all with a vertical accuracy (root mean square error) of 70 cm, and a lateral resolution of 5 x 5 m. NEXTMap was commissioned by the OPW, the lead agency for flood risk management in Ireland, in support of the EU Floods Directive. For simplicity, the NEXTMAP DTM product will hereafter be named 'IfSAR'.

6.1.2 LiDAR

Light detection and ranging (LiDAR) is a remote sensing method that uses light in the form of a pulsed laser to measure ranges (variable distances) to the Earth. These light pulses generate precise three-dimensional information about the shape of the Earth and its surface characteristics. As LiDAR data can go through vegetation it provides a more accurate DTM map than other methods based on visual light. Vertical accuracy is typically between 10 and 20 cm, and lateral resolution between 1 and 2 m. In total, 190 LiDAR datasets were considered for Ireland provided by OPW, GSI, TII, and OSI.



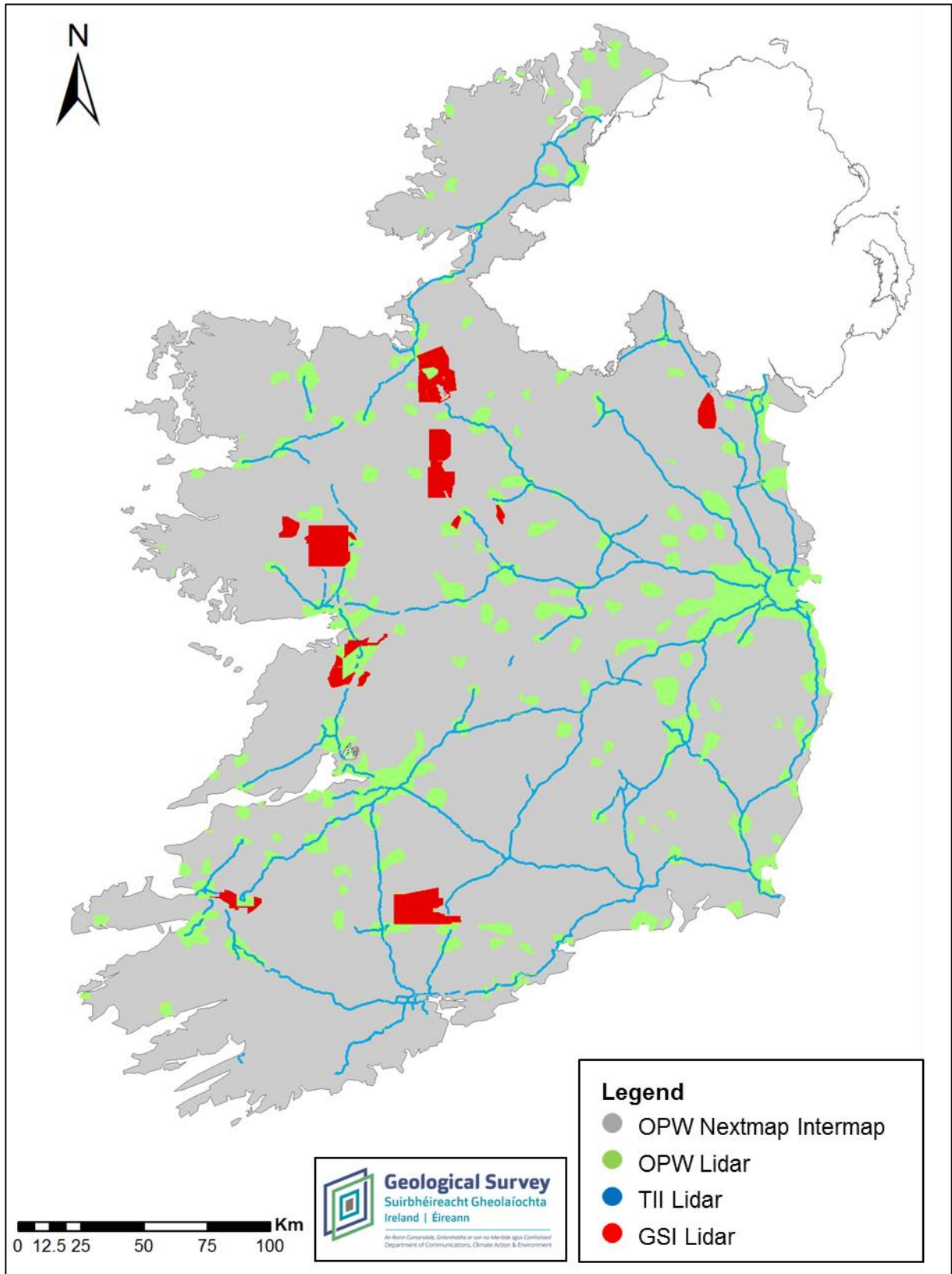


Figure 11: ifSAR (NEXTMap) and LiDAR datasets considered for generating the final DTM.

6.1.3 GPS (topography and bathymetry)

GPS measurements were acquired at selected karst features during dry season, when the water level was lower, to better constrain the shape of the studied karst features (Naughton et al., 2012). Bathymetry data were also acquired near Gort (Coole Lough, Newtown, Hawkhill, Caherglassaun turloughs) by OPW to constrain the shape of karst features that rarely empty.

6.2 Procedure for merging DTM datasets

LiDAR and GPS datasets were considered to improve the vertical resolution of IfSAR when data were available (Figure 11). The process involved three major steps: 1) Addition of LiDAR datasets, 2) addition of GPS datasets, and 3) correction of water levels, using data from IfSAR if the water level of a karst feature was lower when IfSAR data were acquired than when LiDAR data were acquired. The addition of LiDAR and GPS datasets was automatized with Python algorithms developed at GSI. Water level corrections were performed manually at particular karst features with GIS. Below there is a more detailed description of the steps performed for improving the IfSAR, and Figure 12 shows an example of the improvements associated with these steps.



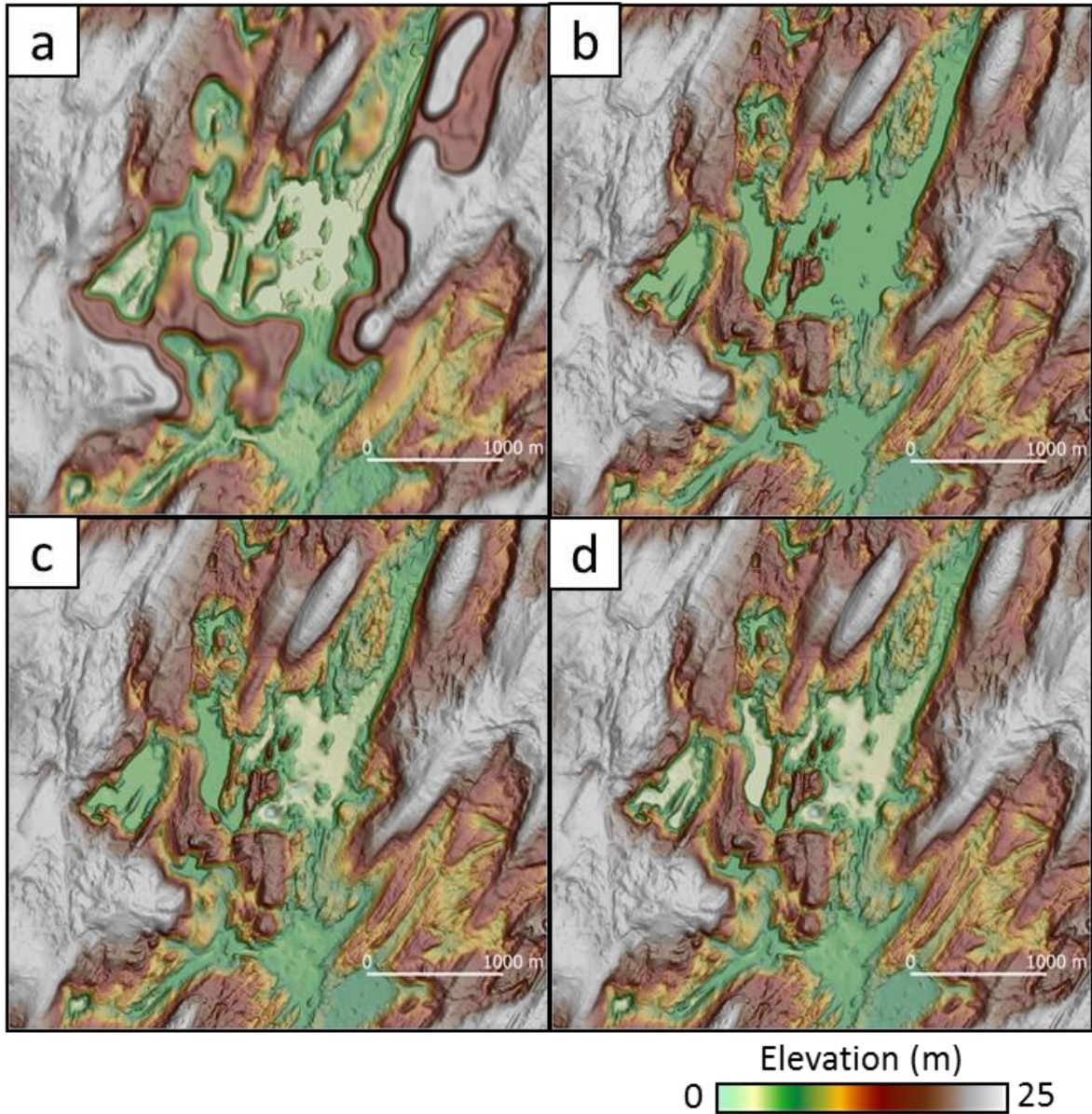


Figure 12: Outputs of the main steps followed to improve the original IfSAR for a particular region close to Gort, Co. Galway: (a) Original IfSAR, (b) addition of LiDAR data, (c) addition of GPS data and (d) correction of water levels.

6.2.1 Addition of LiDAR data

Each LiDAR dataset was considered following the approach described below. Figure 13 shows an example on how LiDAR data were added to IfSAR. The main steps for the addition of LiDAR datasets included:

1. Rescale LiDAR to IfSAR horizontal resolution (5 x 5 m).
2. Select IfSAR data points within the region covered by the LiDAR dataset and surroundings.

3. Discard IfSAR data in the region covered by LiDAR.
4. Define 20 m buffer surrounding LiDAR data. Data points from IfSAR within this region were also discarded. This was performed to smooth the transition between IfSAR and LiDAR.
5. Compute new IfSAR values using LiDAR rescaled points (from step 1) and IfSAR points surrounding LiDAR performing linear interpolation. This step was considered as rescaled LiDAR and IfSAR data points, although having the same horizontal resolution, of 5 x 5 m, may not be centred at the same points.
6. Replace the original IfSAR values with computed values from the interpolation process (step 5).
7. Define a shapefile specifying the source of information used to modify each part of the IfSAR differentiating between IfSAR, LiDAR, and interpolation areas. When more than one LiDAR covered the same region the LiDAR with highest resolution was considered.

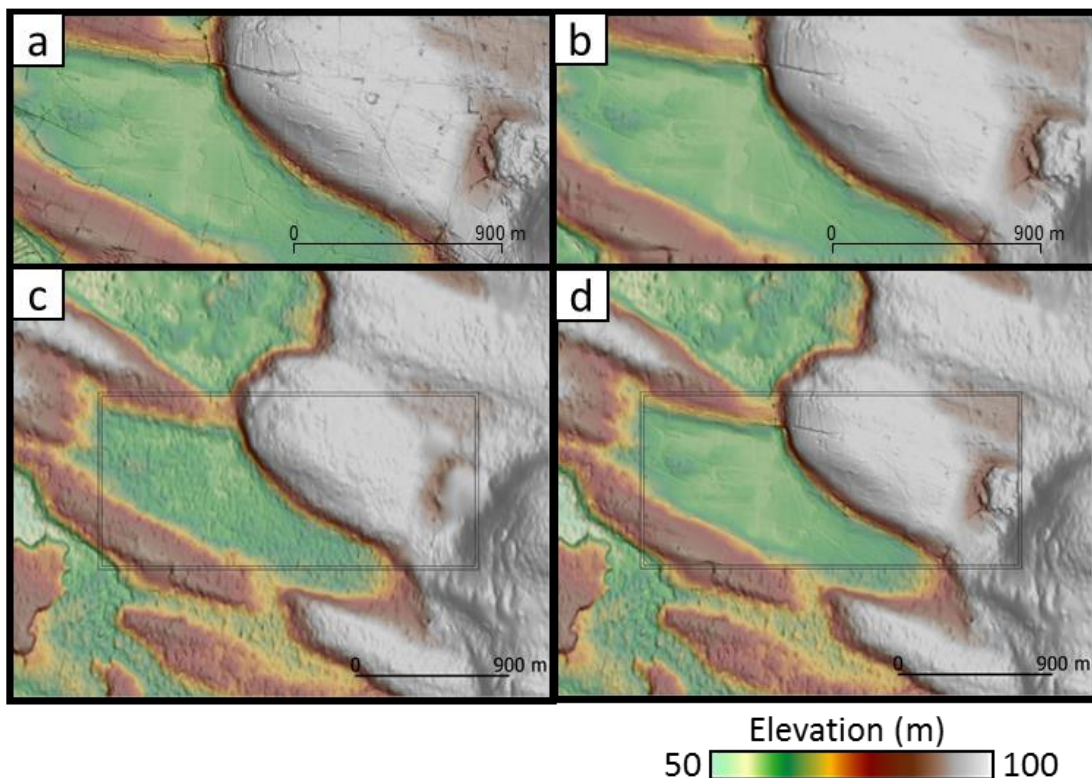


Figure 13: (a) OPW LiDAR data at Four Roads, Co. Roscommon (2 x 2 m resolution), (b) Rescaled LiDAR data at Four Roads, (5 x 5m resolution), (c) Original IfSAR with black outlines showing area covered by LiDAR and area used to smooth transition between LiDAR and IfSAR and (d) Updated IfSAR with LiDAR data. This process was performed for each LiDAR dataset presented in Figure 11.

6.2.2 Addition of GPS data

GPS datasets, including topography and bathymetry, were used to improve the IfSAR-LiDAR merged DTM in karst features that were covered by water when either LiDAR or IfSAR data were collected. Figure 14 shows two examples where the DTM of a karst feature was improved using GPS data.

The main steps followed for the addition of GPS data included:

1. Defining flat areas, associated with the presence of water, from the DTM that were covered by GPS data. This was performed by sliding a window of 3 x 3 cells along the DTM and computing the maximum difference between highest and lower levels. Regions with maximum difference smaller than 5 cm were considered as flat. An additional line of 1 cell was added to the selected areas to account for edges effects.
2. Comparing the elevation values from GPS and the DTM at the vicinity of the flat areas, and define the shift between the two datasets.
3. Correcting the GPS data for shift between the GPS and DTM datasets. The performed corrections were less than 20 cm for most of the karst features.
4. Replacing the DTM values with the GPS data for cells selected in step 2. If more than one GPS point was available within a DTM cell, the average of all GPS points within that cell was considered.
5. Recalculating the elevation at all cells covered by water that did not contain GPS data. This was performed with linear interpolation considering cells in the vicinity of the area covered by water, and cells which values were replaced using GPS points at step 5.



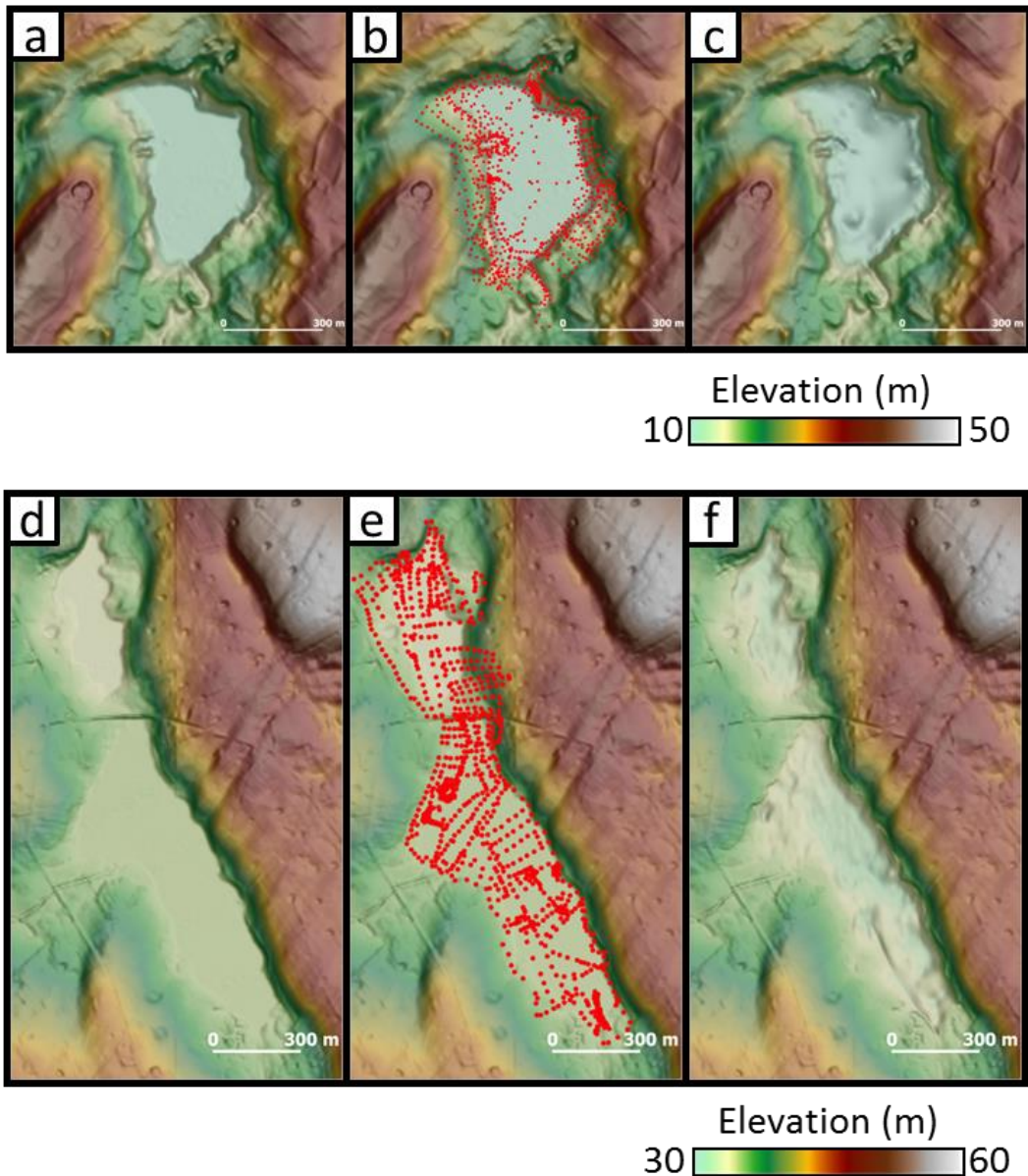


Figure 14: Procedure of merging DTM datasets exemplified by (a) to (c) Lough Coy, Co. Galway and (d) to (f) Kilgassaun, Co. Mayo. (a) and (d) Example of DTM after adding LiDAR information, (b) and (e) location of GPS points (red), and (c) and (f) resulting map after adding GPS information.

6.3 DTM products

Three major sub-products were generated from the final DTM that contributed to the mapping of groundwater floods in the Republic of Ireland: 1) topographic basin mask, based on results from Tarboton et al. (1991), 2) topographic hill mask, equivalent to topographic basin mask but for selecting hills, and 3) height above nearest drainage (HAND) (Rennó et al., 2008, Nobre et al., 2011).

The topographic basin mask map is the result of filling all depressions of the DTM to the spilling point, and subtracting the filled DTM to the original DTM. By subtracting the original DTM from the resulting filled DTM, a new difference grid elevation dataset was produced representative of depression location and depths (e.g. Anders et al. (2011), Siart et al. (2009), Antonić et al. (2001)). The topographic basin mask was used as a filter to rule out false floods and to determine if a flood has spilled outside its basin. Because of changes in elevation within drainage paths caused by the integration of different datasets the topographic basin mask was computed using a smoothed DTM. Using vector data of known drainage paths, the cells corresponding to a drainage path were smoothed by averaging the elevation of each cell with the elevation of the surrounding cells. Equivalent steps were considered for the topographic hill mask.

The HAND model is the result of topographically normalizing the DTM for the drainage network. It represents the topographic difference between a pixel and the hydrologically determined nearest water course. Although HAND grid loses the height reference to sea level it enhances meaningful local relative variations in height, which have hydrological significance and can potentially reveal previously hidden local environments. HAND was used as a filter for ruling out false floods (e.g. from radar shadow on mountain slopes). Any flood with a very high HAND value was unlikely to be real except if it was within a basin.

In order to reduce computational efforts, the DTM was split using a 4 x 4 m grid with overlapping cells (Figure 15). Each of the three sub-products were calculated for each individual cell. The overlaps between cells of the grid secured that any groundwater flood was fully represented in at least one of the maps, which is necessary when generating the topographic basin and hill masks, as basins or hills may not be selected if they are not fully represented within the map. The grids of the generated DTMs and sub-products were aligned to the same grid as the SAR images for consistency between the raster datasets.



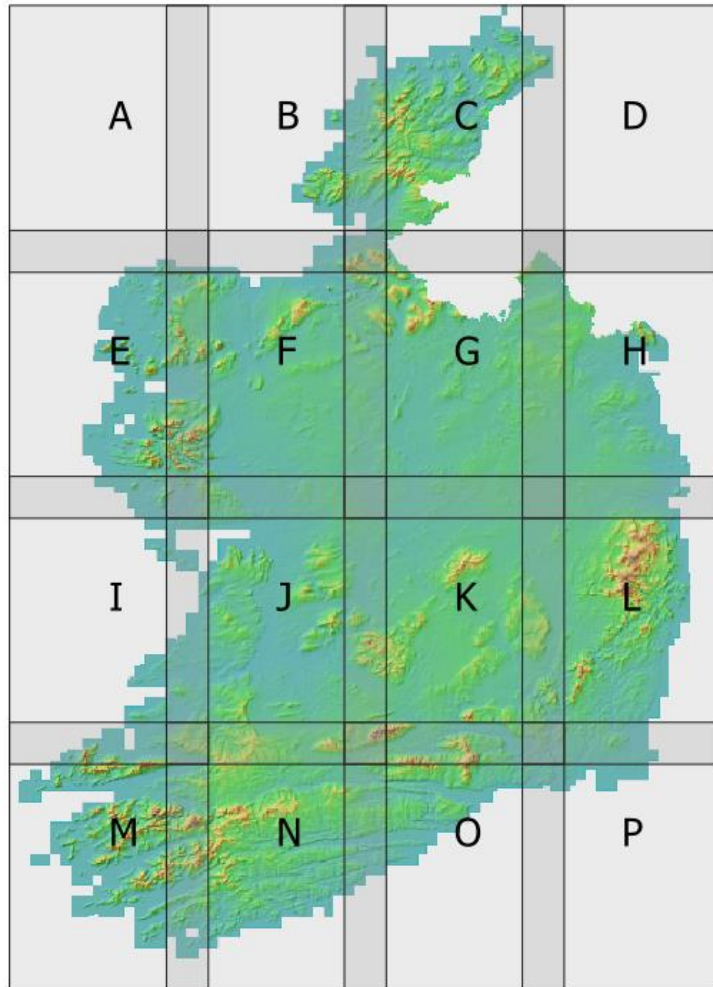


Figure 15: Grid system used to split the DTM and its derivative products. Areas with overlap between cells are represented with darker colour.

7 Flood Mapping Using Sentinel-1 SAR

7.1 Synthetic Aperture Radar

While traditional monitoring is an effective tool at priority sites, the distributed nature of groundwater flooding in karst lowlands hampers any systematic monitoring efforts. Floods tend to occur in isolated basins across the landscape and so would require an impractical amount of field monitoring to provide a complete picture. Earth Observation and Geographical Information System (GIS) approaches offer significant advantages in this respect. Passive satellite imagery, such as the USGS Landsat or ESA Copernicus Sentinel-2 programmes, can be used to image and delineate floods at a catchment scale (Figure 16). In the case of Landsat, a long historical archive of images also allows the observation of past flood conditions and provides some data with which to validate hydrological models. However, an obvious limitation of satellite systems which require a clear view of the earth's surface is the issue of cloud cover. When cloud cover is extensive, as is often the case in Ireland during winter floods, no useful data can be collected. Under these conditions active systems, such as SAR, are extremely useful as they are not impacted by cloud cover (or time of day). In this context, the GWFlood project chose to use SAR imagery from the Copernicus Programme Sentinel-1 satellite constellation as its primary flood mapping tool.

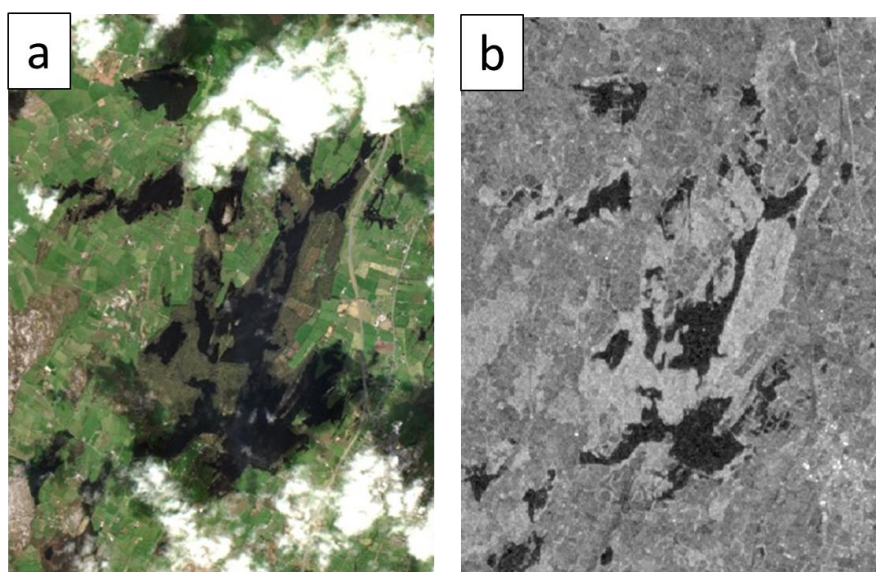


Figure 16: Comparison of (a) Sentinel-2 and (b) Sentinel-1 imagery of flooding near Gort, Co. Galway, March 2020.

The Sentinel-1 mission offers reliable high spatial resolution SAR imagery that is freely available. The mission consists of two satellites: Sentinel-1A and Sentinel-1B, launched in April 2014 and April 2016 respectively. The satellites operate in opposite polar sun-synchronous orbits with a repeat cycle of 12 days. They are dual polarisation C-band SAR systems, capable of transmitting a signal in either horizontal (H) or vertical (V) polarisation, and then receiving both H and V signals simultaneously (i.e. HH+HV or VH+VV). The satellites operate with four acquisition modes: Stripmap (SM), Interferometric Wide swath (IW), Extra-Wide swath (EW), and Wave (WV). These different modes enable the resolution and swath width to be adjusted depending on the setting or purpose (e.g. small-scale high resolution imagery is suitable for small islands or emergency mapping, but not for covering large landmasses). Over Ireland, and landmasses in general, the default acquisition mode is IW. This acquisition mode collects data in 250 km wide swaths at incidence angles of between 29.1° and 46.0°, and provides imagery of 20 m ground resolution (European Space Agency, 2020b).

A significant benefit of SAR for groundwater flood mapping is the frequency of image capture; the ESA Sentinel-1 satellites achieve a global coverage cycle every six days. Within this six-day period, imagery of Ireland is acquired from seven different orbits with large overlapping swaths (Figure 17). As such, a new image of any location in Ireland is typically available at least every 1-3 days. While this revisit time may be inadequate for observing flash floods, which can appear and dissipate within hours, it is suitable for monitoring groundwater flooding which occurs at a much slower rate. Groundwater floods typically appear and recede over a timescale of weeks to months. Thus, the considerable catalogue of Sentinel-1 imagery available allows the tracking of groundwater flood development through time, increasing our understanding of this complex flood form at scale which would otherwise not have been possible by conventional means.



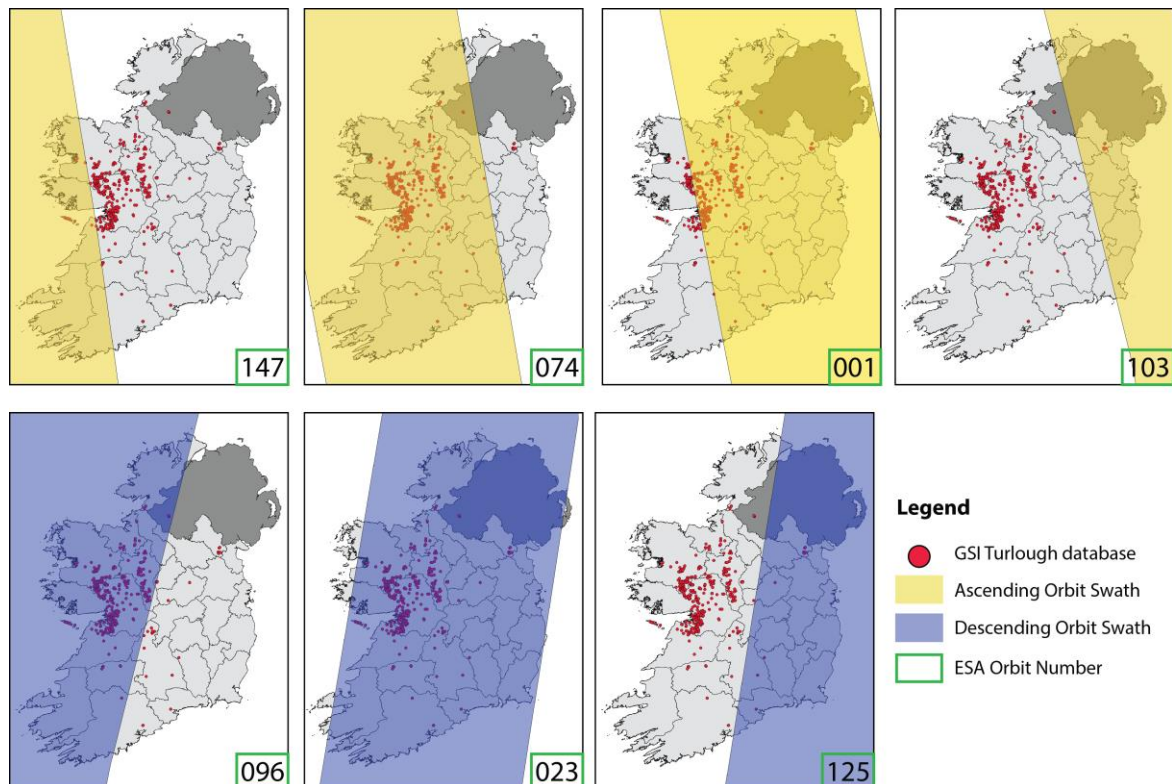


Figure 17: Sentinel-1 orbit coverage over Ireland.

7.1 Water Delineation using SAR

SAR systems emit radar pulses and record the return signal at the satellite. Flat surfaces such as water operate as specular reflectors for the radar pulses resulting in minimal backscatter signal returning to the satellite. Based on this backscatter signal, SAR imagery can be classified into flooded (i.e. flat) and non-flooded pixels (see Figure 18). Numerous studies have demonstrated the efficacy of delineating water bodies using SAR remotely-sensed data (Matgen et al., 2011, Chini et al., 2017, Martinis et al., 2015, O’Hara et al., 2019). Similar image processing techniques were trialled and developed under the GWFlood project to optimise and automate the detection of groundwater flood extents from SAR data.

While water can be detected using any polarisation of SAR imagery (VV, VH, HV, and HH), the backscatter characteristics vary, and some are more suitable than others depending on the scenario. Co-polarised data (VV and HH) is known to be more efficient at classifying water than cross-polarised data (VH and HV), which produces a greater range of

backscatter signals from vegetated land surfaces. This can potentially lead to misclassifications as land with low backscatter, such as sports pitches or golf courses, may be indistinguishable from water (Clement et al., 2017). HH is understood to have the greatest potential for delineating flooding (Brisco et al., 2008, Manjusree et al., 2012) however the default Sentinel-1 acquisition mode over Ireland (IW) only collects images in VH and VV polarisations. Thus, similar to the findings of other studies (Twele et al., 2016), the apparent optimum polarisation is VV. It should be noted, however, that VV is more susceptible to error than VH when there is surface roughening of water caused by wind or rain causing high backscatter. With these considerations in mind, the GWFlood mapping process utilised both VV and VH polarisations for flood delineation.

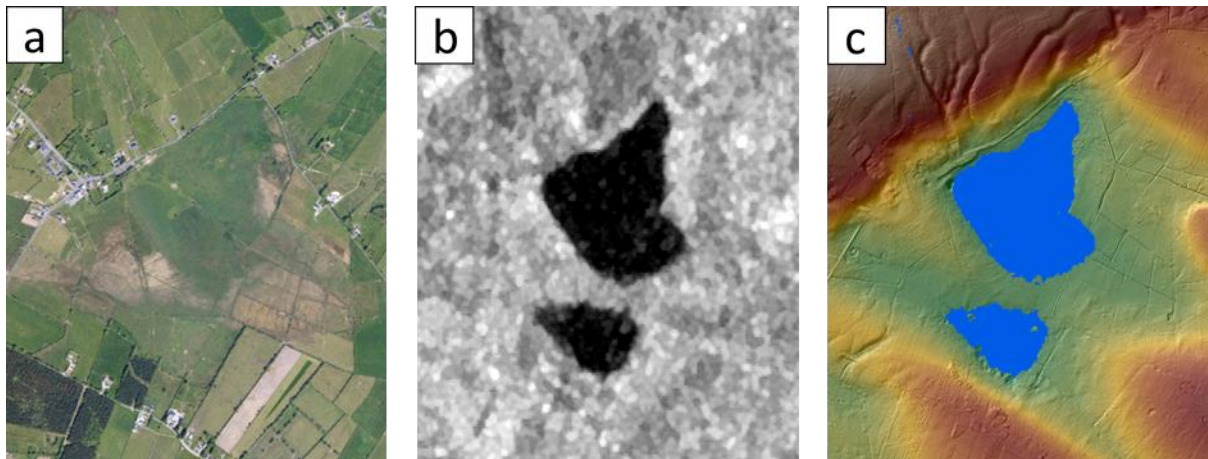


Figure 18: Imagery of Castleplunket turlough Co. Roscommon showing: (a) orthophotography of it empty, (b) pre-processed SAR imagery of it flooded (March 2017) and (c) a SAR based water classification overlaid on LiDAR data.

The GWFlood SAR water classification process was carried out as an automated processing chain using open source Python programming language. It consisted of a sequence of primary processing steps required for both the historic and predictive flood map products as well as a series of subsequent product-specific processing steps. The primary steps and product-specific steps are outlined in Sections 7.1.1 and 7.1.2 respectively. Additionally, the parallel development of a vegetation mask, which was crucial for eliminating false negatives in both historic and predictive maps, is discussed in Section 7.1.3.

7.1.1 Primary Processing

The primary processing steps include data acquisition, pre-processing and water classification and are described in the following sub-sections and illustrated as a workflow in Figure 19. The intermediate products of each of these processing steps are referred to as ‘Stage (X) products’.

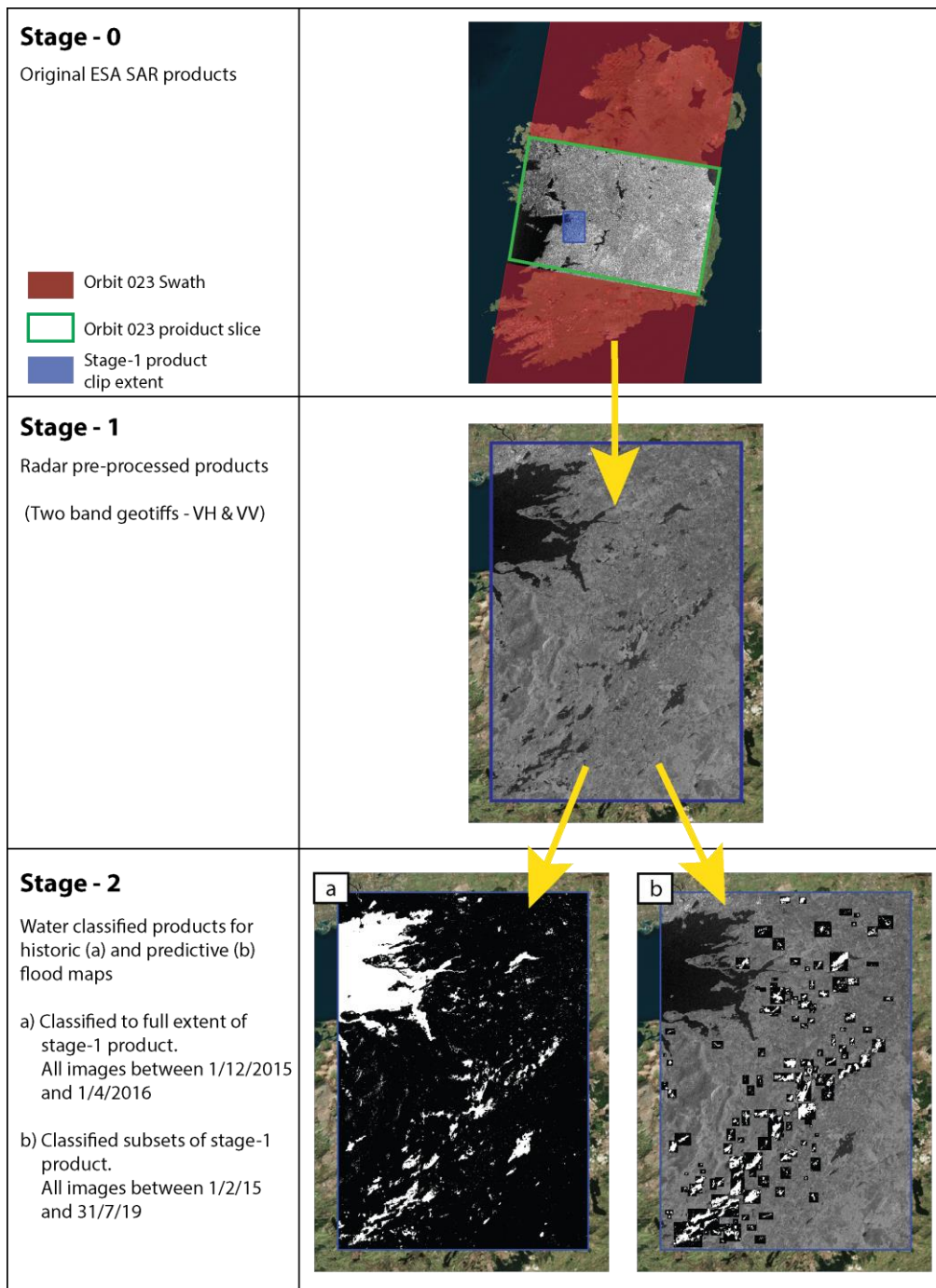


Figure 19: Workflow for producing water classified SAR products. It should be noted that for simplicity a single stage-1 product is shown for both stage-2 products. In actuality, the stage-1 products for the historic and predictive maps were produced on different grids (see Figure 20).

7.1.1.1 Data Acquisition (Stage-0 product)

Level-1 IW Ground Range Detected (GRD) data products were downloaded in batch via an Application Programming Interface (API) from ESA Copernicus Open Access Hub. These products consist of focused SAR data that has been detected, multi-looked and projected to ground range using the Earth ellipsoid model WGS84 (European Space Agency, 2020a). All images fully or partially covering Ireland from the 7 suitable orbit paths (Figure 17) between February 2015 and August 2019 were downloaded and stored. Although being labelled as Level-1 products in ESA terminology, these products are labelled as 'Stage 0' in the GWFlood processing chain due to being unaltered ESA data.

7.1.1.2 Radar Pre-processing (Stage-1 product)

Stage 0 products (or ESA Level-1 products) require a series of standard SAR pre-processing steps before they can be utilised for further analysis or classification (as Stage 1 products). These processing steps were carried out using a Python extension of the ESA Sentinel application platform (SNAP) software. The processing steps included:

- Slice assembly
- Application of orbit file
- Thermal noise removal
- Border noise removal
- Calibration
- Speckle filtering
- Terrain correction
- Conversion to logarithmic scale (dB)

The most influential of these processing steps is speckle filtering. Speckle is a system phenomenon in SAR imagery caused by the variation in the radar return within a pixel due to multiple scattering sources (Lee et al., 1994). It causes the characteristic grainy texture of radar images, reducing their readability. To remedy this, a speckle filter is applied to smoothen the image and enhance its processing capabilities. As part of the groundwater flood mapping process, all available speckle filters were tested. As a result, the Refined-Lee and Lee-Sigma filters were found to be of most value. Lee Sigma was found to reduce



noise in water bodies, yet it also tended to reduce precision at the flood boundaries causing under-prediction. Refined-Lee on the other hand increased noise (i.e. false negatives) within a waterbody but it retained precision at the flood boundary. As such, two separate SAR products were generated for each original image based on each speckle filter. For more information on speckle filtering, and the other SAR processing steps, see Filipponi (2019).

Stage 1 products were produced as geographical subsets of the Stage 0 SAR images. The images were cropped to one of two grids: 1) a full coverage Ireland and Northern Ireland grid for the historic map (Figure 20a) or 2), a groundwater flood targeted grid for the predictive map (Figure 20b). It should be noted that the historic grid was extended to Northern Ireland to allow for basic image processing, but flood map products were not generated due to a lack of necessary datasets (DTMs, drainage system maps, etc.). The resulting grids were optimised based on balancing three chief factors:

1. Memory and computation time

Images were cropped to their minimum necessary size to reduce memory requirements and computation time. This is particularly relevant for the predictive map which did not require national coverage

2. Presence of permanent water

For a water classification to be successful, each image requires sufficient water to be present so that a water signature can be isolated (see Section 7.1.1.3). As Stage 2 images are being created for dry periods as well as flood events, each image must contain a sufficient number of permanent water bodies.

3. Incidence angle

The incidence angle is the angle between the incident SAR beam and the axis perpendicular to the local geodetic ground surface. Over a full Sentinel-1 IW swath, the incidence angle changes from 29.1° at the near-satellite swath edge to 46.0° at the far swath edge. This is noteworthy as incidence angle is understood to have an impact on backscatter signal (Manavalan, 2018), and as such, the processing of



images covering large portions of the swath will result in inconsistent backscatter signatures across the image. To account for this, Stage 1 images are cropped to smaller sizes so that the incidence angle range is small.

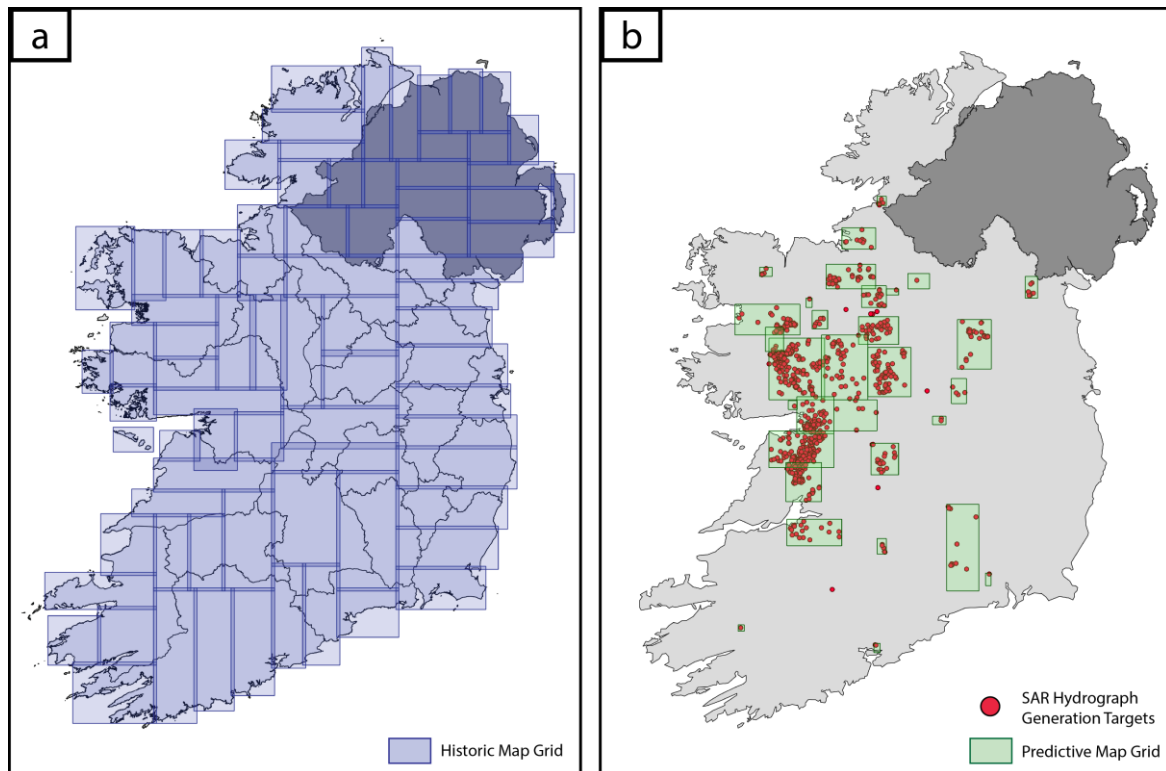


Figure 20: SAR Stage-2 image grids: (a) historic and (b) predictive.

7.1.1.3 Water Classification (Stage-2 Product)

Several methodologies exist to delineate water from SAR imagery. These include visual interpretation (Brivio et al., 2002), histogram thresholding (Matgen et al., 2011), supervised classification (Pulvirenti et al., 2011), change detection (Rémi and Hervé, 2007) and various image texture algorithms (Schumann et al., 2010). A number of these methods were trialled in order to determine the most appropriate for the groundwater flood map. Ultimately histogram thresholding was chosen as it enabled an automated and repeatable process with minimal user interaction. The process involves the generation of a histogram of backscatter intensity values for a SAR image. If the SAR image consists of both wet (i.e. low backscatter) and dry (i.e. high backscatter) pixels, the histogram should exhibit a bimodal distribution, with the peaks representing wet and dry pixels (see Figure 21a). A threshold value between these peaks is then applied to separate the SAR image into a

binary 'wet' and 'dry' image. However, the determination of the threshold value is not trivial as the wet and dry peaks (or curves) overlap to a certain extent. To account for this complexity, the GWFlood mapping procedure used two threshold determination approaches:

Firstly, a wet and dry binary image was generated using the Otsu threshold method (Otsu, 1979). This approach calculates a threshold value by maximizing the variance between the wet and dry classes (see Figure 21a and Figure 21b). This threshold was applied to both the Lee-Sigma and Refined-Lee SAR products and their 'wet' pixels were combined to form a single binary thresholded product.

Secondly, a statistical approach to classification was also developed. Assuming two distinct classes exist in a SAR image (i.e. wet and dry), the uncertainty in classification is highest in the region of the histogram where both classes overlap (Chini et al., 2017). One approach to deal with the issue of overlap, and the unbalanced class populations in an image, is to adopt a statistical approach whereby a probability density function (pdf) is fitted to each class and used to quantify and estimate likelihood of class membership for each pixel (Bazi et al., 2007). The Gaussian pdf has found common use, based on evidence that the distribution of backscatter pixel values for a homogeneous surface in a log-ratio SAR image is Gaussian (Chini et al., 2017, Dekker, 1998, Ulaby et al.). Open water can be considered as a homogeneous surface with low backscatter values in SAR images, and so it can be assumed that the backscatter values of water follow a Gaussian distribution (Matgen et al., 2011). The approach developed involves fitting two Gaussian curves on the histogram pixel values; one curve for the wet peak and one curve for the dry peak. The threshold for distinguishing the two classes could then be chosen based on the relative probability of membership within each class (see Figure 21c). Furthermore, this approach then enables the reverse-calculation of the probability of each pixel being flooded based on the position of a pixel's value on the histogram relative to the wet and dry Gaussian curves (see Figure 21d for example).



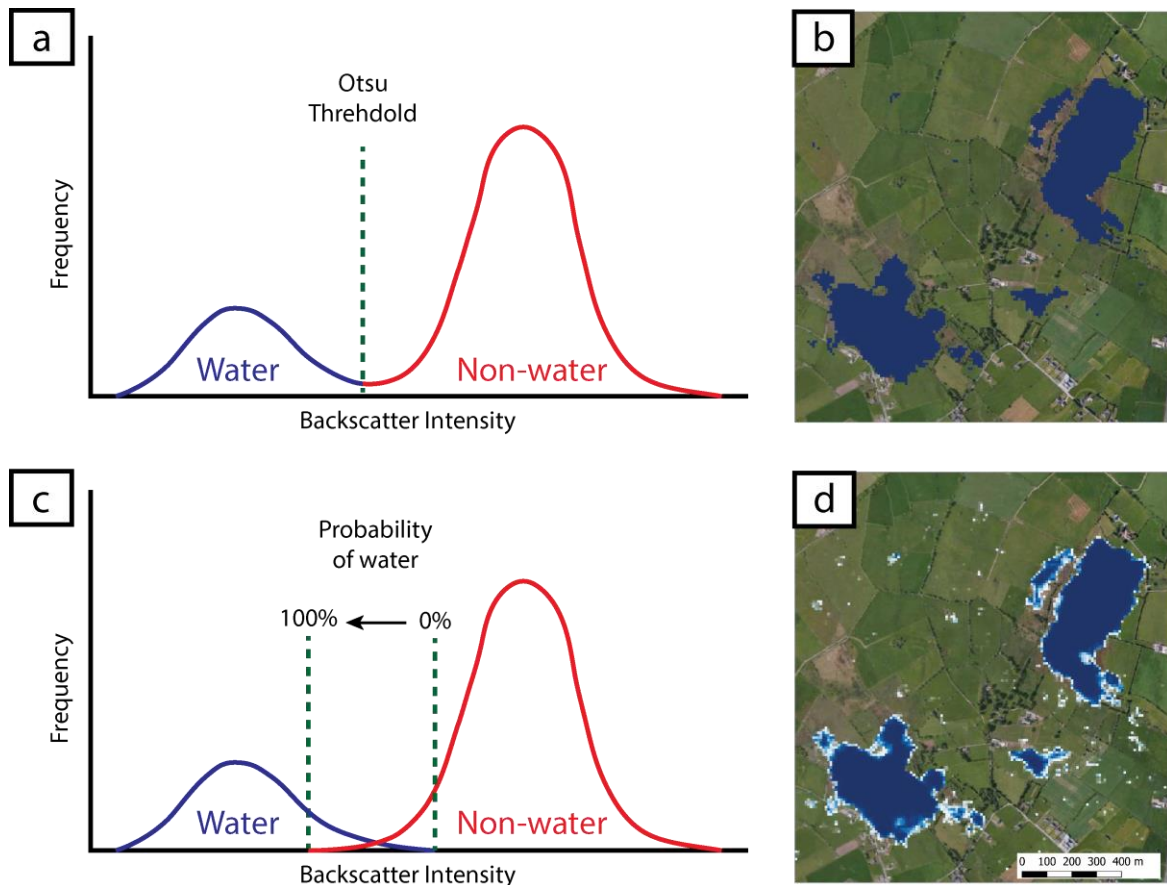


Figure 21: Thresholding Methodologies: (a) applying Otsu threshold to histogram, (b) Otsu thresholded SAR image, (c) applying probability threshold to histogram, showing the percentage likelihood of a pixel being water and (d) probability thresholded SAR image (pixel darkness represents probability of water).

While the histogram threshold process was sufficient to classify SAR imagery in the majority of cases, some regions with very few water-bodies would exhibit single peaked histograms, and thus a separation between wet and dry pixels cannot be established. In order to remedy this, the pixels used to create an image’s histogram were specifically chosen based on pre-determined subsets targeting water bodies (see Figure 22). These sample subsets allowed for greater control in generating a representative bimodal histogram while also minimising computation time. Furthermore, the sample subsets were separated into ephemeral and permanent water bodies to enable an automated test on each image for weather interference. If a permanent waterbody presented a non-bimodal histogram which falsely suggested it was dry, this indicated that the water surface was not flat (e.g. a windy or rainy day) and the image should not be relied upon for classification. Images where this occurred were flagged and not advanced for further processing. For

instances where the weather interference impacts one polarisation and not the other (VV is often affected while VH isn't), the unaffected polarisation image was retained.

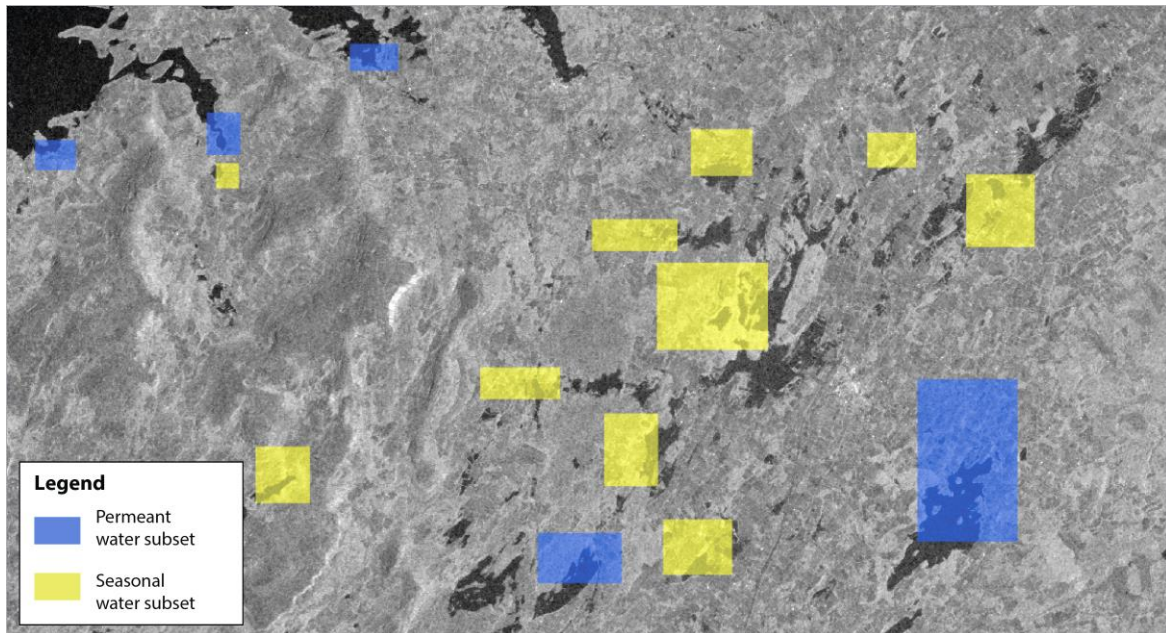


Figure 22: Sampling subsets for SAR histogram calculation.

Stage 2 products were generated as multiband geotiff rasters and each assigned a 9 digit unique label. The spatial extent of Stage 2 products depended on the map they were being produced for. For the historic map, the entire Stage 1 image was thresholded and produced as a Stage 2a product, whereas for the predictive map the Stage 2b products were limited to selected areas of interest for hydrograph generation (or 'target sites', see Figure 19). As the hydrograph generation requires the processing of significant quantities of SAR images, the target sites were optimised to be as small as possible (see Figure 23). This was aided by the fact that the target site images didn't necessarily need to cover the entire flood being observed. The target sites only needed to observe an area which demonstrated the full range of possible water levels. Moreover, some sites such as Lough Funshinagh in Co. Roscommon benefited from partial coverage as the target site could be delineated to ignore known areas of vegetation interference.

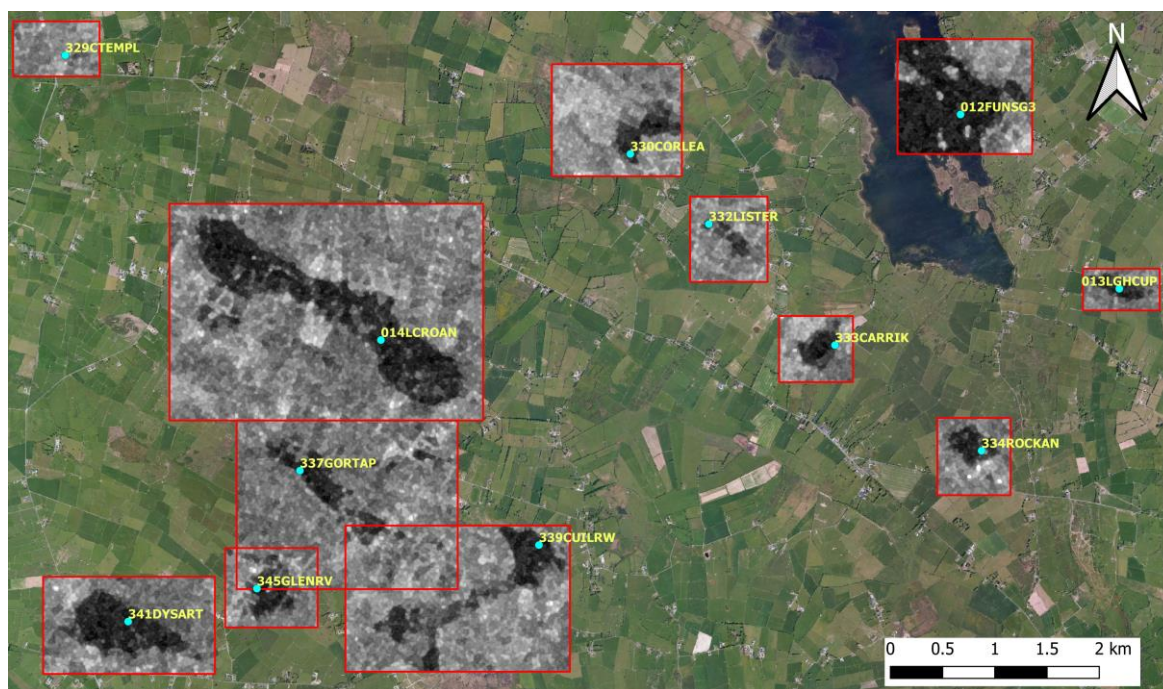


Figure 23: Coverage of Stage 2b products for the predictive map, south Co. Roscommon. Target site boxes shown in red and site reference points (see Section 8.2.1) shown as cyan dots.

7.1.2 Product Specific Processing Steps

While the historic map is created at a national-scale, the hydrograph generation process, which provides the data for the predictive map, is based on specific targeted sites. As such, the subsequent processing steps for the two products are different.

For the historic map, the additional processing steps were primarily focussed on eliminating noise, as well as distinguishing between groundwater flooding and surface water flooding. A series of SAR based filters and contextual filters (e.g. topography, land use, rivers etc.) were utilised to achieve this. In contrast, the hydrograph generation process was only run on areas already known to be susceptible to groundwater flooding, and as such, filtering for noise or non- groundwater flooding was less relevant than for the historic flood map. Instead, the additional processing steps for hydrograph generation were focussed on site specific measures to ensure precise water level calculation (for high and low levels). Further technical information on the product specific processing for the historic and predictive maps is provided in Sections 8 and 11 respectively.

7.1.3 Vegetation Mask

A fundamental limitation of the Sentinel-1 SAR flood mapping process is the inability to detect water through vegetation due to the geometric distortion from the vegetation producing increased backscatter. While this increased backscatter can be exploited by horizontally polarised (HH) SAR systems to map the flooded forests, Sentinel 1 only collects dual vertically polarised (VV&VH) datasets over the majority of Ireland which is not as efficient at flooded forest detection. As such, a vegetation anomaly mask was developed to flag pixels that were likely to be classified as dry, whether they were flooded or not. These pixels were discounted from the flood mapping process.

The Vegetation anomaly mask was developed by exploiting the distinctive polarisation signature (volume scattering) caused by vegetation. It was produced following the procedure of Dostálová et al. (2016) and consisted of the following steps:

1. A 'dry reference' SAR image was generated by aggregating a series of multi-temporal SAR imagery during dry periods at specific locations and calculating the mean value at each pixel. It should be noted that speckle filtering was not applied to each individual dry image as multi temporal averaging is in itself a suitable form of speckle filtering.
2. Dry reference images were generated for both VH and VV bands and a RGB composite image was created using VH as red, VV as blue and the difference between them (VV-VH) as green (see Figure 24a). Forested areas are highlighted in the composite images (appearing as yellow) due to the relatively high backscatter intensities in both polarizations and relatively low difference between them when compared to the surrounding cropland. Other distinct land types include water (appearing as dark blue), bare rock (appearing as near-white) and shallow vegetated water (also appearing as near-white).
3. Exploiting these distinctive patterns in the RGB composite, the image was segmented using random forest semi-automatic classification into four groups: forest, open-land, water, and a mix of shallow vegetated water and bare-rock (see Figure 24b).



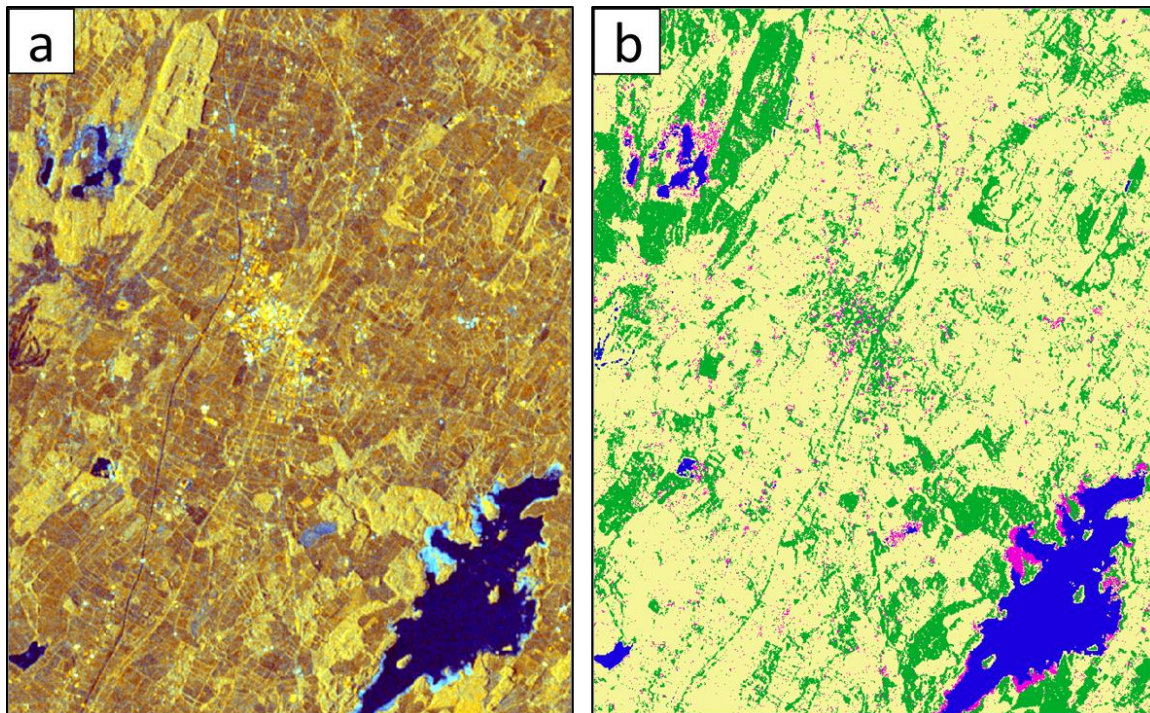


Figure 24: (a) SAR 'Reference' image and (b) classified image showing water (blue), bare rock and shallow water with vegetation (pink), vegetation (green) and open land (yellow).

This process was repeated for each of the 16 raster grids (Figure 15) to produce a national vegetation anomaly mask (as well as by-product water and 'bare-rock' masks). It should be noted that while the vegetation anomaly mask provides a good approximation of vegetated pixels, it is not limited to solely vegetation. Other land use features such as buildings or railways produce similar backscatter signals to vegetation and are thus included in the mask. However, this misclassification is not relevant for this assessment as the purpose of the mask is not necessarily to identify vegetation; it is to identify pixels that cannot be reliably classified as flooded or non-flooded due to permanent high backscatter signal.

8 Hydrograph Generation using SAR

While traditional monitoring is an effective tool for hydrometric data collection at priority sites, the distributed nature of groundwater flooding in karst lowlands hampers any systematic mapping efforts. In this context, the previously described SAR mapping methodology was adapted in order to reconstruct hydrometric data from as many suitable locations as possible. This methodology enabled, for the first time, the collection of concurrent hydrometric data at over 300 turloughs in Ireland. This new data were fundamental to the development and calibration of the hydrological models required for the predictive flood map.

8.1 Site Selection

An initial list comprising 514 turlough sites was compiled from GSI and NPWS turlough databases. Of these sites, 337 were deemed appropriate for SAR analysis as their flooding was consistently large enough to be classified from SAR imagery, and there were enough pixels not covered by forestry to accurately quantify the depth of the floods. The remaining 177 sites were discarded. It should be noted that sites unsuitable for SAR hydrograph generation but with detectable flooding in winter 2015/2016 were included in the historic groundwater flood map.

The process of determining a site's feasibility for SAR hydrograph generation was aided by time-lapse visualisations of SAR imagery. While the purpose of these videos was to assess the feasibility of known turloughs for SAR analysis, a further benefit was the identification of an additional 149 sites which demonstrated seasonal groundwater flooding behaviour (37 of which are listed in the GSI karst database as non-turlough features). These sites were added to the hydrograph generation inventory. A further 75 permanent water bodies (lakes, rivers or fens) were also included as they were deemed to have a seasonal groundwater flood component (e.g. the upper Fergus River). In total, 561 sites were used for hydrograph generation. The locations of these sites are shown in Figure 25.



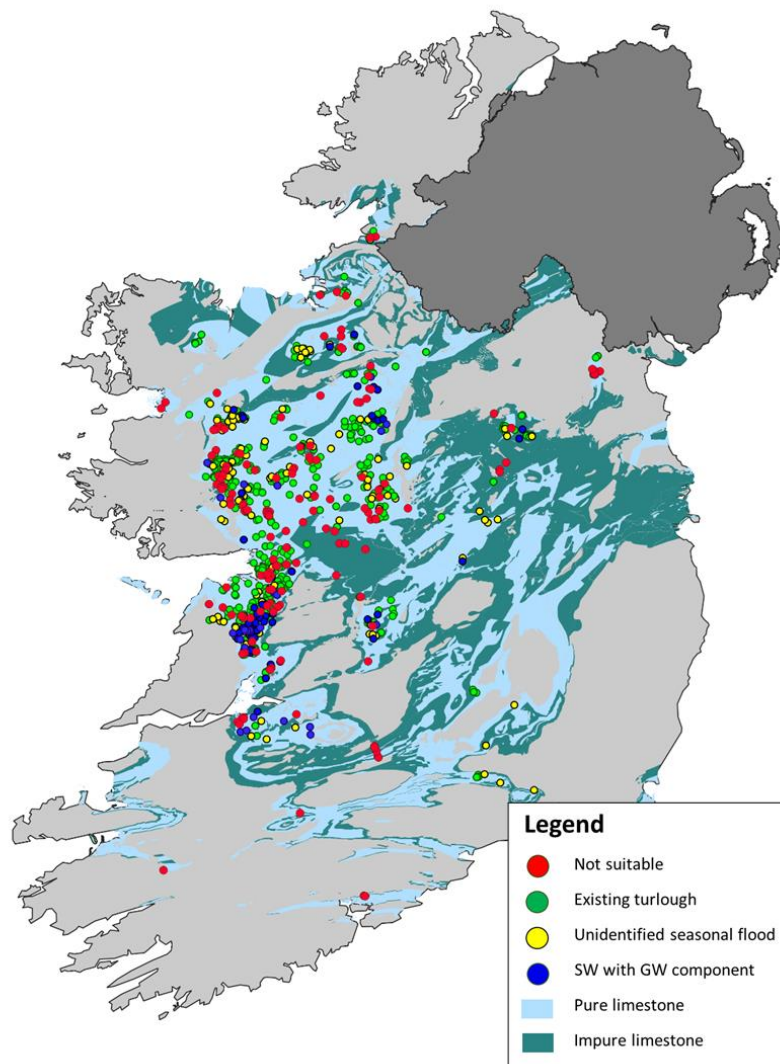


Figure 25: Locations and status of groundwater flood sites used for hydrograph generation (SW: Surface water, GW: Groundwater).

It should be noted that the additional 149 seasonal flood sites are not necessarily turloughs, they just operate in a hydrologically similar manner to turloughs (and can thus be modelled as such). Turloughs are defined as depressions in karst areas, seasonally inundated mostly by groundwater and supporting vegetation and/or soils characteristic of wetlands (Working Group on Groundwater, 2004). Accordingly, the classification of a site as a turlough depends on both its hydraulic regime as well as its ecological characteristics. Assessing the ecological characteristics of groundwater flood sites was beyond to scope of the GWflood project, and as such, sites which demonstrated seasonal groundwater flood behaviour were not classified into turlough or non-turloughs.

8.2 Hydrograph Generation Methodology

The hydrograph generation process was built as an extension of the flood mapping methodology described in Section 7. The process is based on calculating the area of flooding in every available SAR image at selected sites (or ‘target sites’) over specified dates and converting the area values to stage values. The main steps for hydrograph generation are described below.

8.2.1 Assign hydrograph reference point

The hydrograph reference point is the location within the waterbody that the hydrograph is referenced to (see Figure 23 for examples). The elevation of the DTM at this point is the zero depth datum for the hydrograph. The location chosen for this point is relevant as many turloughs split into multiple basins at low levels, and the flood level in each basin may not necessarily be the same. Thus, the reference point enabled the user to control which basin the hydrograph referred to. Typically, the reference point was located at the deepest point of a turlough basin (unless the deepest point was within the vegetation mask).

8.2.2 Calculate Flood Area

For each Stage-2 product (Section 7.1.1.2), the thresholded VH and VV bands were combined into a single thresholded image (a pixel would be designated as water if it was classified as water in either the VH or VV bands). The flooded area associated with the specified reference point was then isolated and its area calculated. However, before the area calculation was made a number of additional filtering steps were applied to the SAR image to exclude suboptimal pixels and enhance precision. The filters were devised through an iterative calibration process (see Section 8.3) and are described in the subsections below. It should be noted that not every filter was required at every site.

8.2.2.1 Vegetation Mask

The vegetation mask (Section 7.1.3) was applied to remove pixels within or adjacent to vegetated areas (see Figure 26b).



8.2.2.2 Adaptive Basin Mask

An adaptive basin mask was used to crop the image being assessed to just the immediate area surrounding the flood. Any flooding occurring in separate sub-basins was thus not included in the area calculation (flood elevation in each sub-basin may be different). The mask adapted to the area of flooding in each image using the DTM, expanding or contracting to include the flood and a perimeter dry zone (see Figure 26).

8.2.2.3 Slope Mask

The slope of each pixel was calculated based on the DTM, and pixels with slopes deemed too low or too high were removed. Extremely low slopes were removed as the interface between water and dry land was difficult to distinguish in these pixels. High slope pixels were removed as the large range of elevation values in a single pixel added to uncertainty in water level estimation. Additionally, high slope pixels are more susceptible to radar shadow effects. Similarly to the adaptive basin mask, the slope filter adapted to the area of the flood in each image and only filtered out pixels near the flood edge. The meant that pixels located in the base of a turlough were not unnecessarily filtered out at high flood levels (see Figure 26d).

8.2.2.4 Surface anomaly mask

During the calibration process it was found that after all of the previously described filters were applied, some 'reliable' pixels would still consistently produce false negatives. To remedy this issue, a method of identifying these anomaly pixels was developed by comparing the DTM with a SAR based flood contour map. The SAR contour map was made by clustering each thresholded flood image into a set of intervals based on their flood area. Each interval cluster was averaged into a single binary image, and then the binary images for each area interval were stacked into a single contour-like image, where the value in each pixel represented the typical area of flood required for that particular pixel to flood (Figure 27b).



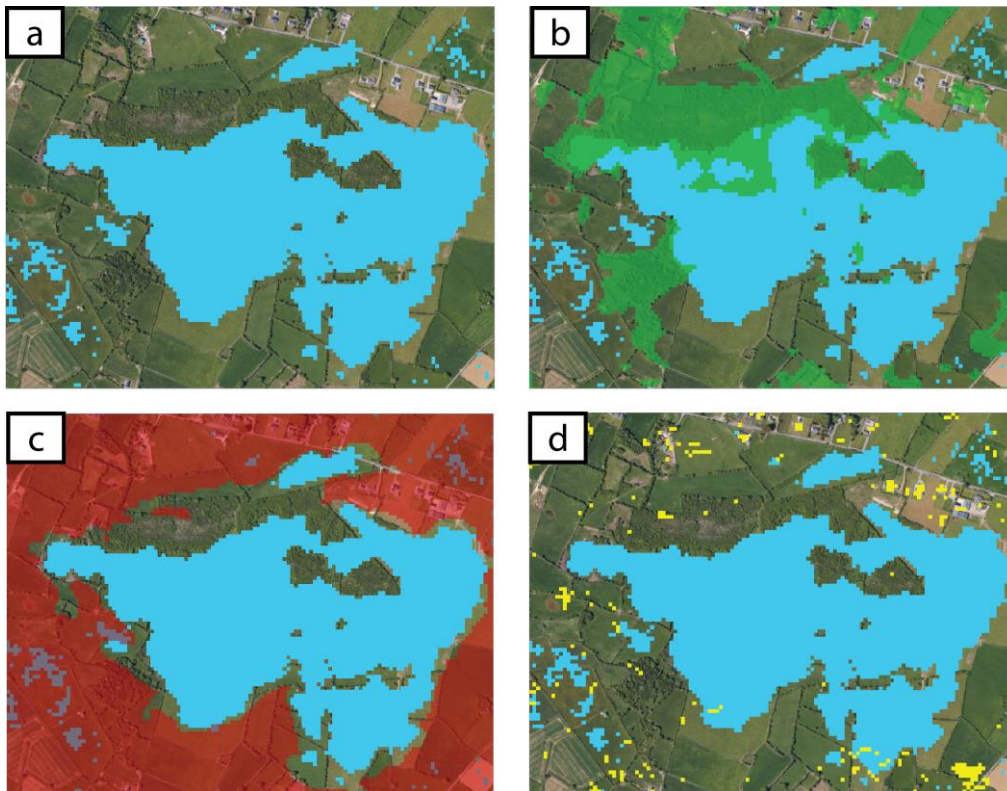


Figure 26: Filters applied for calculating flood area (blue) at Cahermore Turlough, Co. Galway: (a) thresholded SAR image, (b) vegetation mask (green), (c) adaptive basin mask (red) and (d) slope mask (yellow).

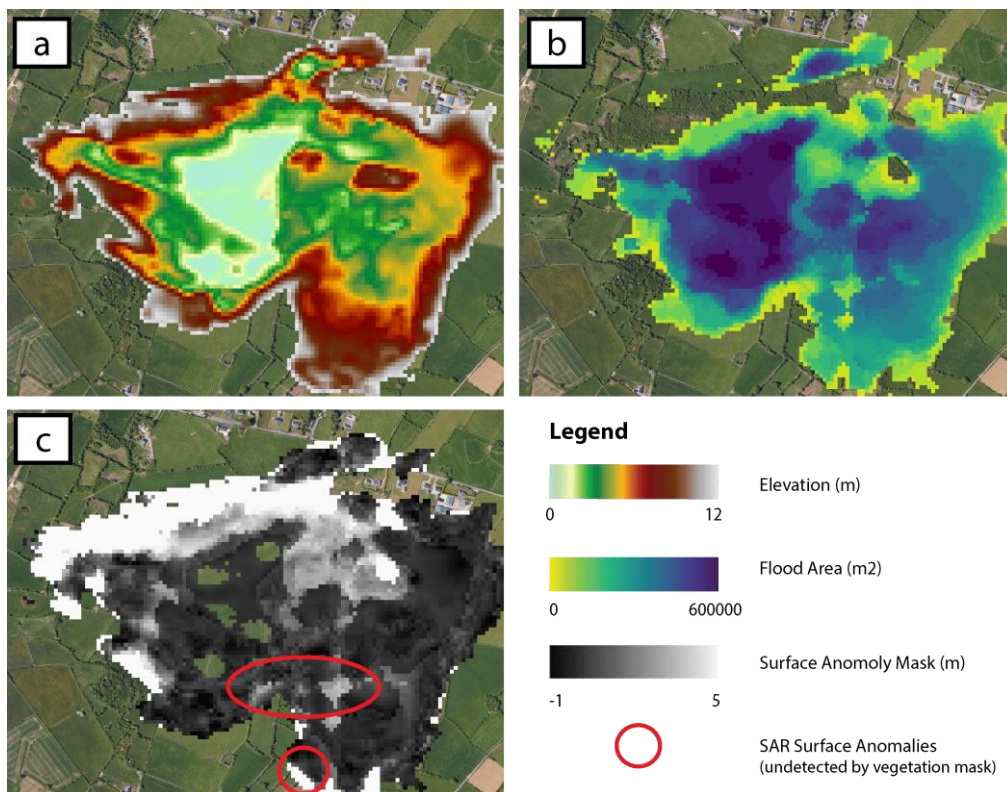


Figure 27: Surface Anomaly Mask procedure at Cahermore Turlough: (a) DTM, (b) flood area contour map and (c) surface anomaly mask (red circles highlights anomalies unseen by other filters).

By comparing the DTM (Figure 27a) to this contour image, an assessment could be made of where the flood should occur (using the DTM) compared to where the SAR observes the flood to occur. The flood contour map was normalised to the same scale as the DTM and the difference between the images calculated. Pixels with high values (i.e. large offsets between the DTM and flood contour image) indicated anomalies that may cause false negatives in the thresholded SAR images. See Figure 27c for an example of an anomaly map. In this figure, pixels with large DTM offset values are shown as white. Many of these anomalies are caused by vegetation and are already detected by the vegetation mask (Figure 26b). However, a number of anomalies (highlighted by red circles) are not present in other filters. These newly detected anomalous pixels were filtered out of the hydrograph generation process.

8.2.3 Convert Area to Stage

Area values were calculated from each of the filtered SAR image and collated into a timeseries. A stage-area curve (or relationship) was developed for each site so that the area timeseries can be converted to stage timeseries. The stage-area curve was generated using the DTM with the same filters applied to it as were applied to the SAR images. This ensured that the area from a filtered SAR image directly corresponds with its associated stage value. See Figure 28 for an example filtered and non-filtered stage area curves.

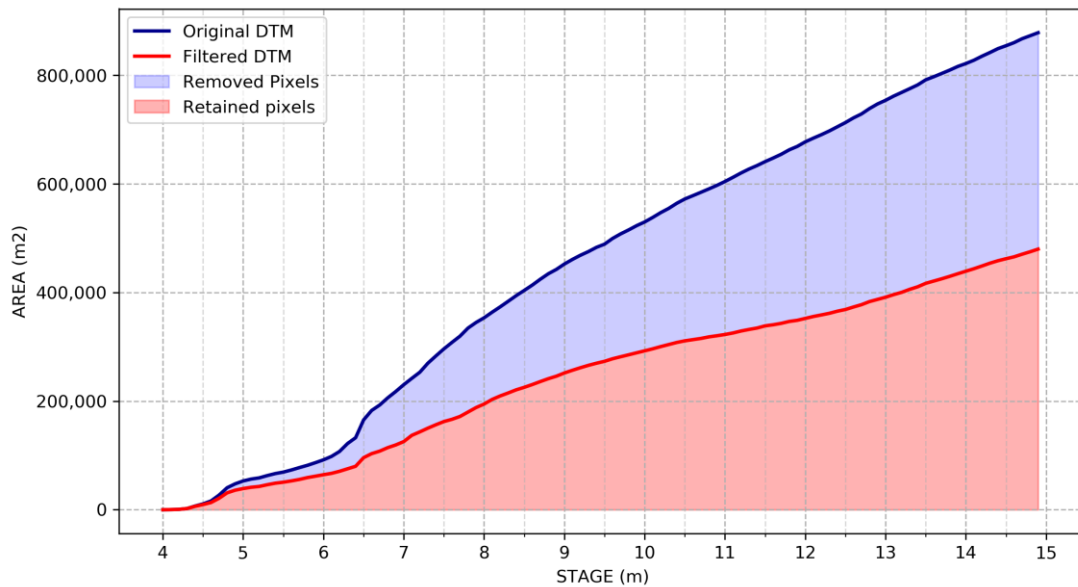


Figure 28: Filtered and non-filtered stage area curves for Cahermore Turlough, Co. Galway.

8.2.4 Discard Low Area Data Points

After these filters were applied and a corrected area was calculated for each image, each data point was subject to a threshold based on how many pixels were available to make the area calculation. The thresholds were based on total area as well as area-per-stage-interval, and are described below:

1. Total Area

Data points with flooded areas of less than 2,000 m² (i.e. 20 pixels) were omitted from the finished hydrograph. Below this value, the accuracy of the hydrograph was found to be poor.

2. Area-per-stage-interval

The previously listed filters often impacted a turlough unequally over its flood range. For instance, some turloughs are surrounded by dense woodland above a certain elevation value (e.g. Coole in Co. Galway). In sites such as these, the visible flooded area on a SAR image may change very little (or not at all) as the water level rises and floods into the woodland, thus hindering any calculation of stage. To remedy this, the number of usable (i.e. not filtered out) pixels at specific stage intervals was calculated. If a stage interval did not contain sufficient usable pixels, any stage values in this interval were discounted.

See for an example of a SAR derived stage timeseries for Ballinduff Turlough, Co. Galway is shown in Figure 29 (pink line). Discarded low pixel intervals at the bottom and top of the flood range are shown by the red band (the errors caused by low pixel counts between 14 and 18 m are clearly apparent).

8.2.5 Apply Smoothing

Due to the inherent noise of a SAR image, the stage timeseries usually includes a degree of noise, especially for small turloughs or at low area stage intervals on larger turloughs. This noise was smoothed using Gaussian Convolution. The blue line in Figure 29 represents a smoothed timeseries with low area intervals removed.



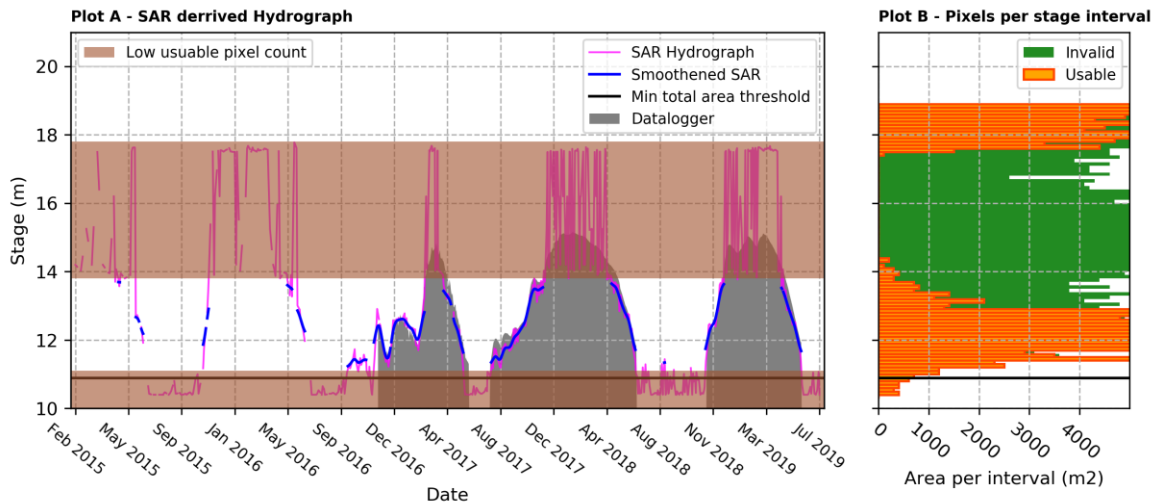


Figure 29: Observed stage (grey), SAR derived stage (pink) and smoothed SAR stage (blue) timeseries at Ballinduff Turlough, Co. Galway. Plot-A shows SAR derived hydrograph. Plot-B shows the total (green) and usable (orange) pixels per stage interval.

8.3 Calibration

Goodness of fit for the SAR hydrograph process was assessed using Nash-Sutcliffe Efficiency (NSE) for flood volume (volume is preferred to stage as it prioritises model efficiency at high flood conditions). Observed water level data were compared to SAR derived hydrographs at 23 sites (out of 47) and the hydrograph generation variables were tweaked to achieve maximum efficiencies. The hydrograph variables were based on the previously described filters and included parameters such as maximum and minimum slope thresholds, area-per-interval threshold or Gaussian kernel size for convolution (i.e. the amount of smoothing applied). Approximately 33,000 combinations of threshold parameters were tested to achieve the optimised threshold parameters for each observed site individually and for the 23 sites collectively (i.e. the single parameter set that achieved the highest average efficiency across the 23 sites). Validation was carried out with the remaining 24 usable sites. For the per-site optimisation, the mean NSE was 0.85 whereas the collective optimisation achieved an average NSE of 0.73 (Figure 30). The collective optimised parameters were then applied to the ungauged sites.

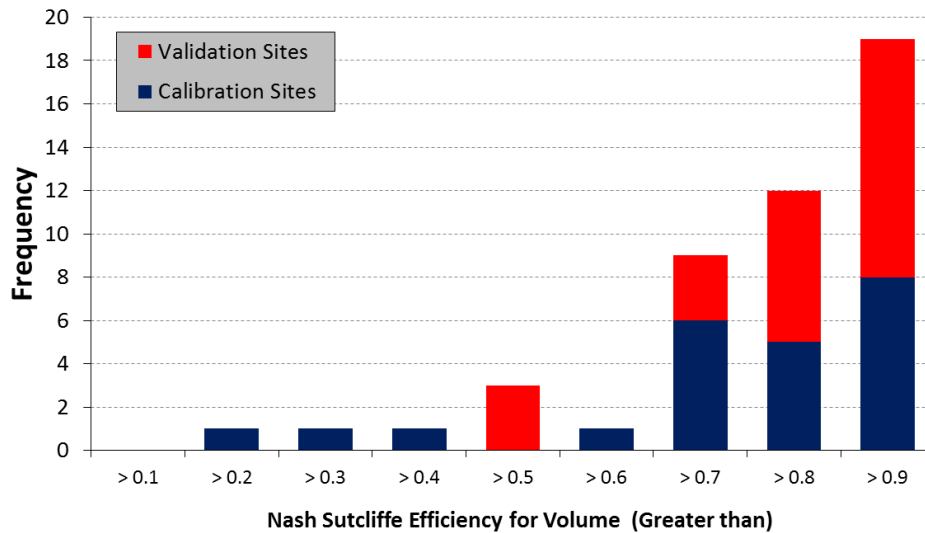


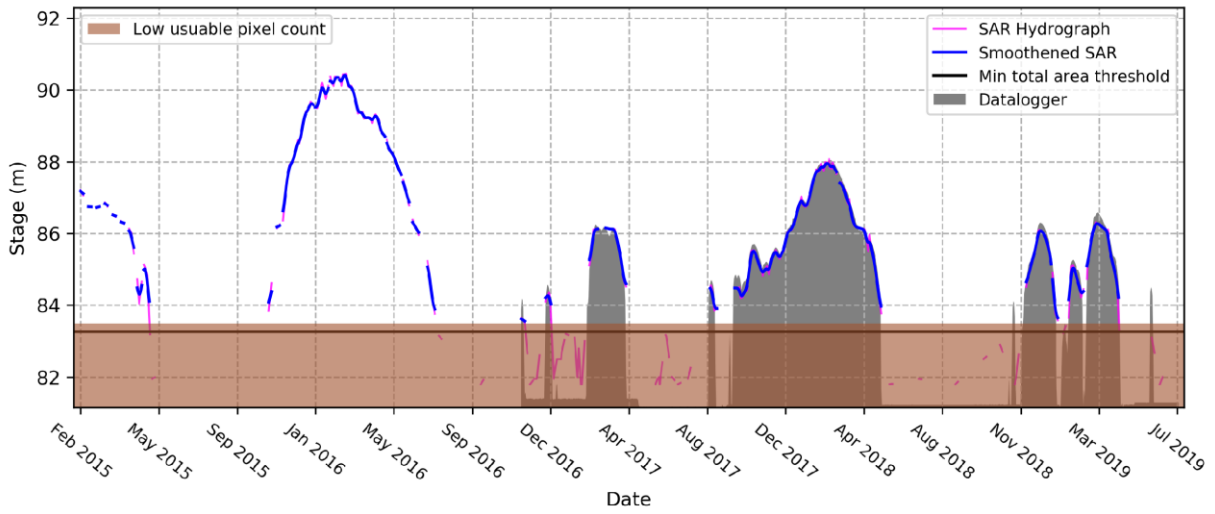
Figure 30: Distribution of Nash Sutcliffe efficiencies (volume) for 47 SAR hydrograph calibration and validation sites.

When additional information was available at ungauged sites, or at gauged sites prior to installation, this information was used to improve the accuracy of the hydrographs. This additional data included flood reports, aerial photography, Sentinel-2 imagery and Landsat imagery.

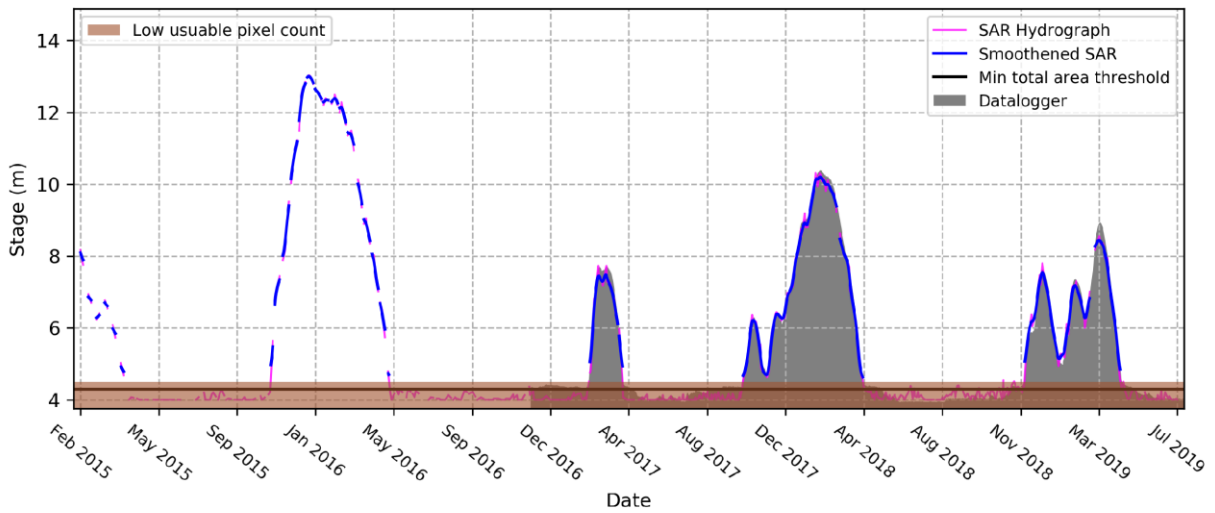
8.4 Results

Hydrographs were produced for 561 sites between February 2015 and July 2019. See Figure 31 and Figure 32 for examples.

Castleplunket, Co. Roscommon NSv: 0.974



Cahermore, Co. Galway NSv: 0.977



Blackrock/Peterswell, Co. Galway NSv: 0.991

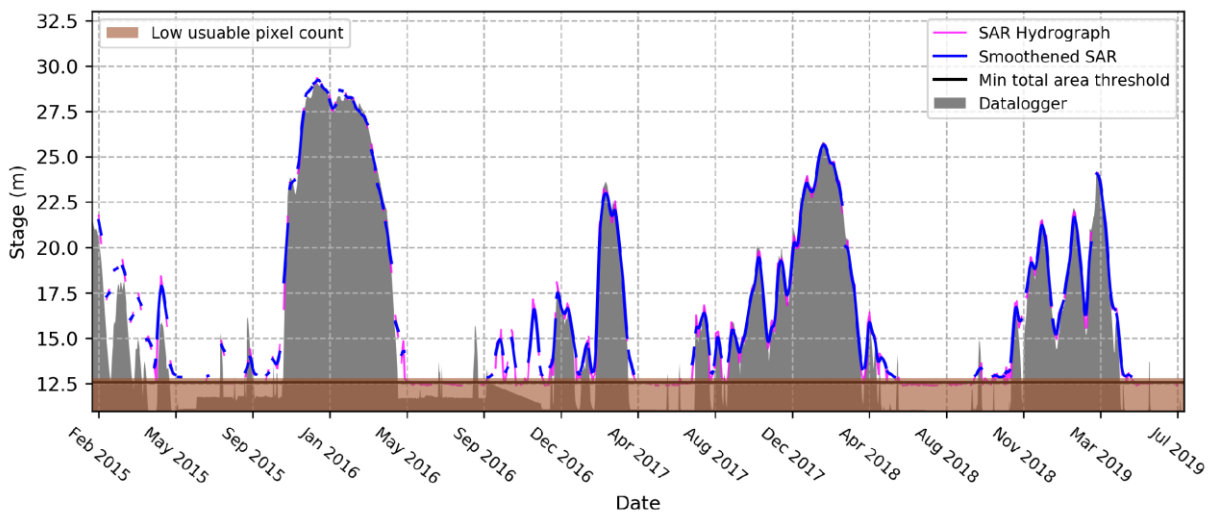
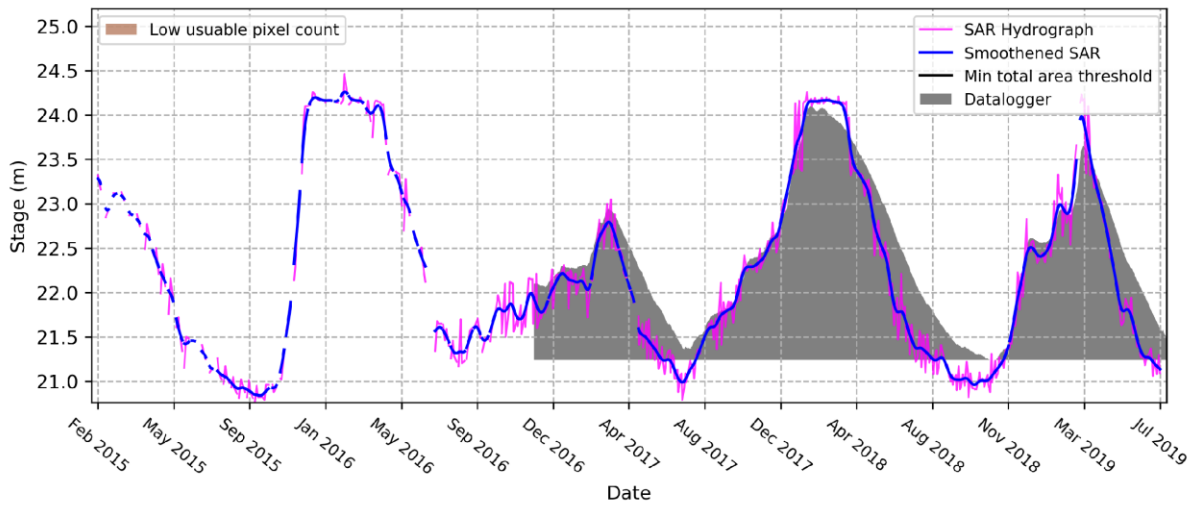


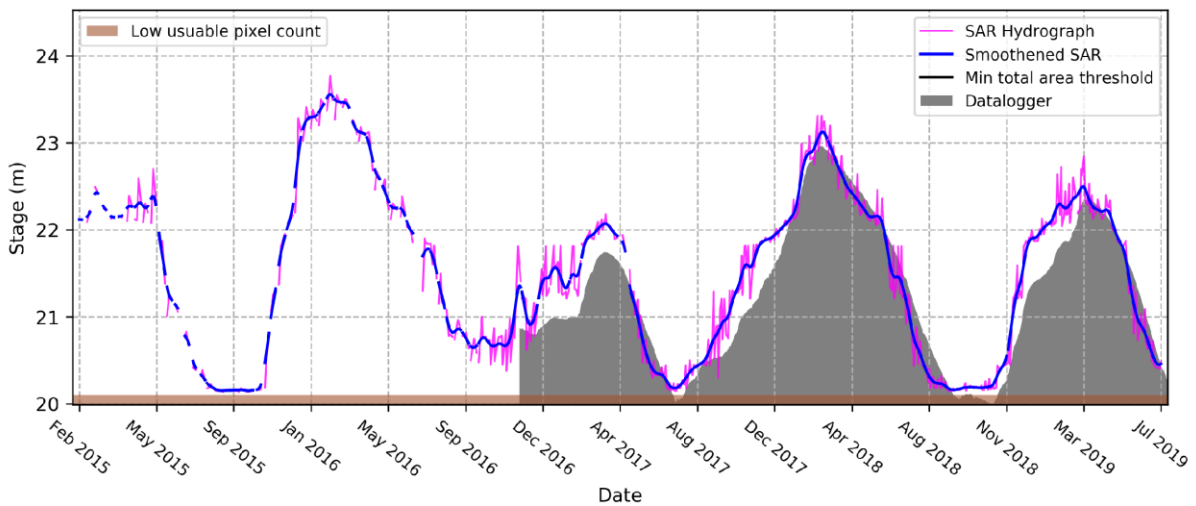
Figure 31: SAR Derived hydrographs and efficiency statistics for selected sites (NSv: Nash Sutcliffe Efficiency for volume).



Termon North, Co. Galway NSv: 0.903



Termon South, Co. Galway NSv: 0.851



Lough Gealain, Co. Clare NSv: 0.836

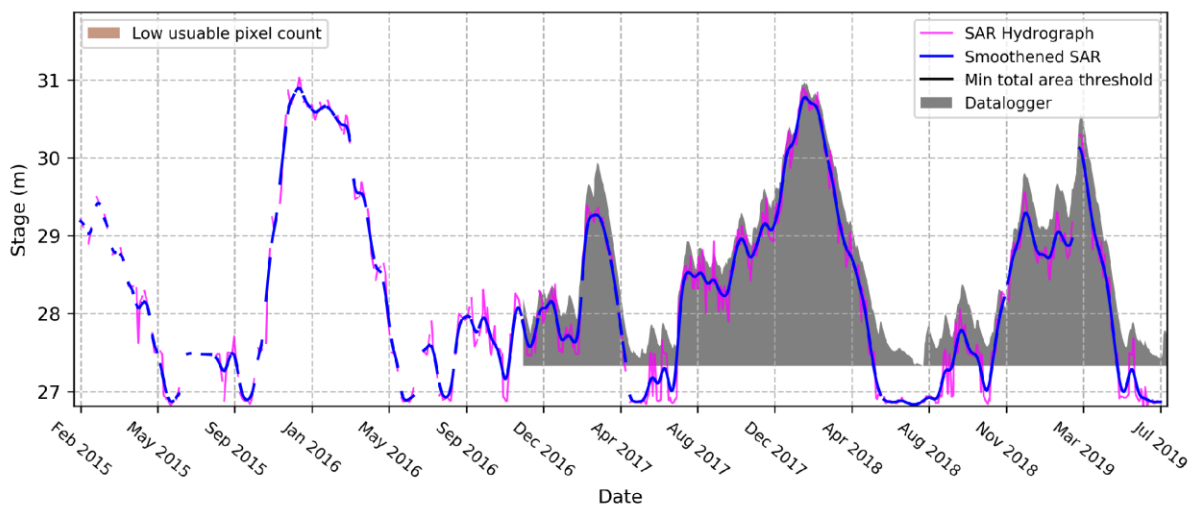


Figure 32: SAR Derived hydrographs and efficiency statistics for selected sites (NSv: Nash Sutcliffe Efficiency for volume).



9 Hydrological Modelling: Global

This section as well as Section 10 describes the hydrological models developed to quantify the relationship between rainfall and groundwater flooding in lowland karst groundwater flow systems, and the approach taken to apply the models for predictive groundwater flood mapping.

The modelling work was broadly divided into two categories;

1. Developing a generic (global) modelling approach that could be applied to individual flood sites based on limited site-specific data such as water level, rainfall and topography. By necessity this approach considered each site independently and did not incorporate information on the wider groundwater system. The predictive flood map was predominantly derived using this approach and the modelling work carried out by the research fellow in the GWFlood project team, based latterly in ITC and formerly in TCD.
2. Refining and applying a distributed groundwater model of the Gort Lowlands catchment, Co. Galway, for predictive flood mapping. The Gort model has been developed by TCD over the last decade and further expansion and refinement carried out by the postdoctoral researcher based in TCD. The distributed model explicitly models connections and interactions between turloughs along the main conduit flow system and peripheral water bodies.

9.1 Modelling Overview

Predictive flood mapping requires long-term hydrological time series to estimate future occurrence probabilities. No such records exist for karst groundwater flow systems in Ireland; however, long-term records of the primary driver of groundwater flooding, rainfall, are available. A hydrological modelling methodology was thus developed to quantify the relationship between rainfall and groundwater flooding in order to allow the reconstruction of long-term hydrological series from observed and stochastic rainfall data to allow predictive flood levels to be estimated.



There are two fundamental approaches to the mathematical modelling of karst systems; distributive models and global models. Distributive models use theoretical concepts such as simplified aquifer geometry and hydrodynamic flow equations to simulate the hydraulic behaviour of karst aquifers (Kovacs and Sauter, 2007). Global (or lumped parameter) models concentrate on mathematically deriving a relationship between input and output, where the input is usually a precipitation event and output the spring discharge time series. Global models consider the karst aquifer as a transfer function, transforming the storm input signal into the output spring hydrograph signal. The transfer function is taken to represent the overall (or global) hydrogeological response of the karst aquifer to storm events (Kovacs and Sauter, 2007).

Given the limited data availability in Irish karst groundwater flow systems, and the broad spatial application of the methodology, global modelling was deemed the most appropriate approach and adopted for national-scale flood mapping. The map was supplemented by outputs from a distributed model developed by TCD for the Gort Lowlands (Morrissey et al., 2020, Gill et al., 2013a, McCormack et al., 2014). A description of global modelling is given in the following sub-sections while the TCD distributive model is discussed in Section 10.

9.2 Global Modelling

The primary objective of the global modelling approach was to develop predictive relationships between antecedent rainfall and flooding within individual turlough basins. Once established, this would allow the reconstruction of hydrological series sufficiently long for flood frequency analysis to be carried out and predictive flood levels to be estimated.

A version of the Antecedent Precipitation Index (API) (Kohler and Linsley, 1951, Smakhtin and Masse, 2000) was used to model flood behaviour. The API assumes the effect of antecedent precipitation can be represented by catchment or site-specific recession coefficient (Beschta, 1998). A modified version of the API, the Current Precipitation Index



(CPI) (Smakhtin and Masse, 2000), has been used to model turlough flood volumes and is given by:

$$CPI = \sum_{t=-1}^{-i} R_t k^{-t}$$

Where i is the number of antecedent days, k is a decay constant and R_t is recharge on day t . The coefficient k represents the percentage water that remains after a specified time interval; a large k leads to a slow recession after the cessation of rainfall while a small k indicates a quick recession (Lee and Huang, 2013). To ensure convergence and remove the influence of initial conditions on analysis, effective rainfall series beginning at least one year before the corresponding hydrological series were used in the calculation of the CPI. CPI series using a range of k values were generated, with the k value showing the highest correlation with observed volume selected. The model then took the form of a simple linear regression between the CPI (predictor) and flood volume (response) where:

$$V = S + C * CPI$$

where S is the intercept C is the slope. Conceptually the intercept S represents a groundwater storage term, or the volume of water required to have built up in the karst groundwater flow system before flooding occurs. The slope term C represents a notional contributing area, defining the minimum zone of contribution required to supply the recorded water volume.

A soil moisture deficit (SMD) model was used to estimate recharge based on the SMD model developed for Irish grasslands by Schulte et al. (2005). The soil and unsaturated zone were represented as a single reservoir with the flux in the reservoir dependent on the inputs and outputs, namely rainfall (R) as input and actual evapotranspiration (ET_A) and recharge (R_E) as output.

Models were calibrated using a combination of observed and SAR hydrographic data (see Figure 33 for examples). Goodness of fit was assessed using the NSE, percentage bias (PBIAS), and annual maxima error (AmaxE) criteria for volume. Model fitting was attempted for 560 sites, of which 120 sites were discarded due to poor SAR and/or model efficiency leaving 440 sites remaining for predictive flood mapping. The average NSE value



for all accepted models was 0.80 and the distribution of NSE values for all accepted models is presented in Figure 34. It should be noted that some models adequately represented the annual maxima, yet displayed relatively low NSE values, were retained.

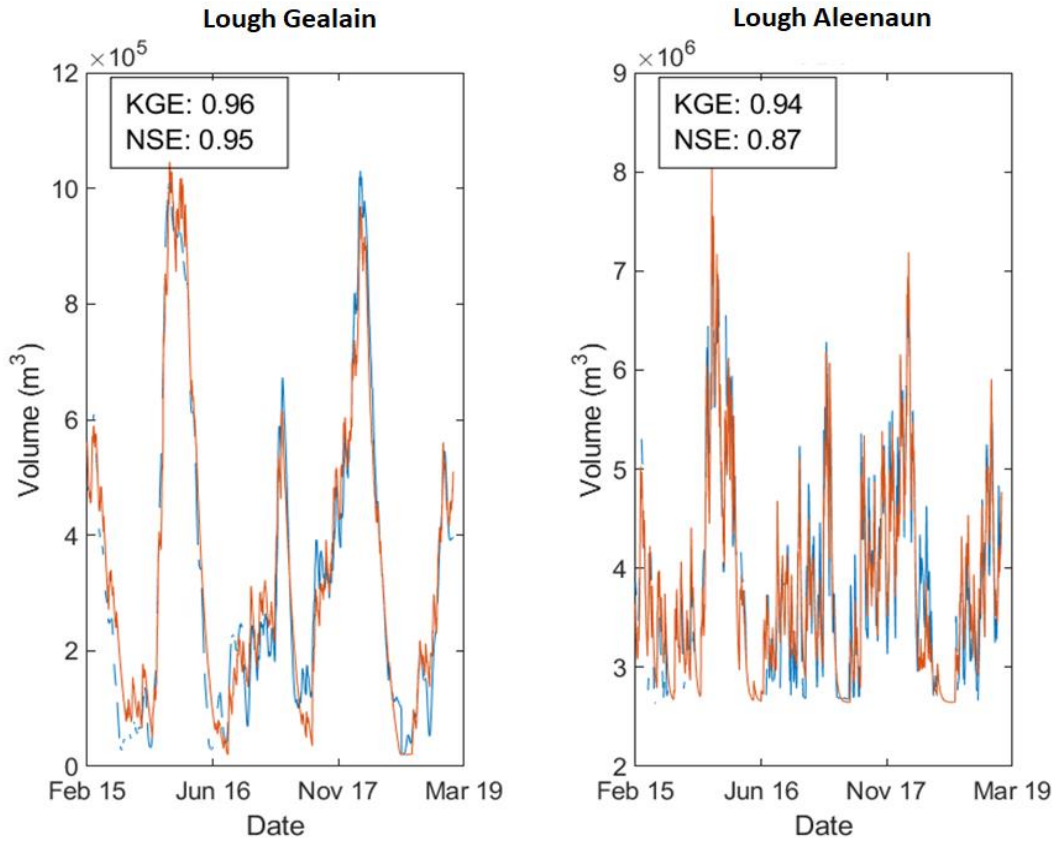


Figure 33: Observed (blue) and modelled (orange) hydrographs for Lough Gealain (left) and Lough Aleenaun (right) turloughs, Co. Clare.

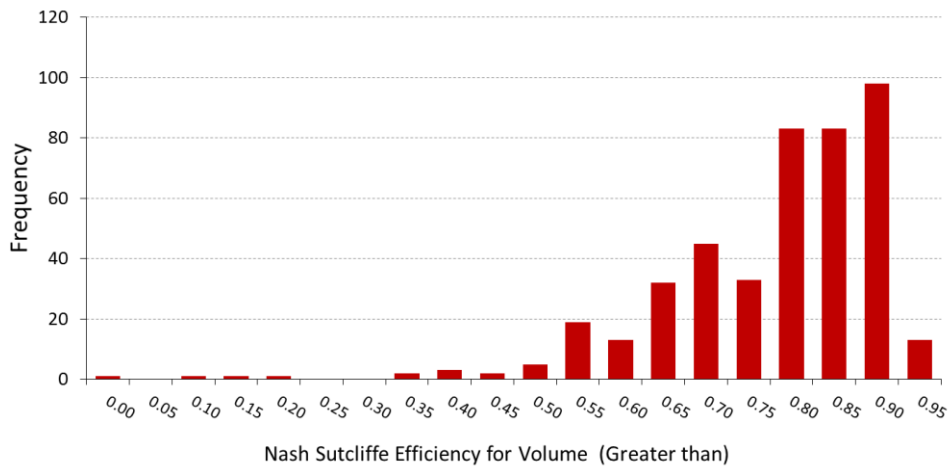


Figure 34: Distribution of Nash Sutcliffe efficiencies related to volume for 440 hydrological models.

While overall the model performed well, several limitations of this approach should be noted. By necessity, due to the limited data availability and high number of sites to be modelled the approach could not incorporate step-changes in hydrological behaviour, such as a stage-dependency in catchment area or localised drainage into/out of the basin beyond the topographic spill point out of the basin. In some cases, this produced a clear divergence between observed and modelled behaviour, e.g. the model fitted well at lower levels but significantly under/over-predicted at higher levels.

In such cases, where possible models were selected that adequately reproduced the peak levels while sacrificing accuracy at lower levels. Were the models applied in another context, for example in an ecohydrological study, the calibration would need to be reassessed. In some cases, this limitation can be overcome by using a non-linear or multiple linear regression approach, but it was not feasible to implement in this project. In others, a global approach is unlikely to replicate flood behaviour adequately and alternatives, such as reservoir or distributed modelling, could be considered.

The total number of sites selected and accepted through the SAR hydrograph generation and modelling process is presented below in Table 4.

Table 4: Breakdown of sites used for SAR hydrograph generation and modelling ('TCD site' indicates that the AEP levels were provided by the TCD research project (see Section 10).

Flood Category	Site Count	Selected for SAR hydrograph generation	Accepted after SAR & modelling	TCD site
Turlough (GSI database)	329	230	182	12
Turlough (external database)	176	107	74	0
Non-turlough feature (GSI database)	44	37	31	0
Unlisted seasonal flood	119	112	99	1
Groundwater flood influenced lake	52	52	39	0
Groundwater flood influenced river	26	22	15	2
<i>Total</i>	<i>746</i>	<i>560</i>	<i>440</i>	<i>15</i>



9.3 Stochastic Weather Generation and Predictive Level Estimation

The hydrological models gave the capacity to construct the long-term time series required for flood frequency analysis, provided rainfall records of sufficient length were available. However, with available rainfall records falling far short of that required to estimate extreme flood events, the alternative of stochastic weather generation was investigated.

Stochastic weather generation uses existing weather records to produce synthetic weather series of unlimited length, thus permitting impact studies of rare occurrences of meteorological variables. A stochastic weather generator algorithm (Chen et al., 2010) was calibrated using approximately 70 years of observed rainfall records provided by Met Éireann, and used to generate long-term (>2000 years) synthetic rainfall data for each site. This stochastic time series, together with long-term average evapotranspiration (ET), was used as input data to the site models to produce long-term CPI series. From this, the annual maxima series were extracted, and a statistical distribution fitted, which enabled estimation of flood levels for a specified range of Annual Exceedance Probabilities (AEP). The probabilities are calculated for the present day (or current) scenario and do not take into account of potential changes due to climate change.



10 Hydrological Modelling: Distributive (Gort Lowlands)

10.1 Project Overview

TCD undertook a focused study of one particular catchment in significant detail. The study catchment covers an area of approximately 500 km² in south Co. Galway known as the Gort Lowland karst system and receives allogenic recharge through runoff from adjacent mountains and autogenic recharge from rainfall over the catchment. The entire catchment drains to a number of intertidal springs at Kinvara Bay via the karst limestone bedrock. During periods of sustained rainfall, the underground karst conduit system surcharges through a system of estavelles and floods low lying basins causing ephemeral lakes, known as turloughs. These turloughs provide additional storage of groundwater not available within the limestone bedrock and thus act as a form of naturally occurring management mechanism for groundwater flooding. The catchment is unique as the natural flow system has not been heavily altered by land reclamation or arterial drainage schemes and has therefore been relatively unaltered by human activities. The associated seasonal inundation cycle has led to the development of unique ecology within the normal upper and lower bounds of flooding providing a habitat for many floral and faunal species of national and international importance. Many of these areas are therefore protected within the European Natura Network. Turloughs are also categorised as GWDTs under the Water Framework Directive (2000/60/EC).

Following the extreme flooding event of winter 1994/1995, the Gort Flood Study was commissioned by the OPW to investigate the nature and causes of flooding in South Galway and to examine potential solutions. The project was a collaboration between Southern Water Global and Jennings & O'Donovan Partners and involved large-scale field studies of the catchment with meteorological and hydrological modelling (Southern Water Global, 1998). A simple Hydroworks model of the catchment was developed which consisted of pipes, weirs and flow controls to simulate the flooding of the rivers and turloughs within the catchment. The modelling effort, which was novel and had some relatively good results, was limited by lack of data with which to either populate or calibrate the model. The study resulted in the publication of a report, which outlined



various potential flood mitigation measures, one of which was the construction of a drainage channel from the lower end of the catchment (Coole complex) to the sea at Kinvara. None of these options were considered viable and therefore were not progressed further. The final project report was issued in 1997 and made a number of recommendations on how to resolve the flooding, the majority of which were ruled out based on cost-benefit.

Since the Gort Flood Study was completed in 1997, a number of consecutive research projects undertaken in Trinity College Dublin, have involved the installation of pressure transducers to record turlough stage (water level) at a number of the turloughs in the south Co. Galway catchment (Gill et al., 2013a, McCormack et al., 2014). This fieldwork also involved developing rating curves on the three main rivers flowing into the lowlands as well as water chemistry analysis. Topographical surveying of the turlough basins was also carried out during dry conditions to accurately determine stage-volume relationships during flooding events. During extreme events, such as what occurred in winter 2015/2016, many turloughs within the catchment overflow at their upper basin elevation and flood adjoining lands which do not flood under normal winter conditions

Research projects, which took place in the mid 2000s at TCD, studied the turloughs in conjunction with the NPWS who were interested in their conservation status and thus the requirement for the development of a numerical model of the catchment. A general conceptual understanding of the catchment was therefore developed at TCD following many years of research which built upon the original Gort Flood Study. The conceptual model was initially informed by extensive tracing studies previously carried out within the catchment. Flows within the main rivers, meteorology across the catchment and water hydrochemistry, all of which has been studied and collected during various TCD research projects, allowed a deeper understanding of the system and how it operates. Time series analysis of the fluctuating turlough water levels was subsequently undertaken. This revealed additional hydraulic characteristics regarding the nature of the catchment such as whether the turloughs act as surcharge tanks or not; and whether a turlough is connected to the mainline system or is located offline.



A semi-distributive model of the complex karst system within the Gort Lowlands was developed at TCD (Gill et al., 2013a). This model represented five turloughs within the catchment (Blacrock, Coy, Coole, Garryland and Caherglassaun) which were represented within a complex pipe network model in the InfoWorks urban storm drainage software package. Karst conduits were represented as pipes with turloughs represented as storage ponds. The boundary conditions at the catchment outfall were represented by the tide level at Kinvara Bay. The stage-volume relationship of the turloughs was determined using the field survey data and provided the input for each pond storage area. The model was calibrated using historical stage data from a number of turloughs, which had been collected over an extended period and was shown to accurately simulate stage within five turloughs in the Gort Lowlands (Gill et al., 2013a, McCormack et al., 2014).

This present study created a new expanded pipe network model of the catchment using the original model as a base reference. An additional 10 turloughs and floodplains were added to the model and the model catchment was expanded from 95.8 km² to 159.2 km². An additional inflow from the south-west of the catchment was also added to the model.

10.2 Model Description

The model developed and used within this study consisted of a semi-distributive pipe network model designed to replicate the hydrological responses of the complex lowland karst system to rainfall and river inputs with the associated downstream outfall to the sea at Kinvara. The pipe network was initially developed with reference to the previously developed model for five turloughs within the catchment by Gill et al. (2013b). The conceptual design of this modelling approach is as follows:

1. Karst conduits are represented as pipes;
2. Turloughs/floodplains are represented as storage nodes;
3. The downstream boundary conditions at the catchment outfall are represented by the tide level at Kinvara Bay;



4. The upstream boundary conditions are represented by the discharge data for each of the three rivers flowing off the Slieve Aughty Mountains, with a fourth river flowing in from the south-west.

An entirely new model was developed for the catchment using the original modelling approach. An additional 10 turloughs and floodplains were added to the model (15 in total) and the model catchment was expanded from 95.8 km² to 159.2 km². An additional inflow from the Cloonteen River located to the south-west of the catchment was also added to the model. A ground model was generated in the InfoWorks ICM software using the DTM data discussed previously. Each of the turloughs or floodplains were then represented by storage nodes with a depth-area relationship developed using this ground model. The geographic location of the 15 storage areas within the catchment is given in Figure 35. The calibration process was carried out by trial and error with pipe dimensions and the various controls varied in an iterative process. Rivers were represented using open channels with dimensions approximated from digital mapping and physical surveys. Overflow channels between basins were added as open channels with dimensions informed by digital mapping, physical surveys and maximum flood extents mapping. The catchment was divided into sub-catchments based on topography and these were connected to the pipe network using conduits and nodes with autogenic recharge applied to these sub-catchments using a Ground Infiltration Module with InfoWorks ICM as described by Gill et al. (2013a).



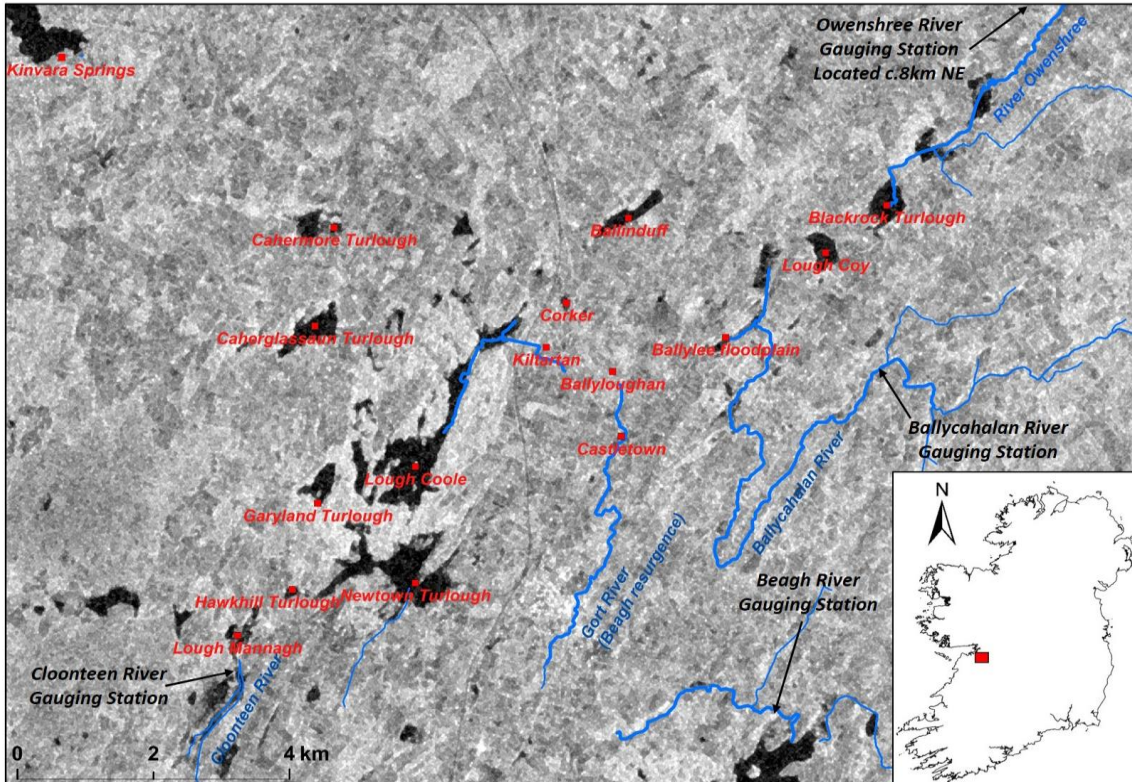


Figure 35: Location of turloughs and floodplains within the catchment and model domain.

The overland flow between turlough/floodplain basins was simplified for incorporation into the 1D environment with channels approximated from the DTM. Thus, whilst the over-spilled volume of water between floodplains that occurred during extreme events could be quantified together with the timing of same, there was no capacity to simulate the overland flow paths. In order to simulate the spatial extent of flooded areas between turloughs/floodplains, a 1D-2D coupled model was required to accurately simulate surface overland flows. A DTM was created using a combination of LiDAR data, GPS data and bathymetric data. These data were combined and a new integrated DTM was constructed using the Kriging method with a 2 m grid spacing. A 2D mesh was then created using this ground model within the model network domain incorporating the full extents of the catchment where overland flooding and flow is known to occur. The 1D pipe network (representing flow within the karst bedrock) was linked to this 2D mesh using 2D nodes. Flow between the 2D mesh towards a 1D node (and vice-versa) was based on a standard head-discharge relationship. Modification of the original calibrated 1D model was kept to the minimum required to effectively incorporate these 2D elements with an aim of reducing the recalibration effort required.

The model calibration period was between 01/11/2016 and 31/03/2018. The calibration process was targeted to matching peaks and did not focus on flashy behaviour at lower elevations. The calibration process was iterative with the catchment roughly broken into two sections based on elevations and close frequency interactions between turloughs. During the calibration process, when the model was nearing an acceptable level of accuracy, the extreme flood period of 2015/2016 was used intermittently to check peak levels for that event against the current calibration. The results of the final model calibration are given below.

It must be noted that the calibration process was for the system as a whole whereby every point was required to be balanced in unison as each storage node is interconnected. It is therefore not possible to tweak the calibration at any one location without affecting some or all of the levels within the system. For this reason, accuracy at limited discrete locations was sacrificed to provide a better calibrated model at multiple other locations.

The final model calibration statistics for model are given in Table 5 with a sample calibration plot given in Figure 36.

Table 5: Summary statistics for the 1D model calibration.

Location	2016 - 2018 Calibration Period Model Efficiency			
	Nash-Sutcliffe (NSE)		Kling-Gupta (KGE)	
	Stage (m)	Volume (m ³)	Stage (m)	Volume (m ³)
Ballinduff	0.87	0.93	0.87	0.88
Blackrock	0.96	0.97	0.97	0.92
Caherglassaun	0.96	0.97	0.95	0.90
Cahermore	0.98	0.98	0.97	0.91
Castletown	0.98	0.85	0.88	0.62
Kiltartan	0.25	0.34	0.27	0.32
Coole	0.95	0.99	0.89	0.93
Coy	0.87	0.89	0.95	0.93
Garyland	0.98	0.99	0.97	0.95
Hawkhill	0.94	0.94	0.91	0.82
Mannagh	0.88	0.85	0.97	0.77
Newtown	0.93	0.99	0.88	0.97



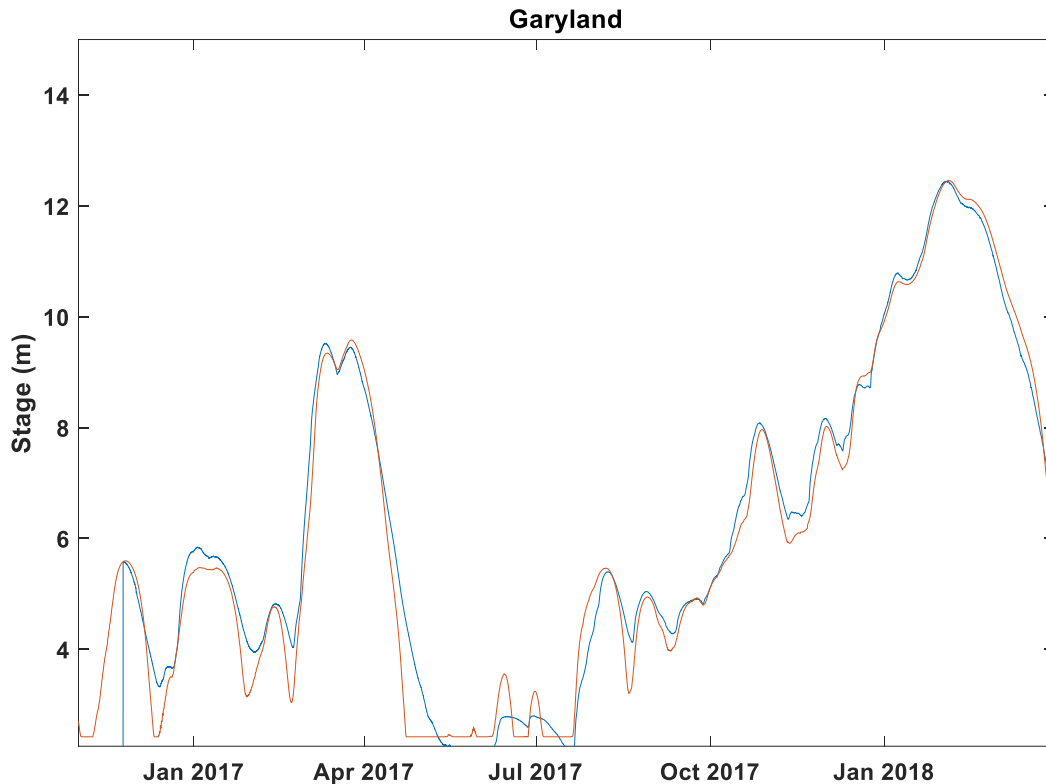


Figure 36: Model calibration for Garryland Turlough – a Nash-Sutcliffe Efficiency (NSE) of 0.98 was achieved for stage (meters above ordnance datum) and 0.99 for volume (m³).

10.3 Main Project Outcomes

10.3.1 Lowland karst modelling – flood alleviation

This study demonstrated the successful development of a 1D/2D pipe network model of a large karst catchment which includes 15 turloughs and floodplains for simulating groundwater flooding. The addition of the 2D aspect of the model coupled with the 1D pipe network, which is a novel achievement for a karst groundwater system, has been shown to successfully simulate overland flooding between basins that are overtopped during extreme flood events. The calibrated model has been used to predict submarine groundwater discharge to Kinvara Bay over a long-term period providing further insight into the catchment hydrology (Morrissey et al., 2020). This study has demonstrated the practical applications for simulating groundwater flood alleviation measures of such models and the results of the study are being used by the OPW and Galway County Council with their consulting engineers to design a flood alleviation scheme for the Gort Lowlands.

10.3.2 Flooding Annual Exceedance Probabilities

This study has demonstrated how Annual Exceedance Probability flood frequency analysis can be implemented for a lowland karst catchment in Ireland using synthetic rainfall with rainfall runoff models and routing the resulting datasets through the calibrated semi-distributed karst model. Statistical analysis was then performed on the resulting annual maxima series using conventional fluvial methodologies. Extreme groundwater flood levels were successfully calculated throughout the catchment and are being used to design a new flood alleviation scheme which is at pre-planning stage. The methodology and resulting data are extremely important both from future planning and flood risk management perspectives in Irish karst hydrological settings.

10.3.3 Climate Change Analysis

This study investigated the predicted impacts of climate change on the Gort Lowland karst catchment by using the calibrated semi-distributed karst model populated with output from high-resolution regional climate models for Ireland. This analysis has shown that mean, 95th and 99th percentile flood levels are expected to increase by significant proportions for all future Representative Concentration Pathway (RCP) emission scenarios. The frequency of events currently considered to be extreme is predicted to increase, indicating that more significant groundwater flooding events seem likely to become far more common. The impacts of increasing mean sea levels were also investigated, however it was found that anticipated rises had very little impact on groundwater flooding due to the marginal impact on ebb tide outflow volumes. Overall, this study highlights the relative vulnerability of lowland karst systems to future changing climate conditions mainly due to the extremely fast recharge which can occur in such systems. The study presents a novel and highly effective methodology for studying the impact of climate change in lowland karst systems by coupling karst hydrogeological models with the output from high resolution climate simulations.



11 Historic Groundwater Flood Map

The historic groundwater flood map shows maximum observed flood extents for locations of recurrent groundwater flooding in limestone regions. The map is primarily based on the winter 2015/2016 flood event, which in most areas represented the largest groundwater flood event on record. It was developed using all available SAR imagery between the 1st of December 2015 and the 31st of March 2016 as well as any available historic records (from winter 2015/2016 or otherwise). The map was produced based on the SAR mapping process described in Section 7 along with a series of additional filtering steps.

In addition to the historic groundwater flood map, the flood mapping methodology was also adapted to produce a surface water flood map of the 2015/2016 flood event. This flood map encompasses fluvial and pluvial flooding in non-urban areas and has been developed as a separate product. It should be noted that this flood map is a snapshot of the 2015/2016 flood event and should not be considered maximum historic flood surface water flood extent map. This is for two chief reasons: 1) the 2015/2016 flood was not the maximum surface water flood event at all locations in Ireland and 2) surface water flooding is typically shorter in duration than groundwater flooding and it is thus less likely that the intermittent flyovers of the Sentinel-1 satellite captured the peak extent of the flood.

11.1 Filtering and Classification

Although the assumption of linking low backscatter signal to the presence of water is a well-established flood mapping technique, there are a number of technical issues that must be addressed. For example, radar shadowing due to local topography often results in false positive pixels on leeward hillsides (i.e. the side of a slope that the side-looking Sentinel-1 sensor cannot see). In addition, not all flat surfaces necessarily indicate water. Artificially flat features such as airport runways, motorways or football pitches can produce false positives. False negatives can occur where surface roughness on water bodies is high due to wind shear or vegetation cover, causing high backscatter. In order to correct for these inherent technical issues, additional filtering and topographical correction techniques were applied to the SAR imagery to enhance the accuracy of the historic flood



map. A flow chart of the complete SAR historic flood mapping process is presented in Figure 37, and the main steps described below.

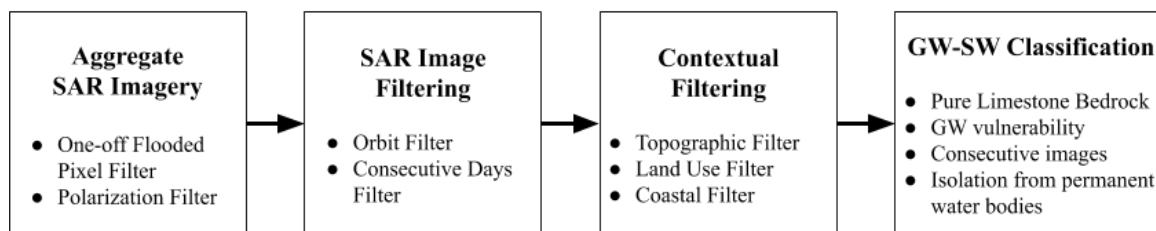


Figure 37: Flow chart with the main steps followed to select floods from SAR images. Each step is described below with more detail.

11.1.1 Aggregate SAR imagery

The first step was to aggregate SAR images (stage-2 products) from relevant orbits between the dates 1st of December 2015 and the 31st of March 2016. The images were stacked into independent arrays for VH and VV where each pixel represents the amount of images where that pixel is classified as flooded (see Figure 38). A threshold was applied to the stacked arrays based on the criteria that pixels had to be classified as flooded in at least one SAR image (One-Off Flooded Pixel Filter) by the two approaches described in Section 7.1.1.3: 1) Otsu threshold method, and 2) the probability method. The VH and VV arrays were then combined onto a single master array with the noise-reducing criteria that only pixels classed as flooded in both VH and VV arrays were retained (Polarization Filter). Furthermore, floods composed of less than six connected pixels (pixel resolution: 10 x 10 m) were removed as an additional noise reduction measure.

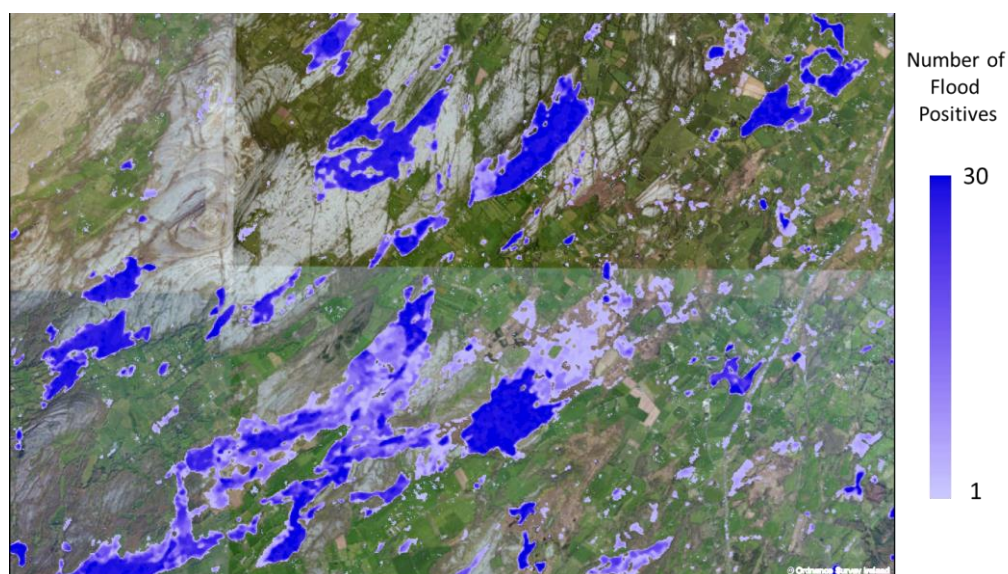


Figure 38: Number of times each pixel was considered as flood (VH band) in North East Co. Clare.

11.1.2 SAR Image Filtering

By using multi-temporal SAR imagery at a specific location, the timing and positioning of the Sentinel-1 satellite during image acquisition can be exploited to provide an initial means for identifying false positive values related to radar shadow and noise. It should be noted that the filtering steps described below were applied in an object-based rather than pixel-based approach. If all flood pixels for an object were not discarded during the filtering process, the object was deemed as representing an area of likely flooding. In this manner, the flood mapping methodology is selective on which floods to retain, but once selected the final flood extent will encompass the largest extent seen in any SAR image.

1. Orbit Filter

This filter omits 'floods' that only appear in images taken from a single orbit direction. Floods that appear in repeated ascending orbit images (viewed from the west) but no descending orbit images (viewed from the east) are likely to be radar shadow. Figure 39 shows an example at applying the orbit filter.

2. Consecutive Images Filter

In order for a potential flood object to be accepted, it must appear to be flooded in consecutive SAR images. This filtering step is crucial for reducing the inherent noise caused by radar speckle, as well as aiding the distinction between groundwater and surface water floods. The greater the amount for consecutive images used, the more noise is removed from a flood map. However, any flood object that exists a shorter duration than the consecutive image threshold will be omitted from the flood map completely. Thresholds of two and four consecutive images were applied to surface water and groundwater flood maps respectively and as a result, the final historic groundwater and surface water flood maps do not include short duration flood extents. While this step has a minor impact on groundwater floods due to their slow flood patterns, it does limit the scope of the surface water flood map. For example, only three images were acquired in the west of Ireland between 30th December 2015 and 6th January 2016. Accordingly, any waterbody that appears and completely disappears between these dates was only observed in a single SAR image and is thus omitted from the map.



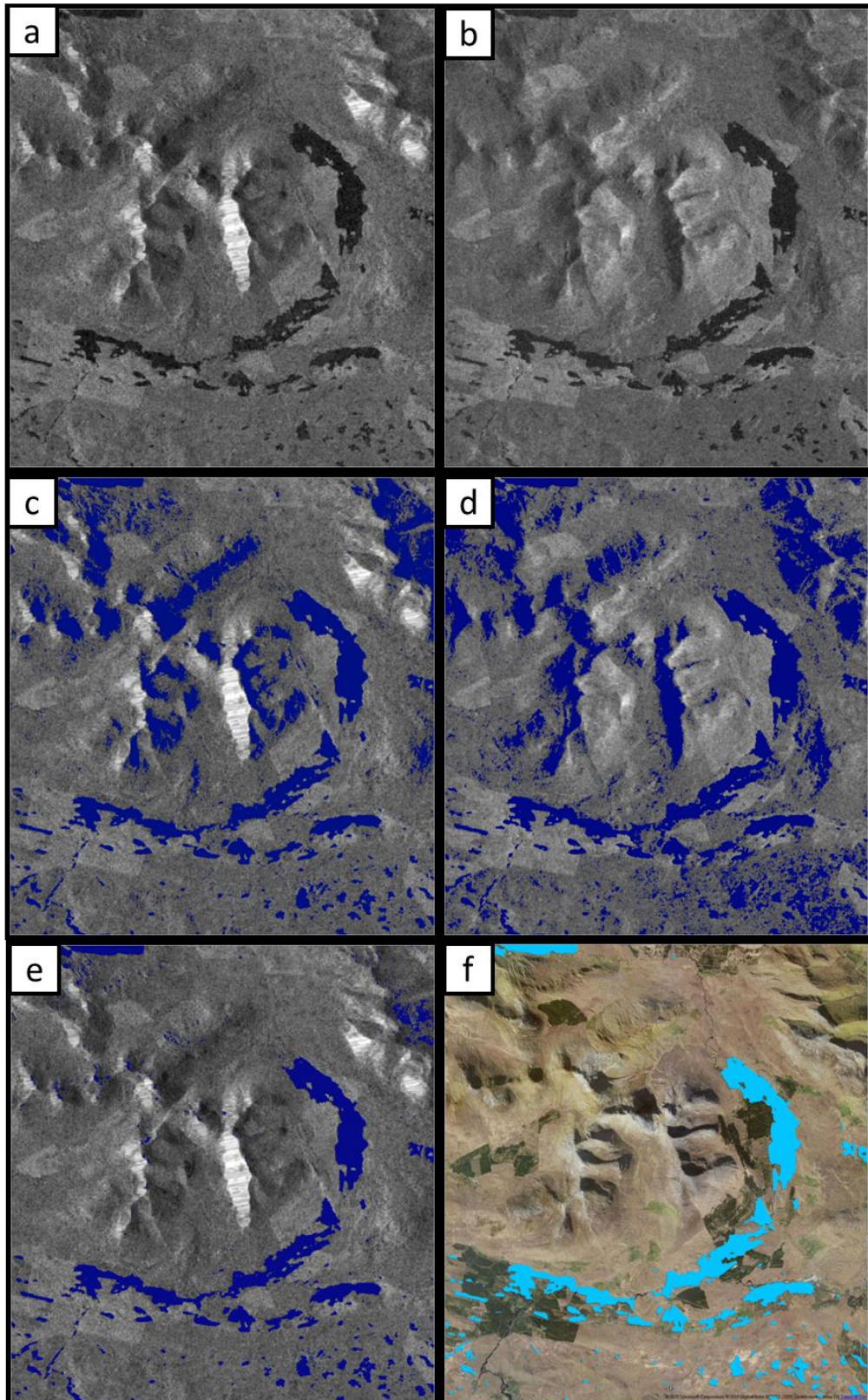


Figure 39: (a) ascending SAR image, (b) descending SAR image, (c) in dark blue water selected from ascending SAR image, (d) in dark blue water selected from descending SAR image, (e) in dark blue water selected using orbit filter and (f) in sky blue water bodies from EPA on top of aerial Bing image. Image Location: Connemara, Co. Galway, Ireland.

11.1.3 Contextual Filtering

11.1.3.1 Topographic Mask

The topographic mask is composed of four subproducts from the DTM including: 1) topographic hill, 2) topographic basin, 3) HAND masks, and 4) slope, and it was used as additional filter for ruling out false positives, such as radar shadow (Figure 40).

The topographic hill mask (Figure 40b) selects hills from the DTM where floods are unlikely to occur, and it is used to remove incorrectly delineated floods occurring on hillsides. The topographic basin mask selects topographic depressions from the DTM, and it is used to select regions where floods are possible. HAND represents the topographic difference between a pixel and the hydrologically determined nearest water course, and the HAND mask is a representation of the regions up to 5 m above the nearest water course where floods are also considered to be possible. The slope mask was combined with the HAND mask by removing areas of possible floods if changes in topography between neighbouring cells were larger than 5 m. Further details on the topographic masks are provided in Section 6.3. Figure 40c shows, in red, regions within topographic basin mask and HAND mask.

The topographic mask works by removing delineated floods occurring on the topographic hill mask, except if the flood is also within either the topographic basin mask or the HAND mask (Figure 40d, e). Figure 40f is used for comparison between the sub-products of this project and data from EPA.

11.1.3.2 Land Use Mask

Land use types which were susceptible to false positive values were omitted from the mapping process. This included airports, quarries, motorways and golf courses. Urban areas were also omitted from the mapping process as results in such areas were poor due to the combined effects of radar shadow, geometric distortion, flat surfaces and inadequate image resolution. Extents for the land use mask were obtained from Open Street Map and CORINE datasets.



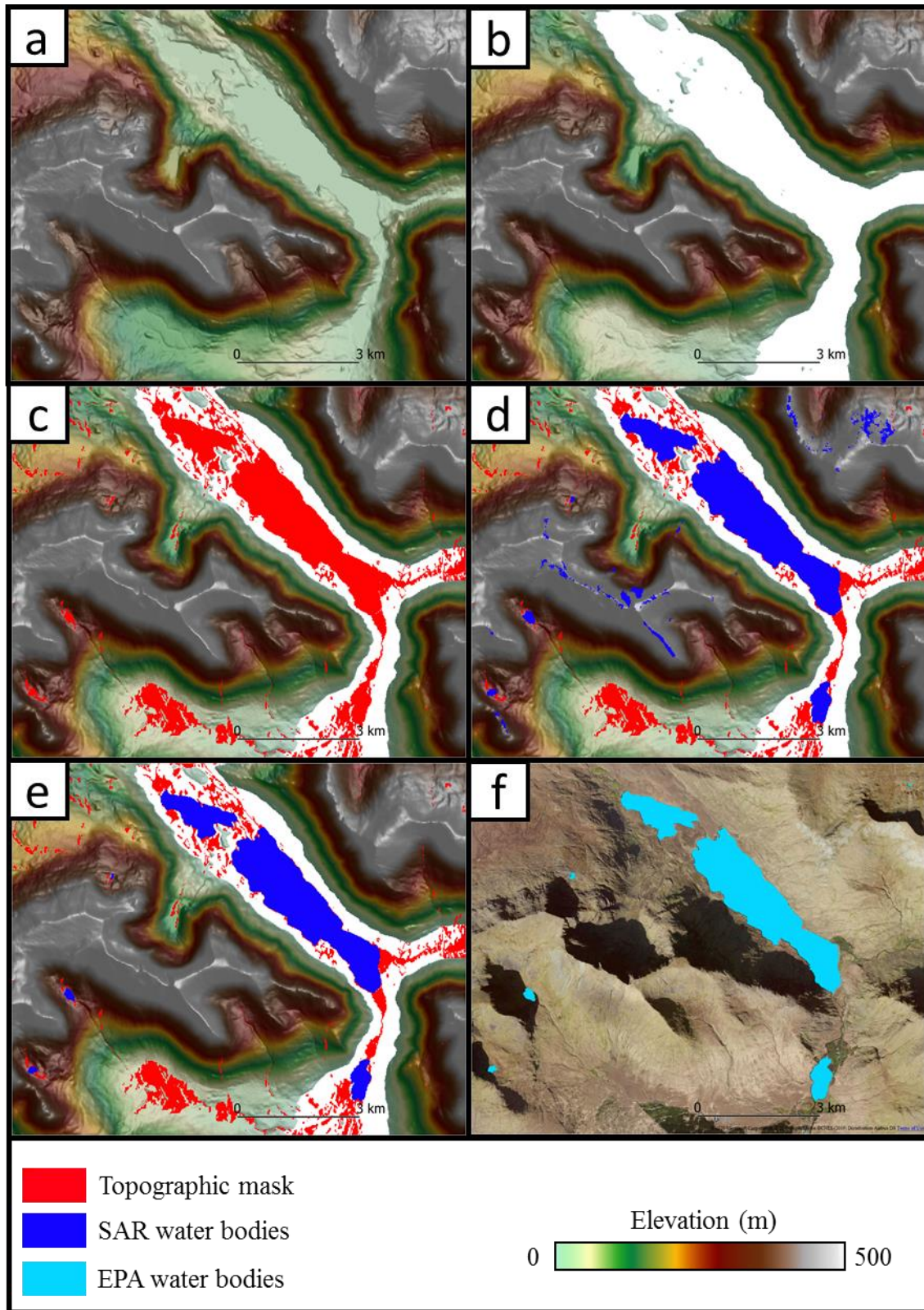


Figure 40: a) Topographic map surrounding Doo Lough (Co. Mayo), b) Topographic map considering only regions within the topographic hill mask, c) in red regions covered by HAND and topographic basin mask, d) in blue SAR water bodies considered after applying the orbit filter, e) in blue SAR water bodies considered after applying topographic filter, d) in sky blue water bodies from EPA on top of Bing Maps orthophotography.

11.1.3.3 Coastal Mask

Flooded pixels within 20 m of the coastline were omitted due to the uncertainty over their attribution as sea water or inland flooding.

11.1.4 Groundwater – Surface Water Classification

Groundwater flooding was distinguished from surface water flooding based on the following criteria:

1. Pure Limestone Bedrock

By definition, karst derived groundwater flooding only occurs on limestone bedrock. While a small number of groundwater floods are present on impure limestones, the overwhelming majority occur on pure limestones. This is due to the substantial amounts of clayey material in impure limestones restricting karstification (Drew, 2018). As such, only floods on pure limestones (according to GSI bedrock mapping) were considered likely to be of karst groundwater origin (unless already designated as a turlough).

2. Groundwater Vulnerability

Groundwater vulnerability embodies the characteristics of the intrinsic geological and hydrogeological features at a site that determine the ease at which water (and contaminants) can transmit from the land surface to groundwater. As a corollary, groundwater vulnerability can be utilised as an indicator for the likelihood of groundwater to emerge from bedrock to surface. In this context, only flooding occurring in areas of high to extreme vulnerability was considered to be of groundwater origin.

3. Consecutive Images

The flood must occur in at least four consecutive SAR images to be classified as groundwater, and at least two consecutive SAR images to be classified as surface water.

4. Isolation from Permanent Water Bodies

Any flood connected to a permanent lake or with a surface water channel draining into it was designated as a surface water flood. This criterion was overridden if a



surface water-linked flood was also designated as a turlough (or a partially groundwater-fed lake). In these instances, the flood was designated as having a mixed groundwater and surface water origin and listed as ‘GWSW’ in the groundwater flood shapefile. Note that floods classified as GW in contact with small rivers, were kept as GW floods if no other contribution from surface water was observed.

Floods that did not meet the criteria listed above were classed as surface water. If floods were unlinked to permanent water, but did not overlies high vulnerability pure limestones, they were designated as ‘SWp’ in the flood map attributes. This classification indicates a possible pluvial origin but also may simply indicate that the surface water feature associated with the flood is absent from permanent water dataset (e.g. small ditches and drains etc.). Table 6 summarizes the criteria used to select GWSW. Green means the flood must agree with the related groundwater flood criteria, in red that it does not meet the criteria, and white that the criteria was not relevant.

Table 6: Summary of the criteria followed to define types of flood. GW: Groundwater flood, GWSW: Floods with significant contribution of both groundwater and surface water, SW: surface water flood, SWp: Isolated floods not classified as GW. Green means the flood has to agree with the related criteria, in red that it has to disagree, and white that the criteria was not relevant.

	Pure Limestone Bedrock	Groundwater Vulnerability	Consecutive Images	Isolation from Permanent Water Bodies
GW			4	
GWSW			4/2	
SW			2	
SWp			2	

11.2 Topographic Correction

An automated process was developed in which flood boundaries from thresholded and filtered SAR images were cross-referenced against topographic data to calculate the elevation of the land-water interface. This calculated flood elevation was then combined with topographic mapping to delineate a topographically corrected flood extent (which



was output in vector format). This filter was only applied to flooding occurring in enclosed isolated basins which can be assumed to have a uniform elevation value, and which are large enough to confidently calculate the mean elevation. As such, floods that overspill their topographic basins were not topographically corrected as they can no longer be assumed to be flat. In these instances, the flood was delineated as the highest possible closed contour. In order to address this overspill limitation (as well as errors caused by localised inaccuracies of the DTM), the original SAR flood object was re-added and merged with the topographically corrected flood object. In this manner, the purpose of the topographic correction process was only to add 'missing' pixels (e.g. forested areas) to a SAR derived flood object but not to remove pixels from SAR flood objects. Floods that were too small for topographic correction were converted directly from raster format to vector format without altering shape. The process is shown in Figure 41 and consists of the following steps:

1. Isolate flooded pixels at the land-water interface that are removed from vegetated areas (non-covered black line in Figure 41b) and calculate the mean elevation value of the pixels from a DTM.
2. Calculate a 'representative point' for the flood object. This point should be a specific location within the flood object that is certain to be within any delineated polygon. It is calculated as the pixel with lowest elevation value within the flood object (white points in Figure 41b).
3. Generate the closed contour for the calculated flood level that completely encircles the representative point. Convert this contour polyline to a polygon (Figure 41c).

This process assumes that the DTM completely controls the flood extent shape and so does not account for any artificial modifications to the flood extent such as flood defence barriers.

It should be noted that this boundary-based method for calculating flood elevation is different to the area based approach used for hydrograph generation (Section 8.2). As the historic map is observing floods at their peak size, there are sufficient flood boundary pixels to confidently calculate their mean elevation. In contrast, the hydrograph generation



process interpreted floods at all stage levels, and as such, there were often too few boundary pixels to confidently calculate elevation. Instead, the hydrograph generation proved more accurate by calculating the flooded area and using a stage-area curve to convert to stage. As the boundary-based method was of comparable accuracy and less computationally intense than the area based method (for large floods), it was the preferred method for the historic flood map.



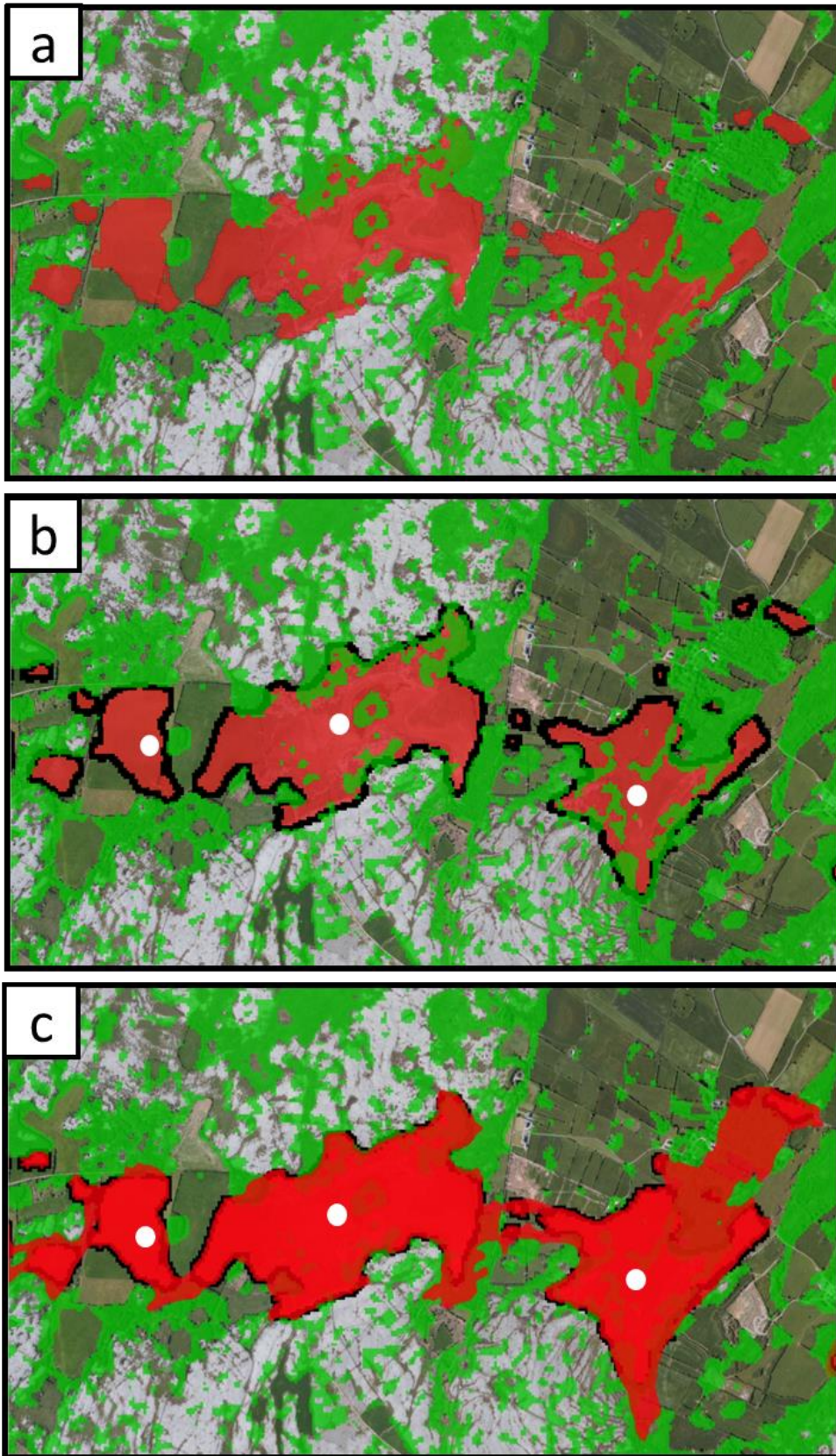


Figure 41: Topographic correction process. (a) SAR delineated flood (red) with surrounding vegetation mask (green), (b) Flood boundary delineated (black) and representative points located (white), (c) Topographic flood delineated (red).

11.3 Application of Supplementary Evidence

Upon completion of the Sentinel-1 based flood map, supplementary evidence for any historic floods that exceed the GSI SAR derived map was added. This included Copernicus Emergency Management Service Rapid Mapping (EMSRI) for the 2015/2016 floods (activations: EMSRI149, EMSRI154 and EMSRI156). This SAR data were acquired at a small number of specific locations using contributing missions to the Copernicus program (e.g. Cosmo-Skymed, TerraSAR-X). Compared to the primary Sentinel-1 mission, these specifically tasked missions operate on smaller target areas but provide higher resolution flood extent products, and as such their mapping products were integrated into both the groundwater and surface water flood maps. However, it should be noted that upon inspection some false positives were found in the EMSRI dataset due to radar shadow and artificial flat surfaces. As such, only selected EMSRI flood objects were used.

In addition, some non-SAR based flood mapping was applied to the groundwater flood map (but not the surface water flood map). This included: aerial photography of the 2009 and 2015/2016 floods (provided by the OPW) and previous flood level reporting such as Naughton (2013), McCormack and Naughton (2016), Ryan Hanley Consulting Engineers (2018) and Ryan Hanley Consulting Engineers (2019).

In February 2020 a groundwater flooding event occurred which was found to show higher flooding in some areas (primarily north Galway and South Mayo) than had occurred over winter 2015/2016. These floods were added manually based on interpretation of Sentinel-2 imagery.

11.4 Dataset Merging

Once floods were delineated, classified, and corrected for each subset defined in Figure 20a, the resulting shape files were merged to create: 1) the national historic groundwater flood map, and 2) the national surface water flood map for 2015/2016. As the subsets had an overlap area between them, there were often a number of duplicate polygons for a given flood. These duplicate polygons were not necessarily identical as they may have derived from different imagery. The overlapping flood polygons were merged, and their



attributes recalculated as appropriate (e.g. if the flood levels were different, the higher flood level was used).

11.5 Manual Editing

The final step of developing the historic flood map was to manually check and remove misclassifications. This step was primarily required due to missing data or misclassifications (e.g. unmapped quarries) in the datasets used by land use mask as discussed in Section 11.1.3.2. Unmapped features such as quarries, golf courses or football pitches which return low backscatter signal and were often incorrectly interpreted as ‘flooded’. It should be noted that due to their manual removal, any ‘true’ flooding occurring at these locations is not included in the flood map.

11.6 Historic Flood Map Limitations and Assumptions

The accuracy of the historic map is subject to a series of assumptions and limitations. The chief limitations are listed below:

1. Identification of Maximum Flood Extents

- The identification of floods as the “maximum historic” extent could only be based on information available at the time of mapping. A lack of flooding presented in any specific location of the map only indicates that a flood was not identified using the described methodology. It does not indicate that a flood cannot occur in that location at present or in the future.
- At the time the map was produced (late 2019), it was assumed that the Winter 2015/2016 flood extent was the largest groundwater flood on record.

2. Flood Delineation using SAR

- Floods smaller than 6 connected pixels are omitted as a noise reduction measure. In addition, long and thin floods (e.g. some rivers) are undetectable to SAR.
- Urban areas are excluded from the flood map due to poor accuracy.
- The fundamental assumption of the SAR flood delineation process is that flat surfaces are classified as water. This assumption can result in false positive



classifications on dry flat land (e.g. airfields, sports pitches) or false negatives due surface roughness on water bodies in windy conditions.

- The presence of vegetation interferes with water classification of SAR imagery. Whilst topographic corrections were applied to mitigate this interference, the correction could only be applied flat surfaced floods (i.e. not rivers, or groundwater floods exceeding their topographic basins).
- Whilst the overall effect of the topographic correction algorithm improves the precision of the flood maps by removing false negatives, it may also cause false positives as it omits the impact of temporary flood defence measures which are not present in the DTM (e.g. sand-bag flood barriers).

3. External Datasets

The accuracy of the delineation and classification (groundwater or surface water) of water bodies was dependent on a number of filtering steps using external data (DTMs, land use data). The ultimate accuracy of the flood map is tied to the accuracy of these external datasets.

11.7 Shapefile Description

The full list of shapefile attributes of the historic groundwater and 2015/2016 surface water flood maps are presented in Table 7 below, and the flood maps are presented in Figure 42.




Table 7: Shapefile Attribute descriptions for Groundwater and Surface water shapefiles.

Field Name	Description
Id	A unique identifier number.
Flood_type	A description of the designated type of flooding. Polygons can be the following: <ul style="list-style-type: none"> • ‘GW’ – Flooding derived solely from groundwater sources. • ‘GWSW’ – Floods likely to be of both groundwater and surface water origin. These floods include lakes and rivers with an apparent groundwater contribution. • ‘SW’ - Flooding derived from surface waters (primarily fluvial). • ‘SWp’ – Surface water flooding which is likely to be of pluvial origin.
Source	The source of data used to produce flood polygon (e.g. SAR imagery, aerial photos, external reports).
Area_m2	The area of the flood extent in meters ²



Maximum Historic Groundwater Flood Map (and Winter 2015/2016 surface water flood extent)

Legend

-  Max historic groundwater flood extent
-  Max historic groundwater/surface water flood extent
-  Winter 2015/2016 surface water flood extent

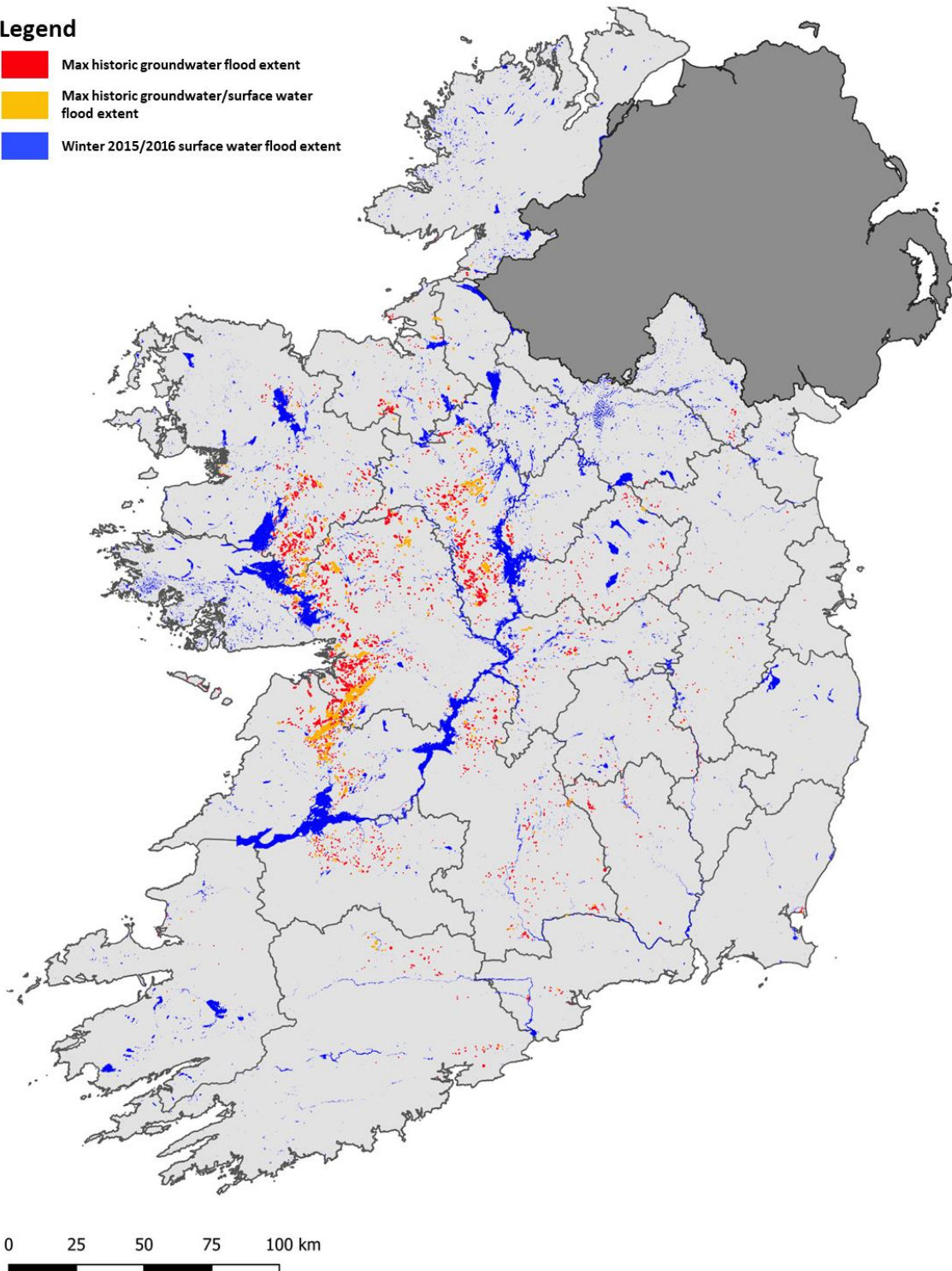


Figure 42: National historic groundwater flood map (including 2015/2016 surface water flood extent)

12 Predictive Groundwater Flood Map

The predictive groundwater flood map presents the probabilistic flood extents for locations of recurrent karst groundwater flooding. The map shows areas predicted to be inundated during a theoretical or 'design' flood event with an estimated probability of occurrence, rather than information for actual floods that have occurred in the past, which is presented on the historic flood map. The map refers to flood event probabilities in terms of a percentage Annual Exceedance Probability, or 'AEP'. This represents the probability of an event of this, or greater, severity occurring in any given year. These probabilities could also be expressed as a return period (e.g. the 100-year flood). Three probabilities of groundwater flood map were generated: high (10% AEP), medium (1% AEP) and low (0.1% AEP). These are presented in Table 8 below. The probabilities are calculated for the present day (or current) scenario and do not take into account of potential changes due to climate change.

Table 8: Shapefile details for each Annual Exceedance Probability (AEP). It should be noted that the number of individual polygons decreases with increasing flood severity due to floods merging together at higher levels

Annual Exceedance Probability (%)	Odds of Occurrence in an Given Year	Return Period (Years)	Flooded area (km ²)	Number of individual floods/polygons
10 (High Probability)	10:1	10	126.38	554
1 (Medium Probability)	100:1	100	150.97	485
0.1 (Low probability)	1000:1	1000	163.41	466

The map is focussed primarily (but not entirely) on flooding at seasonally inundated wetlands known as turloughs. These sites were chosen for inclusion in the predictive map based on existing turlough databases as well as manual interpretation of SAR imagery. The mapping process tied together the observed and SAR-derived hydrograph data, hydrological modelling, stochastic weather generation and extreme value analysis to generate predictive groundwater flood maps for 440 qualifying sites. The overall objective of the method is to generate a hydrological record of sufficient length to estimate the magnitude and frequency of extreme groundwater flood events.



Whilst the map includes flood extents at the majority of known turloughs, it should be noted that it is not a comprehensive datasets of groundwater flooding. The map is limited to locations where the flood pattern was detectable and capable of being hydrologically modelled to a sufficient level of confidence.

The components required for estimating probabilistic flood levels in turloughs have been discussed in previous sections (Sections 7, 8 and 9) and their relationships are presented in Figure 43. In this Section, the mapping procedure is discussed, and the shapefile attributes are listed.

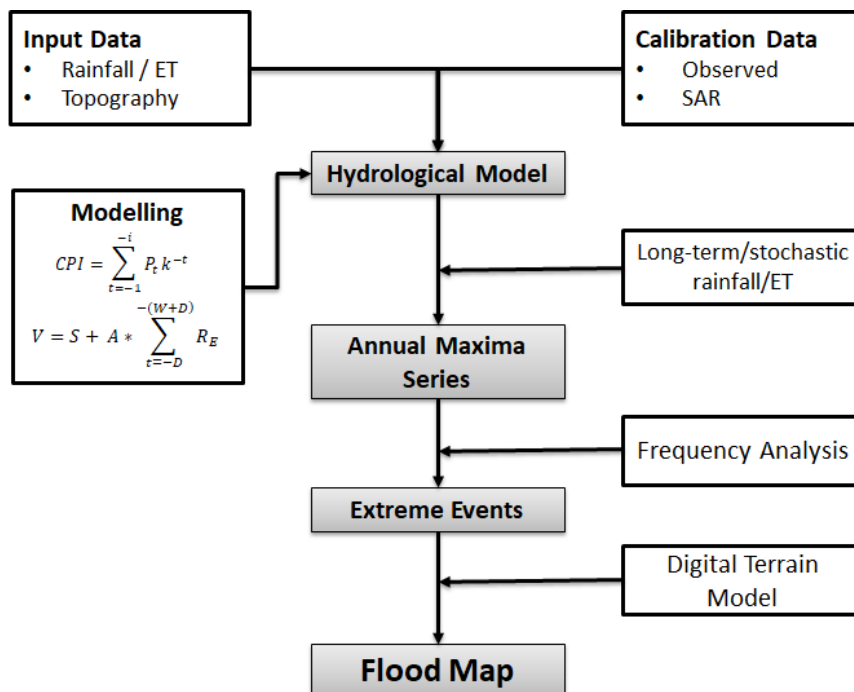


Figure 43: Flow chart for predictive groundwater flood mapping methodology.

12.1 Mapping Methodology

Once the AEP levels were calculated (Section 9), the final stage of producing the predictive map was to delineate polygons at each site for their specific AEP flood levels. Similarly to the historic flood topographic correction procedure (Section 11.2), the mapping procedure was based on isolating a contour of specified elevation that encircles a representative point within the flood. However, unlike the historic map method which automatically calculates the representative points, the predictive map used the preselected 'hydrograph



reference points' (Section 8.2.1) to isolate the appropriate contour. While this process was sufficient for the majority of flood locations, some site-specific alterations were required. These alterations are outlined in the following sub-sections.

12.1.1 Hydraulically Connected Basins

As mentioned above, the mapping process is based solely on the DTM and involves generating one flood polygon per reference point (i.e. per modelled flood). However, in some instances a flood requires more than one polygon in order to be adequately delineated. These multipart floods occur when subsurface hydraulic connectivity exists between separate topographic basins (or when the DTM lacks the resolution to identify narrow surface connections). These hydraulic connections, which may be due to natural karst connectivity or anthropogenic causes (e.g. culverts beneath road embankments), were allowed for in the mapping process by copying the modelled AEP levels to selected neighbouring un-modelled basins. See Figure 44 for an example of mapping a hydraulically connected basin.

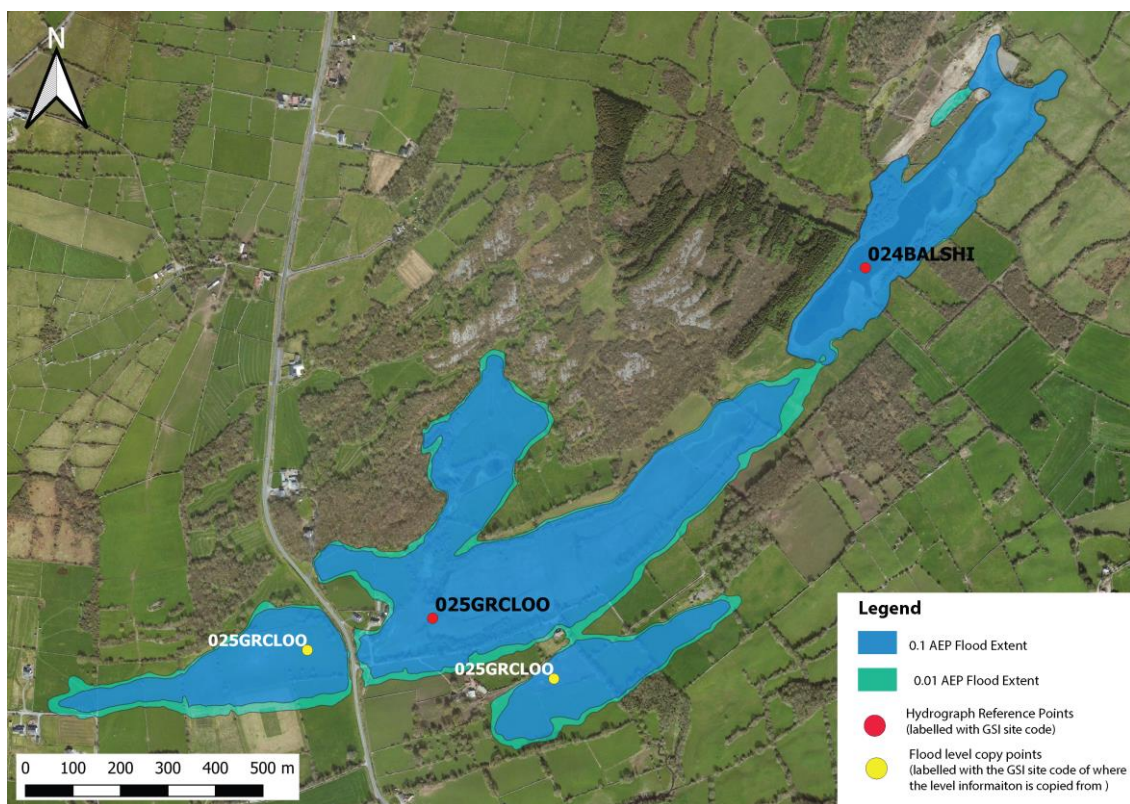


Figure 44: Mapping multipart floods near Cross, Co. Mayo. The primary basin of Garracloon turlough (red point labelled '025GRCLOO') is hydraulically linked to two nearby basins to the west and south (yellow points). The yellow points represent where additional flood mapping is completed for unmodelled basins with the white text label designating where the flood level is matched to.

12.1.2 Overspill Allowance

AEP flood levels that exceeded their topographical basins were capped at the overspill level, and thus produce identical flood polygons for multiple AEP levels. While this is deemed appropriate at certain sites in which the flooding is known to be topographically limited, many sites were incorrectly limited by the DTM. This is often due to river channels causing a low overspill value to be calculated by the DTM when in reality the river channel would also be flooded. Sites such as these were altered to allow flooding in excess of the topographic overspill up to a specified depth. This was implemented by creating a polyline feature to denote topographic boundaries (or walls) where the DTM needed to be altered. These walls were then translated (or burnt) onto the DTM during the flood delineation process resulting in transformed contour lines which better represented the true flood extent. See Figure 45 for an example of applying a topographic boundary to Rahasane turlough in Co. Galway.

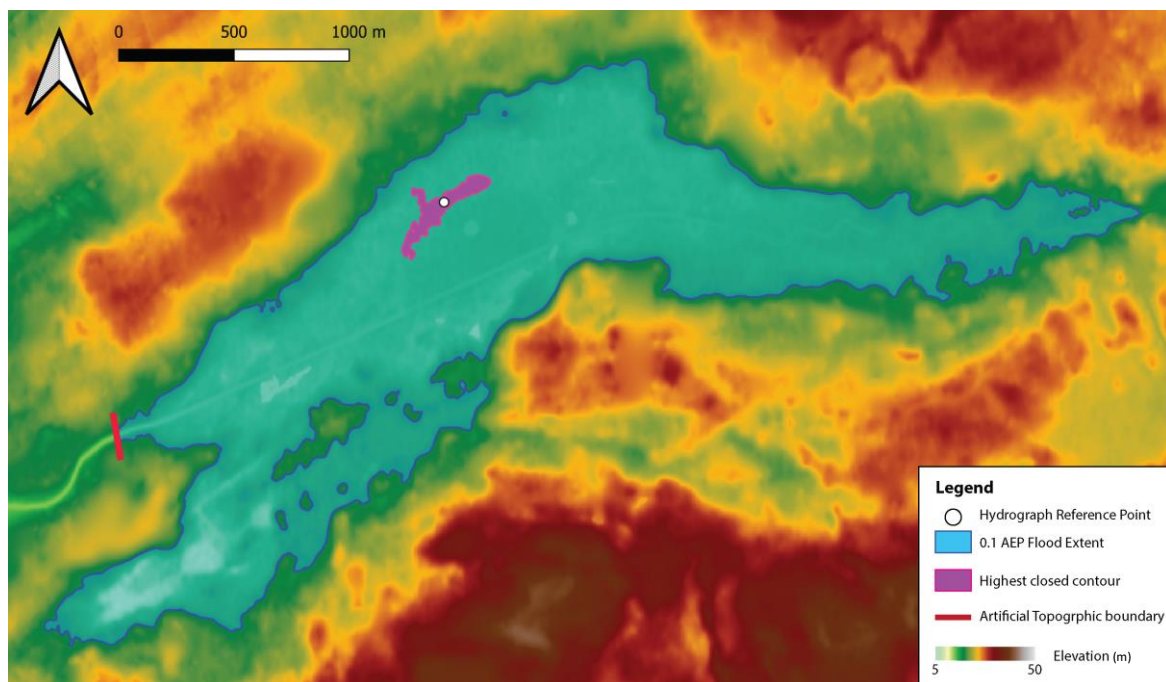


Figure 45: Example of an artificial topographic boundary to enable appropriate flood delineation at Rahasane turlough, Co. Galway. Due to an exaggerated river channel in the DTM, the pink polygon represents the highest possible closed polygon encircling the reference point (white dot). This is corrected by artificially blocking the river channel (red line) to allow a closed contour at the calculated flood level.

In some locations, such as the Gort Lowlands in South Galway, flooding occurs as a series of over-spilling water bodies interlinked by overland flood channels. In these instances, the

overspill channels are a significant component of the flood extent and the flood delineation process was adapted to include them. While some of these overspill channels were modelled explicitly as part of the TCD research project (Section 10), many were not. For these un-modelled channels, the downstream (lower) and upstream (higher) floods were mapped as flat surfaces and the overspill walls were used to step between them (rather than the floods overlapping).

12.2 TCD Gort Lowlands Sites

The results of the TCD research project were directly incorporated into the flood map. This included AEP levels for 16 turloughs/lakes as well as five overland flow channels which were modelled using local 2D hydraulic models. While these sites were modelled in collaboration with the South Galway Flood Relief Scheme, the flood extents used in the GSI predictive flood solely represent the outputs of the research project (and not the flood scheme). The finalised flood scheme maps were not released at the time of the GSI map publication. See Figure 46 for locations of the TCD model sites.

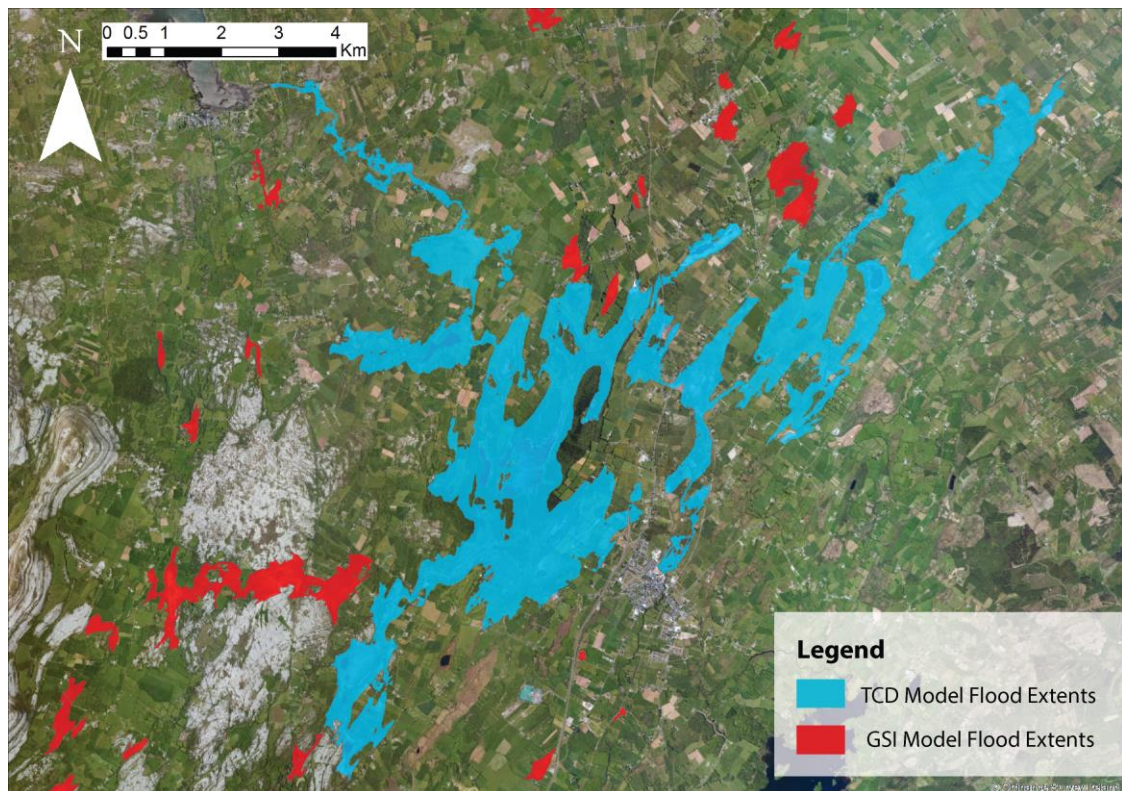


Figure 46: Locations of TCD research project sites integrated into the GSI predictive flood map.

12.3 Predictive Flood Map Limitations and Assumptions

The accuracy of the predictive map is subject to a series of assumptions and limitations. The chief limitations are listed below:

1. Site Selection and Definition of Groundwater Flooding

The predictive flood map was focussed primarily (but not entirely) on flooding at seasonally inundated karst wetlands known as turloughs. These sites were chosen for the predictive map based on existing turlough databases as well as manual interpretation of SAR imagery. While these sites are the most common and impactful sources of groundwater flooding in Ireland, they are not the only sources, and as such, the map should not be considered as a comprehensive dataset of groundwater flooding in Ireland.

2. Data Collection

The predictive flood map could only be generated for sites where the flood pattern was observed, either via physical monitoring or remote sensing. Ungauged turloughs that were too small or too obscured by vegetation for their flood pattern to be quantifiable were omitted from the flood map.

3. Modelling

- The hydraulic models are only functional while a turlough remains within its topographic basin. Once a turlough exceeds its basin, different hydrological processes are occurring which require site specific modelling. In this context, the predictive flood extents at some turloughs are capped by the spill point of their topographic basin (it is assumed that a turloughs do not continue rising once they are spilling out of their basin). It is for this reason that some turloughs demonstrate identical flood extents for multiple AEPs.
- The hydrological modelling procedure was not effective at all attempted sites. If a model could not be calibrated it was omitted from the map.
- Some turloughs did not flood regularly enough to provide enough calibration data for modelling. These sites were omitted from the flood map.



- The modelling process assumes steady state conditions in the turloughs throughout the calibration period (i.e. no subterranean collapses or blockages of swallow holes).

4. Flood Delineation

Predictive flood polygons were delineated based on their calculated flood elevation and the DTM. As such, the polygons represent the flooding that would happen according to the topography and they do not account for the impact of temporary flood defence measures which are not present in the DTM (e.g. sand-bag flood barriers).

5. External Datasets

The accuracy of the SAR derived hydrographs and hydraulic models are dependent on a number of external datasets, particularly the DTM. Inaccuracies in these datasets cause knock-on inaccuracies to the predictive mapping process.

12.4 Shapefile Description

Shapefiles were produced for three probabilities: high (10% AEP), medium (1% AEP) and low (0.1% AEP). The list of attributes for each shapefile are presented in Table 9 and a sample map showing the predictive and historic flood extents in shows in Figure 47

Table 9: Predictive Flood Map Shapefile Attributes.

Field Name	Description
Id	A unique identifier number
Mdl_source	The source of the hydrological model used to produce a polygon (GSI or TCD)
Area_m2	The area of the flood extent in meters ²



Legend

- Max historic groundwater flood extent
- Max historic groundwater/surface water flood extent
- 0.1 AEP groundwater flood extent
- 0.01 AEP groundwater flood extent
- 0.001 AEP groundwater flood extent

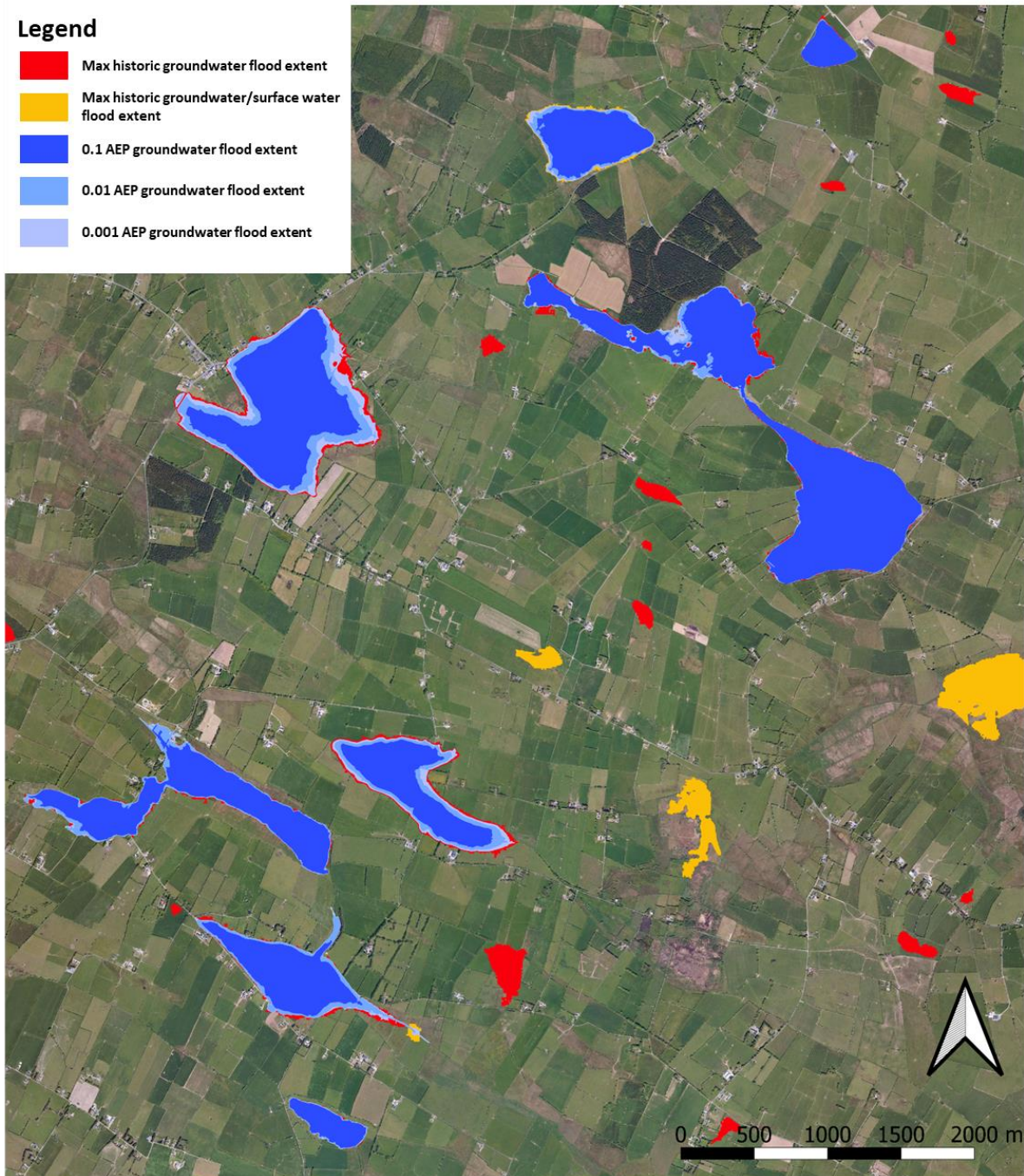


Figure 47: Sample map showing predictive and historic groundwater flood extents at Rathcroghan, Co. Roscommon.

13 Project Recommendations and Future Developments

13.1 Recommendations

Upon completion of the GWFlood project, a series of recommendations were outlined to the technical steering committee. These are listed below.

13.1.1 Capacity Building in Long-Term Groundwater Observation

Long-term multidisciplinary observational data are essential for the sustainable management of water resources and tackling the challenges resulting from global change. However, currently neither the data nor sufficient observational infrastructure exists in Ireland for addressing current and future risks to groundwater and groundwater-dependent ecosystems. GSI could address this deficit could by applying the multidisciplinary scientific approach taken by the GWFlood project to key groundwater and wetland systems representative of Irish geological and climatic conditions.

The remit of such capacity building in long-term groundwater observation would be to monitor and understand the effects of droughts, floods and other climate variability on groundwater levels and groundwater dependent ecosystems in Ireland. This would advance understanding of climate change impacts on groundwater resources, address the deficit of data available in this area and enable scientifically-informed adaptation planning for the groundwater sector. Furthermore, it would assist the EPA and NPWS in their obligations to both the EU Water Framework Directive (2000/60/EC) and EU Habitats Directive (92/43/EEC) which necessitate the monitoring and management of turloughs habitats to ensure favourable conservation and groundwater status.

13.1.2 Non-karst Groundwater Flooding

The GWFlood project focussed on flooding caused by the emergence of groundwater from karstified bedrock. While this is the most common and impactful form of groundwater flooding in Ireland, it is not the only form. Other forms include flooding from permeable superficial deposits (e.g. water moving laterally through a river embankment and flooding surrounding land), groundwater rebound or urban groundwater flooding. These forms of



flooding are anecdotally known to occur in Ireland yet their impacts have not been quantified. These non-karst groundwater flooding mechanisms should be explored by GSI.

13.1.3 Further Development of Remote Sensing Mapping Tools

The production of the historic and predictive groundwater flood maps necessitated the development of Sentinel-1 processing tools. Whilst these tools have served their purpose under the GWFlood project, they are readily adaptable for future earth observation endeavours by GSI. Future enhancements to the Sentinel-1 processing tools should include: 1) automated national flood mapping at regular intervals or after extreme rainfall events, 2) extending the hydrograph generation process to near real-time, and 3) extending the hydrograph generation process to permanent surface water features. Furthermore, the predictive groundwater flood maps should be re-evaluated at a future date when lengthier satellite derived hydrometric datasets are available to calibrate hydrological models.

13.1.4 Groundwater Flood Forecasting

The potential application of near real-time groundwater flood monitoring and modelling developed during this project to groundwater flood forecasting should be examined. Such a system could be developed to provide dynamic information regarding impending groundwater flood risk, and could ultimately integrate into the Met Éireann National Flood Forecasting and Warning Service. This would enable local communities, businesses and authorities to pre-empt groundwater flood emergencies.

13.1.5 Impacts of Climate Change on Groundwater Flooding

Climate change will be a major driving force in shaping Ireland's water resources and natural environment in coming decades. The latest downscaled climate change data for Ireland could be interpreted using established hydrological models to quantify and analyse the potential impact of climate change on karst groundwater systems in terms of flood duration, frequency, and extent.



13.2 Future Developments

In January 2020 GSI initiated a new three year climate change focussed project: GWClimate. This project was designed to build from the experience gained through the GWFlood project and will address many of the GWFlood project recommendations. The primary aims of GWClimate are 1) to establish a long-term strategic groundwater level monitoring network and 2) to develop modelling and analytical approaches for evaluating the impacts of Climate Change to Irish groundwater systems.

A series of focussed hydrometric observatories will be deployed at specific groundwater systems where climate change is anticipated to have an impact on groundwater. Observatory sites will be thoroughly instrumented to provide long term level and physicochemical reference data. Observatory sites will be modelled and their groundwater system behaviour assessed at both short- (flood forecasting) and long- (climate change impact) timescales. The data and analyses will greatly improve the national capacity to understand how groundwater resources respond to climatic stresses and improve the reliability of planning and forecasting, which will inform climate adaptation strategies. Specifically, the work will support decision-making for:

- Areas impacted by groundwater flooding due to changes in rainfall amounts and timing.
- Areas impacted by reduced groundwater recharge (“drought issues”) due to seasonally lower precipitation and higher temperatures, which will have direct consequential impacts on sustainable water supplies for clean drinking water, agricultural and industrial uses, and ecosystems.

The GWClimate project will make significant advances in meeting obligations under the National Climate and Biodiversity Emergency, the National Adaptation Framework, recommendations from the Citizen’s Assembly on Climate Change and the All of Government Climate Action Plan to Tackle Climate Breakdown.



14References

- ABBOUD, J. M., CATHRYN RYAN, M. & OSBORN, G. D. Groundwater Flooding in a River-Connected Alluvial Aquifer. *Journal of Flood Risk Management*.
- ANDERS, N. S., SEIJMONSBERGEN, A. C. & BOUTEN, W. 2011. Segmentation optimization and stratified object-based analysis for semi-automated geomorphological mapping. *Remote Sensing of Environment*, 115, 2976-2985.
- ANTONIĆ, O., HATIĆ, D. & PERNAR, R. 2001. DEM-based depth in sink as an environmental stimator. *Ecological Modelling - ECOL MODEL*, 138, 247-254.
- ASCOTT, M. J., MARCHANT, B. P., MACDONALD, D., MCKENZIE, A. A. & BLOOMFIELD, J. P. 2017. Improved understanding of spatio-temporal controls on regional scale groundwater flooding using hydrograph analysis and impulse response functions. *Hydrological Processes*, 31, 4586-4599.
- BAZI, Y., BRUZZONE, L. & MELGANI, F. 2007. *Image thresholding based on the EM algorithm and the generalized Gaussian distribution*, Elsevier Science Inc.
- BESCHTA, R. L. 1998. Forest hydrology in the Pacific Northwest: additional research needs. *JAWRA Journal of the American Water Resources Association*, 34, 729-741.
- BRISCO, B., TOUZI, R., VAN DER SANDEN, J. J., CHARBONNEAU, F., PULTZ, T. J. & D'IORIO, M. 2008. Water resource applications with RADARSAT-2 – a preview. *International Journal of Digital Earth*, 1, 130-147.
- BRIVIO, P. A., COLOMBO, R., MAGGI, M. & TOMASONI, R. 2002. Integration of remote sensing data and GIS for accurate mapping of flooded areas. *International Journal of Remote Sensing*, 23, 429-441.
- CHEN, J., BRISSETTE, F. P. & LCONTE, R. 2010. A daily stochastic weather generator for preserving low-frequency of climate variability. *Journal of hydrology*, 388, 480-490.
- CHINI, M., HOSTACHE, R., GIUSTARINI, L. & MATGEN, P. 2017. A Hierarchical Split-Based Approach for Parametric Thresholding of SAR Images: Flood Inundation as a Test Case. *IEEE Transactions on Geoscience and Remote Sensing*, 55, 6975-6988.
- CLEMENT, M. A., KILSBY, C. G. & MOORE, P. 2017. Multi-temporal synthetic aperture radar flood mapping using change detection. *Journal of Flood Risk Management*, n/a-n/a.
- COBBY, D., MORRIS, S., PARKES, A. & ROBINSON, V. 2009. Groundwater flood risk management: advances towards meeting the requirements of the EU floods directive. *Journal of Flood Risk Management*, 2, 111-119.
- COPERNICUS EMERGENCY MANAGEMENT SERVICE 2016a. (© 2016 European Union), [EMSRI149] Floods in Ireland: Delineation Map.
- COPERNICUS EMERGENCY MANAGEMENT SERVICE 2016b. (© 2016 European Union), [EMSRI154] Floods in Roscommon: Delineation Map.
- COPERNICUS EMERGENCY MANAGEMENT SERVICE 2016c. (© 2016 European Union), [EMSRI156] Floods in Roscommon II: Delineation Map.
- COXON, C. E. 1986. *A Study of the hydrology and geomorphology of turloughs*. Ph.D. (unpublished), Department of Geography, Trinity College Dublin.
- DEKKER, R. J. 1998. Speckle filtering in satellite SAR change detection imagery. *International Journal of Remote Sensing*, 19, 1133-1146.
- DOHERTY, D. 2019. Gort Lowlands Karst Multi-Dye Trace. Geological Survey Ireland.



- DOHERTY, D., DUNCAN, N. & KELLY, C. 2018. Groundwater Trace at Neale, April 2018. Geological Survey Ireland.
- DOSTÁLOVÁ, A., HOLLAUS, M., MILENKOVIĆ, M. & WAGNER, W. 2016. FOREST AREA DERIVATION FROM SENTINEL-1 DATA. *ISPRS Annals of Photogrammetry, Remote Sensing and Spatial Information Sciences*, III-7, 227-233.
- DREW, D. 2018. *Karst of Ireland: Landscape Hydrogeology Methods*. , Dublin, Geological Survey Ireland.
- EUROPEAN SPACE AGENCY. 2020a. *Sentinel-1 SAR Technical Guide* [Online]. Available: <https://sentinel.esa.int/web/sentinel/technical-guides/sentinel-1-sar> [Accessed January 2020 2020].
- EUROPEAN SPACE AGENCY. 2020b. *Sentinel-1 SAR User Guide* [Online]. Available: <https://sentinels.copernicus.eu/web/sentinel/user-guides/sentinel-1-sar> [Accessed 18th January 2020].
- FILIPPONI, F. 2019. Sentinel-1 GRD Preprocessing Workflow. *Proceedings*, 18, 11.
- FINCH, J. W., BRADFORD, R. B. & HUDSON, J. A. 2004a. The spatial distribution of groundwater flooding in a chalk catchment in southern England. *Hydrological Processes*, 18.
- FINCH, J. W., BRADFORD, R. B. & HUDSON, J. A. 2004b. The spatial distribution of groundwater flooding in a chalk catchment in southern England. *Hydrological Processes*, 18, 959-971.
- GILL, L. W., NAUGHTON, O. & JOHNSTON, P. 2013a. Modelling a network of turloughs in lowland karst. *Water Resources Research*, 49, 3487-3503.
- GILL, L. W., NAUGHTON, O., JOHNSTON, P. M., BASU, B. & GHOSH, B. 2013b. Characterisation of hydrogeological connections in a lowland karst network using time series analysis of water levels in ephemeral groundwater-fed lakes (turloughs). *Journal of Hydrology*, 499, 289-302.
- GOTKOWITZ, M. B., ATTIG, J. W. & MCDERMOTT, T. 2014. Groundwater flood of a river terrace in southwest Wisconsin, USA. *Hydrogeology Journal*, 22, 1421-1432.
- HUGHES, A. G., VOUNAKI, T., PEACH, D. W., IRESON, A. M., JACKSON, C. R., BUTLER, A. P., BLOOMFIELD, J. P., FINCH, J. W. & WHEATER, H. S. 2011. Flood risk from groundwater: examples from a Chalk catchment in southern England. *Journal of Flood Risk Management*, 4, 143-155.
- JACOBS 2004. Strategy for flood and coastal erosion risk management: Groundwater Flooding Scoping Study (LDS 23). Final Report for Defra. .
- KELLY, C. 2018. Groundwater Trace at Neale, County Mayo, February/March 2018. Geological Survey Ireland.
- KOHLER, M. A. & LINSLEY, R. K. 1951. *Predicting the runoff from storm rainfall*, US Department of Commerce, Weather Bureau.
- KOVACS, A. & SAUTER, M. 2007. Modelling karst hydrodynamics. In: GOLDSCHIEDER, N. & DREW, D. (eds.) *Methods in karst hydrogeology*. Taylor & Francis.
- LEE, J. S., JURKEVICH, L., DEWAELE, P., WAMBACQ, P. & OOSTERLINCK, A. 1994. Speckle filtering of synthetic aperture radar images: A review. *Remote Sensing Reviews*, 8, 313-340.
- LEE, K. T. & HUANG, J.-K. 2013. Runoff simulation considering time-varying partial contributing area based on current precipitation index. *Journal of Hydrology*, 486, 443-454.



- MANAVALAN, R. 2018. Review of synthetic aperture radar frequency, polarization, and incidence angle data for mapping the inundated regions. *Journal of Applied Remote Sensing*, 12, 021501.
- MANJUSREE, P., PRASANNA KUMAR, L., BHATT, C. M., RAO, G. S. & BHANUMURTHY, V. 2012. Optimization of threshold ranges for rapid flood inundation mapping by evaluating backscatter profiles of high incidence angle SAR images. *International Journal of Disaster Risk Science*, 3, 113-122.
- MARTINIS, S., KERSTEN, J. & TWELE, A. 2015. A fully automated TerraSAR-X based flood service. *ISPRS Journal of Photogrammetry and Remote Sensing*, 104, 203-212.
- MATGEN, P., HOSTACHE, R., SCHUMANN, G., PFISTER, L., HOFFMANN, L. & SAVENIJE, H. H. G. 2011. Towards an automated SAR-based flood monitoring system: Lessons learned from two case studies. *Physics and Chemistry of the Earth, Parts A/B/C*, 36, 241-252.
- MAYES, E. 2008. Turlough Database Consolidation Project. Unpublished report for National Parks & Wildlife Service.
- MCCARTHY, M., SPILLANE, S., WALSH, S. & KENDON, M. 2016. The meteorology of the exceptional winter of 2015/2016 across the UK and Ireland. *Weather*, 71, 305-313.
- MCCORMACK, T., GILL, L. W., NAUGHTON, O. & JOHNSTON, P. M. 2014. Quantification of submarine/intertidal groundwater discharge and nutrient loading from a lowland karst catchment. *Journal of Hydrology*, 519, Part B, 2318-2330.
- MCCORMACK, T. & NAUGHTON, O. 2016. Groundwater flooding in the Gort Lowlands. *Irish Groundwater Newsletter* [Online].
- MORRIS, S. E., COBBY, D. & PARKES, A. 2007. Towards groundwater flood risk mapping. *Quarterly Journal of Engineering Geology and Hydrogeology*, 40, 203-211.
- MORRISSEY, P. J., MCCORMACK, T., NAUGHTON, O., MEREDITH JOHNSTON, P. & WILLIAM GILL, L. 2020. Modelling groundwater flooding in a lowland karst catchment. *Journal of Hydrology*, 580, 124361.
- MOTT MACDONALD 2010. Preliminary Flood Risk Assessments: Groundwater Flooding. Dublin.
- NAUGHTON, O. 2013. An Overview of Groundwater Flooding in Ireland. *Groundwater Newsletter* [Online]. Available: <https://www.gsi.ie/NR/ronlyres/91A8739D-9F0D-437A-89A5-F73EDAAB7A6F/43869/GWNewsletterNo55.pdf>.
- NAUGHTON, O., GILL, L., JOHNSTON, P., MORRISSEY, P., REGAN, S., MCCORMACK, T. & DREW, D. 2018. The hydrogeology of the Gort Lowlands. *Irish Journal of Earth Sciences*, 36, 1-20.
- NAUGHTON, O., JOHNSTON, P. M. & GILL, L. W. 2012. Groundwater flooding in Irish karst: The hydrological characterisation of ephemeral lakes (turloughs). *Journal of Hydrology*, 470-471, 82-97.
- NAUGHTON, O., JOHNSTON, P. M., MCCORMACK, T. & GILL, L. W. 2017a. Groundwater flood risk mapping and management: examples from a lowland karst catchment in Ireland. *Journal of Flood Risk Management*, 10, 53-64.
- NAUGHTON, O. & MCCORMACK, T. 2018. Monitoring Groundwater Flooding in Ireland Using Sentinel-1 SAR. *NEREUS/ESA/EC "The Ever Growing use of Copernicus across Europe's Regions"*.
- NAUGHTON, O., MCCORMACK, T., GILL, L. & JOHNSTON, P. 2017b. Groundwater flood hazards and mechanisms in lowland karst terrains. *Geological Society, London, Special Publications*, 466.



- NOBRE, A. D., CUARTAS, L. A., HODNETT, M., RENNÓ, C. D., RODRIGUES, G., SILVEIRA, A., WATERLOO, M. & SALESKA, S. 2011. Height Above the Nearest Drainage – a hydrologically relevant new terrain model. *Journal of Hydrology*, 404, 13-29.
- NOONE, S., MURPHY, C., COLL, J., MATTHEWS, T., MULLAN, D., WILBY, R. L. & WALSH, S. 2016. Homogenization and analysis of an expanded long-term monthly rainfall network for the Island of Ireland (1850–2010). *International Journal of Climatology*, 36, 2837-2853.
- O’HARA, R., GREEN, S. & MCCARTHY, T. 2019. The agricultural impact of the 2015–2016 floods in Ireland as mapped through Sentinel 1 satellite imagery. 58, 44.
- O’NEILL, F. H. & MARTIN, J. R. 2015. Summary of findings from the Survey of Potential Turloughs 2015. Unpublished Report for National Parks & Wildlife Service. Volume I: Main Report.
- OTSU, N. 1979. A Threshold Selection Method from Gray-Level Histograms. *IEEE Transactions on Systems, Man, and Cybernetics*, 9, 62-66.
- PINAULT, J.-L., AMRAOUI, N. & GOLAZ, C. 2005. Groundwater-induced flooding in macropore-dominated hydrological system in the context of climate changes. *Water Resources Research*, 41.
- PULVIRENTI, L., PIERDICCA, N., CHINI, M. & GUERRIERO, L. Monitoring flood evolution in agricultural areas using COSMO-SkyMed data: analysis of the Tuscany inundation of December 2009. *SPIE Remote Sensing*, 2011. SPIE, 12.
- RÉMI, A. & HERVÉ, Y. 2007. Change detection analysis dedicated to flood monitoring using ENVISAT Wide Swath mode data. *Proceedings of the ENVISAT Symposium 2007, Montreux, Switzerland, SP-636*.
- RENNÓ, C. D., NOBRE, A. D., CUARTAS, L. A., SOARES, J. V., HODNETT, M. G., TOMASELLA, J. & WATERLOO, M. J. 2008. HAND, a new terrain descriptor using SRTM-DEM: Mapping terra-firme rainforest environments in Amazonia. *Remote Sensing of Environment*, 112, 3469-3481.
- RYAN HANLEY CONSULTING ENGINEERS 2018. South Galway (Gort Lowlands) Flood Relief Scheme Surveyed Historic Flood Levels - Draft.
- RYAN HANLEY CONSULTING ENGINEERS 2019. South Mayo (The Neale) Flood Relief Scheme Historic Flood Levels - Draft.
- SCHULTE, R. P. O., DIAMOND, J., FINKELE, K., HOLDEN, N. M. & BRERETON, A. 2005. Predicting the soil moisture conditions of Irish grasslands. *Irish Journal of Agricultural and Food Research*, 44, 95-110.
- SCHUMANN, G., DI BALDASSARRE, G., ALSDORF, D. & BATES, P. D. 2010. Near real-time flood wave approximation on large rivers from space: Application to the River Po, Italy. *Water Resources Research*, 46, n/a-n/a.
- SHEEHY SKEFFINGTON, M., MORAN, J., O’CONNOR, Á., REGAN, E., COXON, C. E., SCOTT, N. E. & GORMALLY, M. 2006. Turloughs - Ireland’s unique wetland habitat. *Biological Conservation*, 133, 265-290.
- SIART, C., BUBENZER, O. & EITEL, B. 2009. Combining digital elevation data (SRTM/ASTER), high resolution satellite imagery (Quickbird) and GIS for geomorphological mapping: A multi-component case study on Mediterranean karst in Central Crete. *Geomorphology*, 112, 106-121.
- SMAKHTIN, V. Y. & MASSE, B. 2000. Continuous daily hydrograph simulation using duration curves of a precipitation index.



- SOUTHERN WATER GLOBAL 1998. An investigation of the flooding problems in the Gort-Ardrahan area of South Galway. Final Report, April 1998. Produced by Southern Water Global and Jennings O`Donovan and Partners for the Office of Public Works, Dublin.
- TARBOTON, D. G., BRAS, R. L. & RODRIGUEZ-ITURBE, I. 1991. On the extraction of channel networks from digital elevation data. *Hydrological Processes*, 5, 81-100.
- TWELE, A., CAO, W., PLANK, S. & MARTINIS, S. 2016. Sentinel-1-based flood mapping: a fully automated processing chain. *International Journal of Remote Sensing*, 37, 2990-3004.
- ULABY, F. T., MOORE, R. K. & FUNG, A. K. *Microwave Remote Sensing Active and Passive- Volume III: From Theory to Applications*, Artech House, Inc.
- WORKING GROUP ON GROUNDWATER 2004. Guidance on the assessment of pressures and impacts on groundwater dependent terrestrial ecosystems, Risk Assessment Sheet GWDTERA2a – Risk to Turloughs from Phosphate. Guidance Document no. GW9.
- ZHOU, W. 2007. Drainage and flooding in karst terranes. *Environmental Geology*, 51, 963-973.

